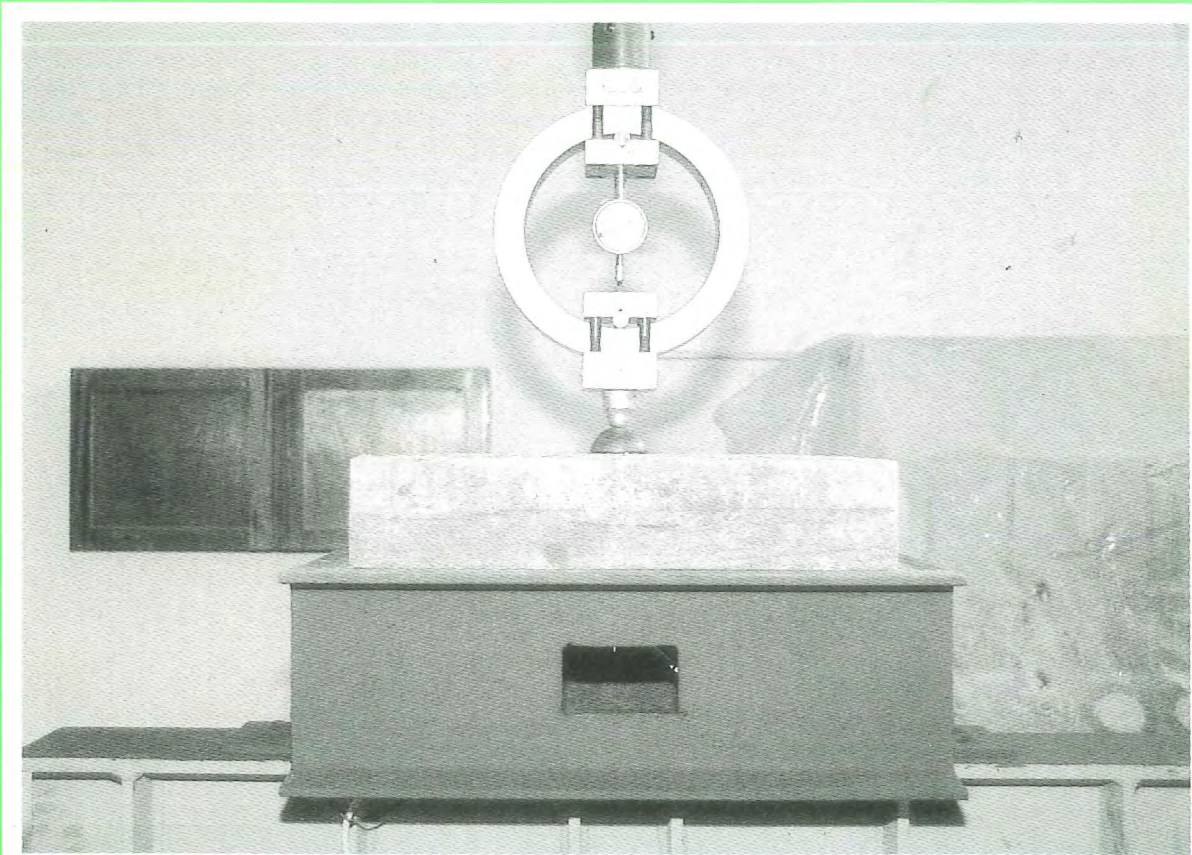




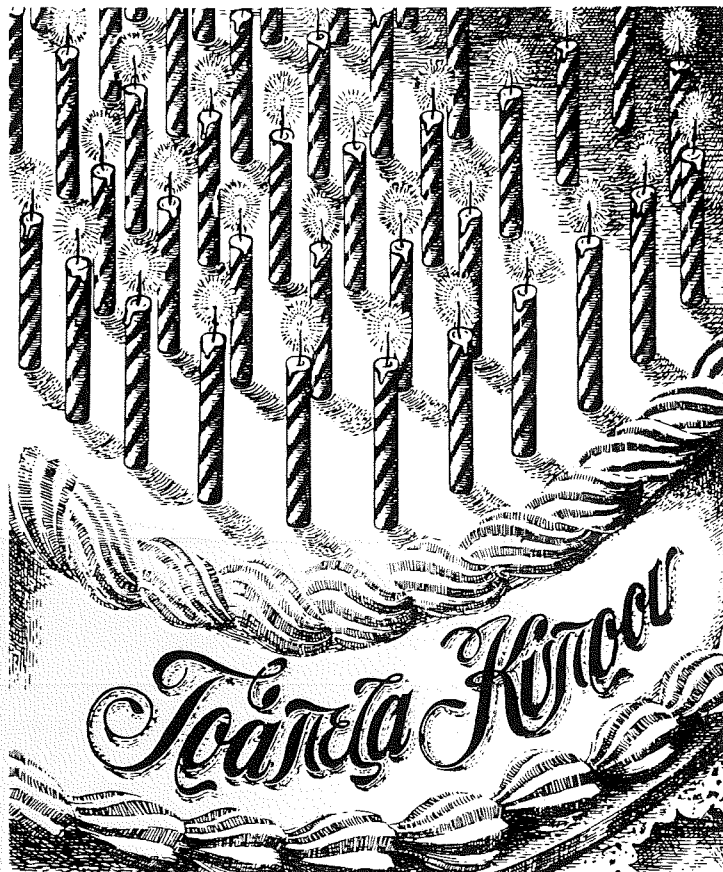
No. 18 June 1989 Nicosia Cyprus

Review

THE HIGHER TECHNICAL INSTITUTE



ενενήντα χρόνια πρώτη!



Πριν 90 ακριβώς χρόνια, μια τράπεζα ξεκίνησε δειλά-δειλά να προσφέρει τραπεζικές υπηρεσίες στον τόπο. Ήταν η πρώτη Κυπριακή τράπεζα.

Στο πέρασμα του χρόνου, η τράπεζα αυτή προχώρησε, μεγάλωσε, απλώθηκε σ' ολόκληρη την Κύπρο και στο εξωτερικό. Είναι η Τράπεζα Κύπρου, ο μεγαλύτερος Τραπεζικός Οργανισμός του τόπου.

Σήμερα 90 χρόνια μετά οι φιλοδοξίες μας παραμένουν αναλλοίωτες και προχωρούμε δυναμικά στις δεκαετίες που μας έρχονται.

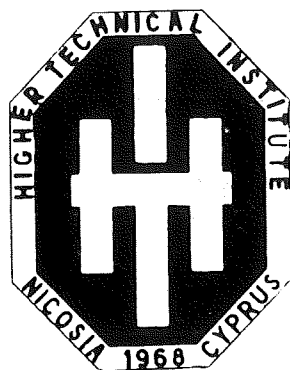


**ΤΡΑΠΕΖΑ
ΚΥΠΡΟΥ**

δυναμικά στον κόσμο του αύριο



The Higher Technical Institute (HTI) was established in 1968 as a Government of Cyprus project with assistance by the United Nations Special Fund (UNDP), the United Nations-Educational Scientific and Cultural Organisation (UNESCO), and the International Labour Office (ILO). Cyprus Government Executing Agency: The Ministry of Labour and Social Insurance.



Review

No. 18 June 1989 Nicosia Cyprus

Director HTI

Dr T. Drakos MSc PhD CEng FIEE FIMechE

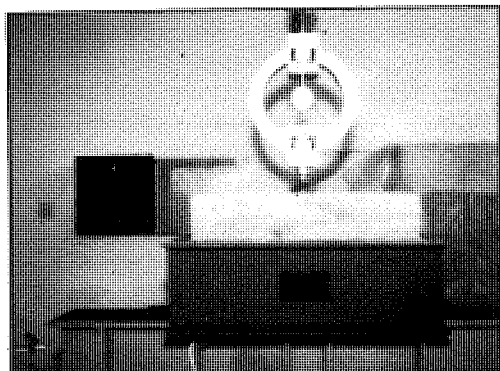
Chief Editor

P. Vassiliou BSc MSc CEng MICE

Assistant Chief Editors

A. Kaplanis MSc AMIEE MBES FIHospE

E. Michael BSc MSc CEng MIEE



Testing of Steel Fibre Reinforced Concrete slabs at HTI

Cover Photograph by Dr H. Stavrides

HTI Review is published by the Press and Information Office in cooperation with the Higher Technical Institute, Nicosia. It accepts articles which promote and further new developments and knowledge in technology, especially with reference to Industries of Cyprus. Requests for further copies of the magazine and for information concerning the published articles should be made to Chief Editor HTI Review, Higher Technical Institute, P.O.Box 2423 - Nicosia.

The HTI is not as a body responsible for the opinions expressed in the HTI Review unless it is stated that an article officially represents the HTI's views.

P.I.O. 48/89-500

CONTENTS

Page	
2	Artificial Neural Net Algorithms in Classifying Electromyographic Signals <i>by Dr C. N. Schizas, C. S. Pattichis, L. T. Middleton, I. S. Schofield & P.R. Fawcett.</i>
3	Parallel Processing via Artificial Neural Systems <i>by Dr C. N. Schizas.</i>
7	The flexural and toughness characteristics of steel fibre reinforced concrete <i>by Dr H. Stavrides</i>
16	Acoustoelectronic and Acousto-optic devices for signal processing in real time <i>by Prof. Y.N. Culyaev</i>
24	Comparative tests on plain, steel fabric reinforced and steel fibre reinforced concrete ground floors <i>by Derrick Beckett</i>
27	Computer information system for the III games of the small states of Europe <i>by Dr C. N. Schizas</i>
30	Concrete pumping and associated problems <i>by A.D. Ioannides</i>
36	Theoretical computation of acoustic emission signal trends for monitoring metal cutting tool wear <i>by Dr V. Messaritidis</i>
39	Cold Fusion or Nuclear Confusion? <i>by Dr A.Y. Stathopoulos</i>
42	Microprocessor Controlled Three-phase Transistor Inverter <i>by S. Hadjoannou</i>
45	Acoustic Intensity and its applications <i>by Dr P. Eleftheriou</i>
48	Thermography in medicine <i>by A.K. Kaplanis</i>
51	Solar Radiation <i>by S. Kaloyirou</i>
55	Contingency Plans for Time-Constrained Systems <i>by A. Solomou</i>
60	Calendar of Activities Academic Year 1988-89 <i>by D. Charalambidou-Solomi</i>

Artificial Neural Net Algorithms in Classifying Electromyographic Signals*

A research paper

C.N. Schizas, B.Sc., MBA, Ph.D., MIEE, CEng, MIEEE, FABAC, MBCS^{1&2}
C.S. Pattichis, B.Sc, M.Sc., MIEEE & L.T. Middleton, M.D.²
I.S. Schofield, M.D. & P.R. Fawcett, M.D.³

Motor Unit is the smallest functional unit of the muscle which can be activated. This unit consists of an anterior horn cell, an axon and the muscle fibers innervated by this neuron. Structural reorganization of the motor unit takes place by disorders affecting peripheral nerve and muscle. Motor Unit morphology can be studied by recording its electrical activity using several types of needle electrodes. The data used in this study has been acquired by using the macro needle electrode. The recorded waveform during weak muscle contraction is referred as the macro motor unit action potential (Macro MUP).

The shape features of the Macro MUP are described by the following parameters: (1) **amplitude** (the difference between the minimum positive peak and the maximum negative peak), (2) **area** (the sum of the rectified signal integrated over the 50ms analysed epoch), (3) **average power** (the sum of squares of each sample over the 50ms epoch, divided by the number of samples) and (4) **duration** (the segment of the epoch which contains 90% of the power of the analysed epoch).

Eight hundred and forty (840) Macro MUP's have been acquired from forty-one (41) subjects, analytically shown in the following table.

Group	No of subjects	Age range	No of Macro MUP's
Normal	7	19-46	147
Becker's Muscular Dystrophy	14	17-63	285
Motor Neuron Disease	9	27-59	183
Spinal Muscular Atrophy	11	21-72	225

The methodology which is proposed in this study will be tested and evaluated by using the above data.

Current methods of diagnosis and classification of pathological cases are based on the amplitude value of the Macro MUP. Stalberg and Fawcett (1982) have developed a table which provides the normal range of amplitudes, depending on the age of a subject.

The aim of this work is to examine how Parallel Distributed Processing via Artificial Neural Nets (ANN) can be used in providing a computerised

method of electromyographic diagnosis. Automatic analysis of the electromyographic signal (EMG) involves high computation rates and many hypotheses to be pursued in parallel. Therefore ANN models may be considered as ideal candidates for this analysis.

It has been previously demonstrated that cluster analysis using Macro EMG data, result in a low diagnostic yield because cluster boundaries identifying each group overlap (Pattichis et al., 1988). In the present study the Back-Propagation Training Algorithm by Rumelhart, Hinton and Williams (1986) is utilised. A three layer perceptron net is implemented in this investigation due to its ability to differentiate among arbitrarily complex decision regions. The flexibility of this algorithm and its parallel processing nature enabled the examination of different ways of structuring the input data. Two architectures are under study; one with eight inputs, three layers and four outputs, and the other with eighty inputs, three layers and four outputs. In the first ANN model the median and the semi-inter quartile range of each subject are forming a set of inputs, where in the second ANN model the parameters of each Macro MUP for each subject are forming the set of inputs. Half of the available data is used as a training set and the rest as evaluation data. A comparative study between existing manual methods and the proposed automatic method will be demonstrated.

Bibliography and References:

1. D.E. Rumelhart, G.E. Hinton, R.J. Williams, *Learning representations by Back propagating errors*, NATURE Vol. 323, 533-536, 1986.
2. R.P. Lippman, *An Introduction to computing with neural nets*, IEEE ASSP magazine, 4-22, 1987.
3. R. Rosenblatt, *Principles of neurodynamics*, New York, Spartan Books, 1959.
4. E. Stalberg, P. Fawcett, *Macro EMG in health subjects of different ages*, Journal of Neurology, Neurosurgery and Psychiatry, 45, 870-878, 1982.
5. C.S. Pattichis, I.S. Schofield, P.R. Fawcett, *A morphological analysis of the macro MUP*, III International conference of quantitative EMG, Cyprus, June 1988.

* Abstract submitted to the first IEE International Conference on Artificial Neural Networks.

1 Lecturer, Higher Technical Institute, Nicosia, Cyprus

2 MDRTC, Neurodiagnostic centre, Makarios Hospital, Nicosia, Cyprus

3 Department of Clinical Neurophysiology, Newcastle General Hospital,

Newcastle Upon Tyne, UK

Parallel Processing via Artificial Neural Systems

A research paper

*Dr Christos N. Schizas,
Lecturer HTI*

The field of neural networks is a unique field in that from the point of view of the neurobiologist, it is a mature one, but from the perspective of signal processing and computing, it is a rapidly developing, new, and exciting area of research. Interest, however, within the engineering community in neural modeling and neural computing is not recent. It can be traced to the work of McCulloch and Pitts in the early 1940's. In fact, devotees of historical roots can legitimately claim that some of the early publications of Aristotle could easily appear as abstracts for modern neural network papers.

Neurons are living nerve cells and neural networks are networks of these cells. An example of a natural neural network is the organization of the cerebral cortex of the brain. Investigators attempted to build biological models for studying and understanding the function of real brains. Technological modeling has as main objective the study of the brain for extracting concepts and using them for developing new computational methodologies such as parallel processing. The latter structure has been taken by scientists and engineers mainly, who are working in the area of artificial neural networks (ANN) and neurocomputers.

The first objective of research in ANN is to understand how the brain imparts abilities like perceptual interpretation, associative recall, common sense reasoning and learning of humans. It is necessary, however, to understand how "computations" are organized and carried out in the brain. These computations are of a different kind than the formal manipulation of symbolic expressions. The second objective is to understand the subclass of neural network models that emphasize "computational power" without having necessarily all the experimental evidence to support it.

Traditional digital computers are extremely good at executing sequences of instructions that have been precisely formulated for them with the Von Neuman "stored program" representing the processing steps that need to be done. The human brain, on the other hand, performs well at such tasks as vision, speech, and information retrieval in the presence of noisy and distorted data; tasks that are very difficult indeed for sequential digital computers. How does the brain accomplish these tasks, given that its "processing elements" (neurons) are significantly slower than the processing elements of contemporary supercomputers?

Neurons are electrochemical devices and they respond in milliseconds, whereas modern electronic components can respond in nanoseconds.

Interest in ANNs has been prompted recently by advances in technology as well as through deeper understanding of how the brain works. The desire to build a new breed of powerful computers (the sixth generation computers) is about to become a reality. These intelligent machines will be able to solve a variety of problems that are proving to be very difficult with conventional digital computers. Cognitive tasks such as recognizing a familiar face, learning to speak and understand a natural language, and guiding a mechanical hand to grasp objects of different shape, weight, size and ingredients are some typical objectives being set. Tasks such as these, typically involve pattern recognition, fuzzy pattern matching, nonlinear discrimination which are analogous to those typically performed naturally by the brain, and are beyond the reach of conventionally programmed computers as well as the rule-based expert systems.

The development of cognitive models which will form the foundation for artificial intelligence has always been one of the main objectives of research because it is closely related to the associative property and self-organizing capability of the brain; associative means the capability of recalling an entire complex of information by using a small part of it as a searching key, done extremely well by the brain, and self-organizing means the ability to acquire knowledge through a trial-and-error learning process.

Tasks such as autopiloting, handwritten-character recognition, spoken language translation, for which algorithms do not yet exist, or for which it is virtually impossible to write down a series of logical or arithmetic steps that will arrive at the answer are candidates for this new way of computing using neural nets, called "neurocomputing". In formal terminology as specified by R. Hecht-Nielsen, neurocomputing is the engineering discipline concerned with nonprogrammed adaptive information-processing systems that develop associations (transformations or mappings) between objects in response to their environment. Instead of being given a step-by-step procedure for carrying out the desired transformation, the neural network itself generates its own internal rules governing

the association, and refines those rules by comparing its results to its training set. As mentioned above, through trial and error, the network literally teaches itself how to do the task.

Eventhough neurocomputing does not, replace algorithmic programming, is indeed a fundamentally new and different information-processing paradigm; the first alternative to algorithmic programming. Wherever it is applicable, totally new information-processing capabilities can be developed, and development costs and time often decrease by an order of magnitude.

negative for inhibitory inputs. The combination of all inputs most probably in an additive way form the net total input which determines whether to fire or not.

A model of neural network can be formed by a collection of neurons, each of which is connected to as many as 10,000 others, from which it receives stimuli, inputs and feedback, and to which it sends stimuli. Some of those connections are strong; others are weak as could be indicated by the weighting factor. In the case of the brain, it accepts inputs and generates responses to them, partly in accordance with its

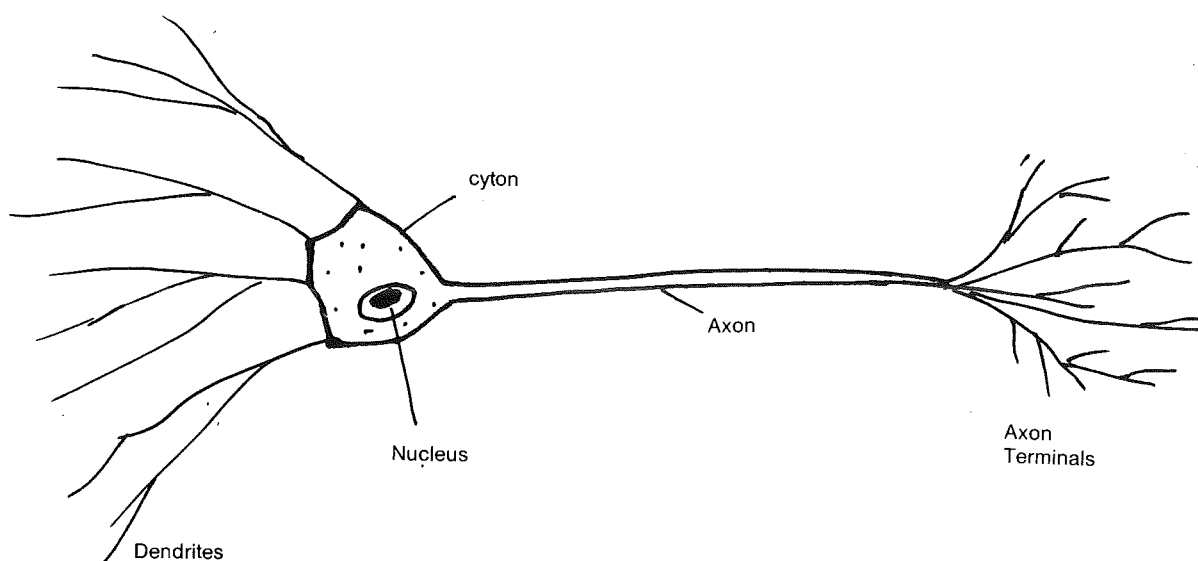


Figure 1
Structure of nerve cell (neuron)

It has not yet been completely understood how a biological neural network stores, retrieves, represents, and manipulates data such as images, smells, and thoughts. It has been estimated however that the number of neurons in the human brain is of the order of 10^{11} , and that they are organized in highly complex structure. Under a microscope where the structure of a nerve cell can be revealed, as illustrated in fig. 1, one can observe a cell body, or cyton; many input fibers, or dendrites; and a single output fiber, or axon, which branches out to send signals to the input fibers of other nerve cells.

Dendrites are of two main types; those which tend to cause the neuron to produce an output and those which tend to prevent the neuron from firing. The first type of dendrites which cause firing are called 'excitatory' inputs and the second type which in fact discourage firing are called 'inhibitory' inputs. Each input has a "weighting factor" which is positive for excitory inputs and

genetically programmed structure, but mainly through learning, organizing itself in reaction to input. As it has already been mentioned the way neural networks are used by engineers are only loosely based upon nerve physiology. At best, the only comparison is that they behave in a vaguely similar way. Eventhough it will be a long time before one can re-create in a machine all the capabilities of the brain, neurocomputing is already offering some valuable, specialized, brain-like capabilities that in all likelihood lie beyond the reach of algorithmic programming.

As an example of a practical model the "multi-layer perceptron" will be used in order to illustrate its structure and functioning. This model consists of a collection of processing units, each of which has many input signals, but only a single output signal. The output signal is distributed out along many paths to provide input signals to other processing units at deeper levels which form layers containing many hidden units that are

not directly connected to both the input and output nodes. A three-layer perceptron with two layers of hidden units is illustrated in fig. 2.

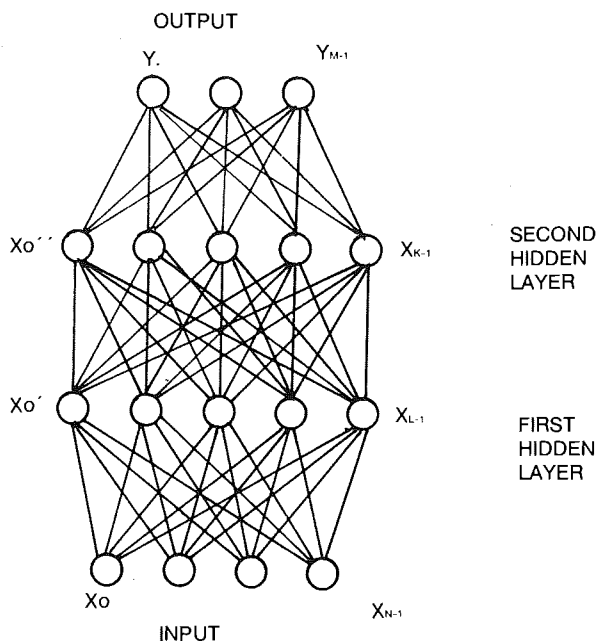


Figure 2

A three-layer perceptron with two layers of hidden units

Each unit has its own small local memory, which stores the values of some previous computations along with adaptive coefficients basic to neural-network learning. The processing that each element does is determined by a transfer function which is often subject to non-linearities. Every connection entering a processing unit has an adaptive coefficient which we called "weighting factor" assigned to it. This weight, which is stored in the local memory of the processing element, is generally used to amplify, attenuate, and possibly change the sign of the signal in the incoming connection. Often, the transfer function sums this and other weighted input signals to determine the value of

the processing element's next output signal. Thus the weights determine the strength of the connections from neighboring processing elements.

Recently developed, effective training algorithms for such models have made possible the practical use of multi-layer perceptrons. ANN models have already been applied in speech processing, classification of sonar waves, adaptive filtering, etc. A recent application of ANN is under development for classifying electromyographic signals, recorded from subjects suffering from neuromuscular diseases.

An electronic device that behaves somewhat like a neuron is the electronic analog operational amplifier, configured as an integrator. If hundreds of these integrators are visualized as being interconnected through potentiometers, whose settings represent the strengths of real neurons, then what is generated is a crude model of an ANN. With the recent developments in VLSI technology it has become possible to build high-density custom circuits to represent the neurons via thresholding amplifiers. Constraints which may be imposed by VLSI limitations in areas such as density of interconnectivity could be overcome by using opto-electronics and optical computing.

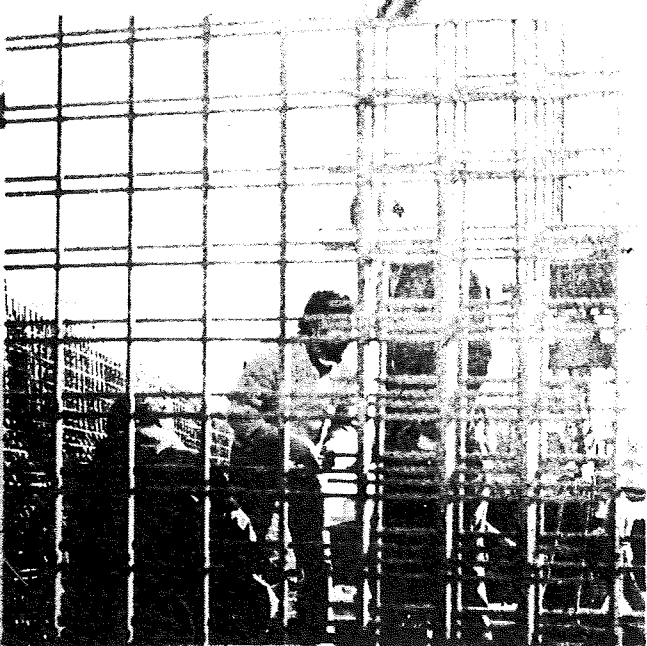
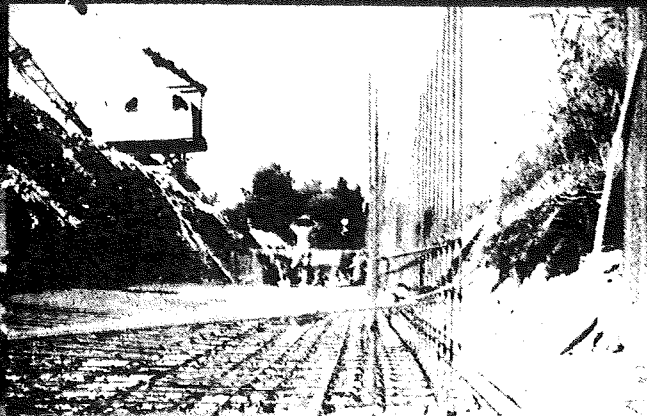
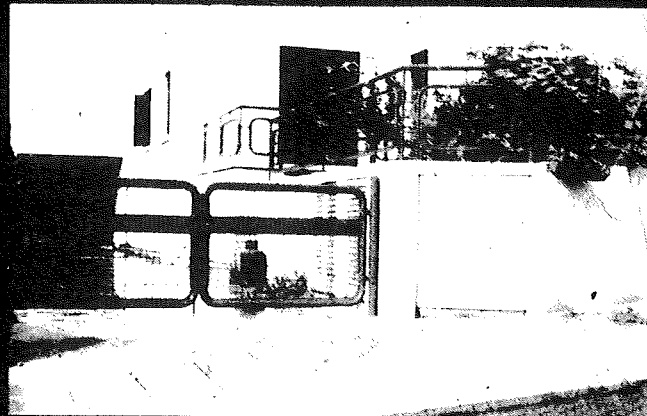
Bibliography

1. *Artificial Neural Systems*, Computer Magazine, Computer Society of the IEEE, March 1988.
2. Robert J.B., *Artificial Neural Network Experiment*, Dr Dobbs Journal of Software Tools, April 1987.
3. McCulloch and Pitts, *A Logical Calculus of the Ideas Immanent in Nervous Activity*, Bulletin of Mathematical Biophysics, 5, 1943
4. Rober Hecht-Nielsen, *Neurocomputing: Picking the human brain*, IEEE spectrum, 36-41, March 1988
5. Rosenblatt F., *The Perceptron, a probabilistic mode for information storage and organization in the brain*. Psychological Review, 62, 1958.
6. Minsky, M. and S. Papert, *Perceptrons: An introduction to computational geometry*, Cambridge, MIT Press, 1969
7. Rumelhart D.E., Hinton G.E., Williams R.J., *Learning Internal Representations by Error Propagation*, Parallel Distributed Processing, vol 1, MIT Press, 1986.
8. Schizas C. et. al, *Artificial Neural Net Algorithms in classifying Electromyographic Signals*, ibid, 1989.

δομικό πλέγμα

DOMOPLEX

για λιγότερο κόπο, χρόνο και χρήμα



- Σύγχρονη λύση προηγμένης τεχνολογίας, πρακτική, γρήγορη και οικονομική.
- Ψηλότερη αντοχή, οικονομία υλικού, μηδενισμός αποκομμάτων.
- Ειδικευμένοι πολιτικοί μηχανικοί και πλήρης σειρά προγραμμάτων κομπιούτερ (Domus) για στατικούς και αντισεισμικούς υπολογισμούς, στη διάθεσή σας.
- Παγκύπρια διανομή από τα καταστήματα υλικών οικοδομής.
- Εξαγωγές στη Μέση Ανατολή και Ευρώπη.

Παραγωγή από 1.000.000 τετραγωνικά μέτρα τοιχώματα και δαπεδοσκελετούς.
Παράδοση DOMOPLEX στην Κύπρο.

DOMOPLEX LTD

Τ.Κ. 4185 Λεμεσός

Τηλ. 051-23862



The Flexural and toughness characteristics of steel fibre reinforced concrete

A research paper

Dr Herodotos Stavrides
Senior Lecturer
Civil Engineering Dept HTI

1. INTRODUCTION

Fibre reinforced cement and concrete have "invaded" the construction industry internationally since the mid-seventies. Research on concrete and cement reinforced with a large variety of fibres ranging from glass, mainly for cement, to steel as reinforcement for concrete, started seriously in the early sixties. Since those early days a considerable amount of research on fibre reinforced cement composites has been carried out both on the material properties and the structural behaviour. Research on the material properties covered such properties as flexural behaviour, shrinkage both free and restrained, creep, toughness and energy absorption, impact and abrasion resistance etc. As far as structural behaviour is concerned, research was carried out on the contribution of steel fibres in R.C. beams and slabs. The applications of fibre reinforced cement composites are numerous ranging from road construction for both overlays and new road construction, to industrial floors. Steel fibre reinforced concrete has been used successfully in the repair of damaged concrete pavements, in the replacement of airfield taxiway, storage and refuelling areas etc.

The main fibre types that have been used as reinforcement to cement or concrete include, ceramic, asbestos, glass, vegetable, nylon, polypropylene and steel, the latter being the more widely used.

2. FIBRE REINFORCED CONCRETE IN CYPRUS

In Cyprus steel fibre reinforced concrete has not been used as yet, even though recently another form of fibre reinforcement has been employed, namely polypropylene. In the recent construction of the Sheraton Hotel marina, polypropylene fibre reinforced concrete sections were used.

It is hoped that in the near future, with the contribution of the present work, steel fibre reinforced concrete will find its first major application. The Cyprus Ports Authority who has sponsored this research programme is planning to construct a heavy duty rigid pavement at the Port of Limassol. The total area of the pavement will be about 5000 m².

3. THE EXPERIMENTAL PROGRAMME

3.1 Preamble-Aim of Research Programme

The aim of the experimental programme was to establish the influence of the steel fibre inclusion in concrete made with local materials.

The main parameters chosen for investigation were the flexural strength and toughness. It was

thought that apart from the classical prism specimens employed for the evaluation of modulus of rupture, slab elements ought to be cast as well.

In deciding upon the mix proportions to be employed during the trial mixes several factors were taken into consideration, the main two being:

(a) Steel fibre reinforced (S.F.R.) concrete mixes require a larger amount of fine material - cement/sand matrix - in which to be embedded effectively, than ordinary plain concrete mixes.

(b) The effectiveness of the fibre reinforcement is considerably enhanced with the use of smaller maximum size aggregate.

Thus taking both these two factors into consideration but also bearing in mind the cost effectiveness of S.F.R concrete which per se is considerably more expensive than plain concrete due to the high cost of fibres, the following decisions were reached.

(a) The trial mixes were to be such that the cement content should not exceed a value of 350 kg/m³.

(b) The maximum aggregate size to be used was to be 20 mm. However this was to be used in conjunction with 10mm maximum size aggregate in various proportions. Thus after a series of trial mixes the field was narrowed down to two different mixes, one containing 70% of 20mm maximum size aggregates and 30% of 10mm maximum size aggregates, and the other containing the above maximum sizes in equal proportions.

Obviously the use of 10mm maximum size aggregates only, would enhance the performance of SFR concrete, but it was thought that this compromise ought to be made in order to limit the cost of production per cubic metre.

The percentage of fibres was another item to be decided upon. Since steel fibre percentages of the order of 0.5% by volume have been known to give good results in general performance, it was decided to use different fibre contents with a maximum value of 40 kg/m³ which is just over 0.5% by volume.

3.2 The Test Programme

3.2.1 Materials/Mix Proportions

The materials used and their mix proportions are shown in Table 1. The crushed sand had a coarse grading as it can be seen from Fig. 1. The inclusion of fibres which can be thought of as an extra amount of aggregates with very high surface area, causes workability problems. Therefore the use of finely graded sand is

prohibitive, due to its high demand for water at a given workability.

The fibres used were DRAMIX steel fibres which exhibited an excellent performance during fabrication. The author has considerable experience on fibre reinforced cement based materials and indeed has come across a large variety of fibres of different materials and shapes. One of the major problems of SFR concrete is the "balling effect" which occurs with normal steel fibres. This takes place during mixing when the fibres have the tendency to lock together into small balls resembling tiny "hedgehogs". This obviously affects not only workability but performance, since these fibre-balls give rise to segregation and a considerable loss of homogeneity of the mix.

The ingenious fabrication of the DRAMIX Steel fibres, whereby the fibres are glued together in small bundles, makes mixing a joy to watch. The glue holding a number of fibres together upon contact with water, and after a very short period of wet mixing, dissolves, thus freeing the fibres to disperse in the mix in a very homogeneous manner. The final result is a very "healthy looking" mix free of cancerous parts such as fibreballs.

3.2.2 Fabrication and Specimens Cast

The aggregates both coarse and fine were weighed in a saturated surface dry condition and mixed dry with cement for two minutes. Then the water was added to the mix together with the plasticizer for a wet mixing of two minutes. Finally the fibres were dispensed into the mix for a further 90 seconds mixing.

All the specimens cast were compacted by means of external vibration.

Specimens

In each batch the following specimens were cast.

- (a) Three 150mm cubes for compressive strength
- (b) Three 100x500 mm prisms for modulus of rupture tests
- (c) One 100x100x500mm prism for shrinkage readings
- (d) Two 100x500x500mm slabs for flexural (central point load) tests.

Curing:

All specimens were demoulded in 24 hours and put in a curing tank at a temperature of 20 to 28°C, except the prism used for shrinkage readings, which was left to dry freely in air.

Table 2 shows the mix details and the 7-day compressive strength of all mixes.

3.2.3 Test Results-Analysis-Comments

3.2.3.1 Flexural strength of prisms & Toughness Index

For each mix three prisms were tested in flexure in a Denison Testing machine. The load was applied centrally with the supports being 300mm apart. This distance does not conform to the specifications which require a 400mm distance between supports. The smaller support distance gave rise to increased values of flexural

strength. However due to the short span of the prism, the influence of fibre inclusion does not seem to be pronounced. That is, with the 400 mm span between supports of the prisms the influence of the fibre inclusion would have been more marked.

The single central point load was added incrementally and at each load increment the central deflection was recorded by means of a dial gauge.

Table 3 summarizes the 7 day flexural strength of all mixes and the toughness index. This is a measure of the amount of energy required to deflect the prism used in the modulus of rupture test a given amount, compared to the energy required to bring the fibrous beam to the point of first crack. The toughness index is calculated as the area under the load-deflection curve out to 1.9mm divided by the area under the load-deflection curve of the fibrous beam up to the first crack strength.

Referring to Figs 2-10 it can be seen that toughness index is given by:

$$\text{Toughness Index} = \frac{\text{Area 1} + 2}{\text{Area 1}}$$

Referring to Table 3 it can be seen that the toughness index increases with increasing fibre content in the mix. That is the higher the content of fibres the higher the absorption of energy in the post cracking stage of the specimen, a very useful property to have, especially in the case of cyclic and impact loading.

The increase in the flexural strength or Modulus of Rupture (M.o.R) is also evident with increasing fibre content. Thus in the case of Series A mixes, with 70% of the aggregate content being of 20mm maximum size, increases of up to 17.5% in Modulus of Rupture were recorded compared to the plain concrete beam. This 17.5% increase was observed in the case of Mix A6 with a fibre content of 40 kg/m³.

The better performance of the mixes of series B is obvious. Thus referring to Table 3 it can be seen that the larger proportion of smaller maximum size aggregates (10mm - 50% instead of 30%) led to even higher values of Modulus of Rupture. However the better performance of the mixes with a higher content of smaller maximum size coarse aggregates, is manifested in the percentage increase in M.o.R with respect to the plain concrete beam. Thus in Series B mixes increases of up to 39.5% were observed. The comparative percentage increases in M.o.R are shown in Fig. 11a. Fig. 11b summarizes the direct comparison between series B and series A mixes. It can be seen that the influence of the higher amount of smaller maximum size aggregates (Series B) is even more pronounced at high fibre contents, with a maximum increase of 24.5% recorded in the case of mixes with 40 kg/m³ of fibres.

3.2.3.2 Slabs

Fig. 12 shows the experimental set-up and the instrumentation of the slabs under testing. The square slabs of thickness 100mm and side 500 mm were positioned in a rigid frame made of heavy duty steel channels. The frame had internal dimensions 460 mm so that the slab would have a support of 20 mm perimetrically. Load was applied centrally by means of a hydraulic jack fitted with a calibrated proving ring.

The load was applied incrementally and the corresponding central deflection was obtained at each load increment by means of a dial gauge.

Like the prisms the slabs with steel fibre concrete showed a vast improvement in post-cracking behaviour. However the improvement in the post-cracking characteristics of fibre reinforced concrete slabs was even more spectacular than that of the corresponding prisms. That is in the case of prisms the first visible crack load, coincided with the ultimate load, with load capacity continuing in the post cracked stage. In the case of slabs however, there was a very distinct difference between first crack load and ultimate load. Table 4 shows the test results of all slabs in the form of First Crack Load and Ultimate Load. The plain concrete slabs just like the corresponding prisms, on reaching their first crack load failed immediately with the first cracks opening up and thus not allowing the slab to carry any more load with non-existent post-cracking behaviour.

Table 5 shows the influence of fibre content, which summarizes the percentage increase in both First Crack and Ultimate Load of all slabs with respect to the plain concrete slabs. The influence of the fibre content is also shown diagrammatically in Fig. 13.

Increases of up to 88% in ultimate load capacity have been recorded. The superior performance of series B is again evident with increases in both first crack and ultimate loads with respect to the plain concrete slabs especially at high fibre contents. Thus whereas in the case of mix B6 an increase in ultimate load capacity of 88% was observed, in the case of mix A6 the corresponding increase with respect to mix A1 was only 69%. In fact in Table 6 a direct comparison is made between corresponding mixes in Series A and Series B. From this table it can be seen that as the fibre content increases so does the difference in performance between the mixes with a higher amount of finer coarse aggregates (Series B) and the mixes with higher coarse aggregate content. (Series A).

Crack Pattern and Deflection of Slabs

Fig. 14 shows the load-central deflection of slabs A6 and B6, the two slabs with the maximum fibre content of 40 kg/m³. The load deflection characteristics of the fibre reinforced concrete with 50% of 20mm aggregates are obviously superior with a considerable increase in energy absorption in the post-cracking stage.

Whereas the plain concrete slabs failed by the formation of the first two major cracks from edge to edge, the fibre reinforced slabs showed an increase in the number of cracks of smaller order of magnitude, the number of small cracks in fact increasing with fibre content.

3.2.3.3 Shrinkage

The early age shrinkage values were recorded by means of a 200 mm gauge length and 8.1 x 10⁻⁵ gauge factor mechanical demec gauge. The results show a positive influence of the fibre presence on shrinkage values. Fig. 15 shows the variation of free shrinkage strains with time in the first ten days of the two extreme cases in series A. That is mix A1 (plain concrete) is compared to mix A6 (S.F.R concrete with 40 kg/m³ of fibres). The influence of steel fibres in arresting the shrinkage strains is obvious.

3.3 General Conclusions

1. The Modulus of Rupture increases with increasing fibre content. In this work increases of up to 39.5% were recorded in concrete with 40 kg/m³ fibre content.
2. The Toughness Index which is a measure of the capacity of an element to absorb energy in its post-cracking stage is increased considerably. Bearing in mind that plain concrete which fails on the appearance of the first crack has a toughness index of unity, and considering the Toughness Index values recorded in this work (of up to 23.70) the benefits accruing from the presence of steel fibres in a mix, are obvious.
3. The behaviour of concrete slabs reinforced with steel fibres is superior to that of plain concrete slabs, with considerable increases in ultimate load carrying capacity. In this work concrete slabs with steel fibres at a rate of 40 kg/m³ exhibited an increase in ultimate load of 88%.
4. The failure mode of concrete slabs reinforced with steel fibres differs from that of plain concrete, in that failure is the result of a larger number of smaller magnitude (crack width) cracks.
5. Free drying shrinkage is another property that benefits from the presence of fibres with shrinkage strains decreasing with increasing fibre percentages.
6. The presence of fibres especially at high percentages causes workability problems which must be overcome by a balanced mix design, by the use of a higher proportion of smaller maximum size coarse aggregates and by means of plasticizers. In this work it was established that for laboratory purposes the V.B. test is the best means for assessing workability since the more widely used slump test may yield erroneous results.
7. In S.F.R. concretes the use of a high proportion of coarse aggregates of small maximum size (10mm) is a must. This is so because high proportions of the larger maximum size aggregates (20mm) hinders the performance of the steel fibres, not allowing them the

necessary space to be distributed evenly and uniformly in the mix. The effectiveness of steel fibres is very much dependent on the existence of the necessary amount of paste to be embedded in, and hence the need for higher cement factors is necessary. Furthermore coarser sands must be used so that the "water demand" of the sand is kept to a minimum. In this work coarse sand was used and mixes containing 50% of 10mm

maximum aggregate size were found to be superior than mixes with 30% of 10mm maximum aggregate size. Obviously the use of 100% of 10mm maximum aggregate size would yield still better overall results. However it was thought that using the 50% figure as the top ceiling for 10mm aggregates would sacrifice some of the performance but with some benefits in the overall cost of production of S.F.R. concrete.

Table 1 Materials

Material	Information
Cement	Ordinary portland Cement
Fine Aggregate	Crushed Sand (Diabase) of coarse grading Specific gravity = 2.69
Coarse Aggregate	Crushed Stone (Diabase) Series A: 70% 20mm Max. Size 30% 10mm Max. Size Series B: 50% 20mm Max. Size 50% 10mm Max. Size. Specific Gravity = 2.55
Steel Fibres	Dramix fibres with hooked ends d = 0.55 mm l = 40 mm
Admixtures	A plasticizer at a rate of 150 ml per 50 kg. cement
Mix Proportions	1:2:3/0.6

Table 2 Mix Details and 7-Day Compressive Strength

Mix	Content of Materials (kg/m ³)					V.B time (secs)	Slump (mm)	7-Day Cube strength (N/mm ²)
	Cement	Sand	C. Agg. (10mm)	C. Agg. (20mm)	Fibres			
A1	350	700	315	735	0	0	collapse	17.80
A2	350	700	315	735	20	1.5	100	17.40
A3	350	700	315	735	25	4	25	19.60
A4	350	700	315	735	30	6	10	18.80
A6	350	700	315	735	40	10	zero	18.50
B1	350	700	525	525	0	1	collapse	22.00
B2	350	700	525	525	20	2.5	80	23.70
B3	350	700	525	525	25	5	10	21.80
B6	350	700	525	525	40	10	zero	21.00

Table 3 Flexural Strength and Toughness Index (Prisms)

Mix	7-Day Flexural Strength (N/mm ²)	Percentage Increase in flexural strength w.r.t. plain Concrete	Toughness Index
A1	3.15	-	-
A2	3.33	6%	16.00
A3	3.60	14.5%	15.85
A4	3.60	14.5%	17.50
A6	3.70	17.5%	19.00
B1	3.30	-	-
B2	3.68	11.5%	18.80
B3	4.05	22.5%	20.80
B6	4.60	39.5%	23.70

Table 4 First Crack and Ultimate Load of slabs

Mix	First Crack Load (KN)	Ultimate Load (KN)
A1	22.5	22.5
A2	25.0	30.0
A3	26.5	32.0
A4	27.0	34.0
A6	29.0	38.0
B1	28.4	28.4
B2	31.5	37.0
B3	34.0	42.0
B6	38.0	53.3

Table 5 Influence of fibre Content on First Crack and Ultimate Load of slabs

Fibre Content kg/m ³	Percentage Increase with respect to plain concrete	
	First Crack Load	Ultimate Load
Series A		
20	11%	33%
25	18%	42%
30	20%	51%
40	29%	69%
Series B		
20	11%	30%
25	20%	48%
40	34%	88%

Table 6 Comparison between performance of Series A and Series B slabs

Mixes	Fibre Content kg/m ³	Percentage increase in First Crack and Ultimate Loads in Series B slabs w.r.t. corresponding Series A slabs	
		First Crack Load	Ultimate Load
B2 Vs A2	20	26%	23%
B3 Vs A3	25	28%	31%
B6 Vs A6	40	24%	40%

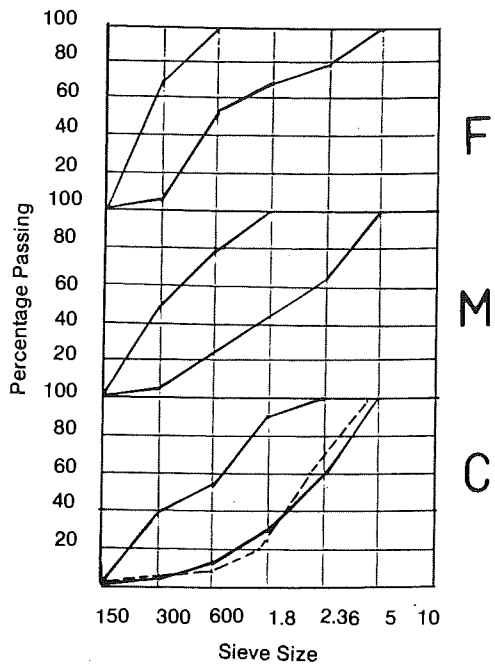


Fig. 1 Sieve Analysis of Sand.

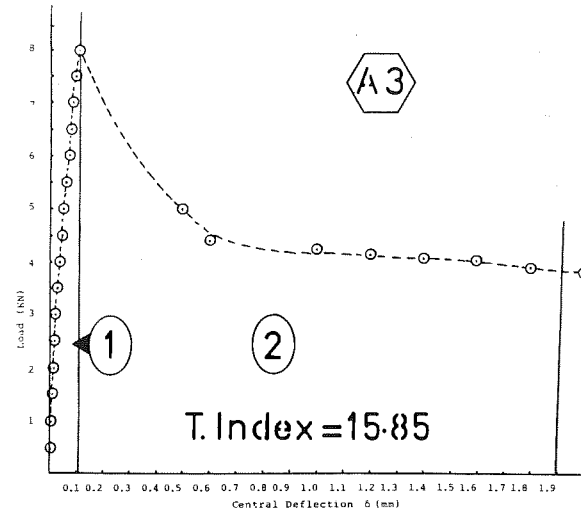


Fig. 4 Load-Deflection (mix A3)

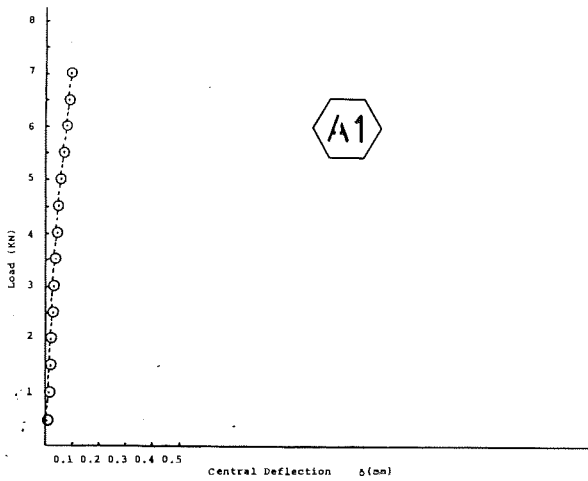


Fig. 2 Load Deflection (mix A1)

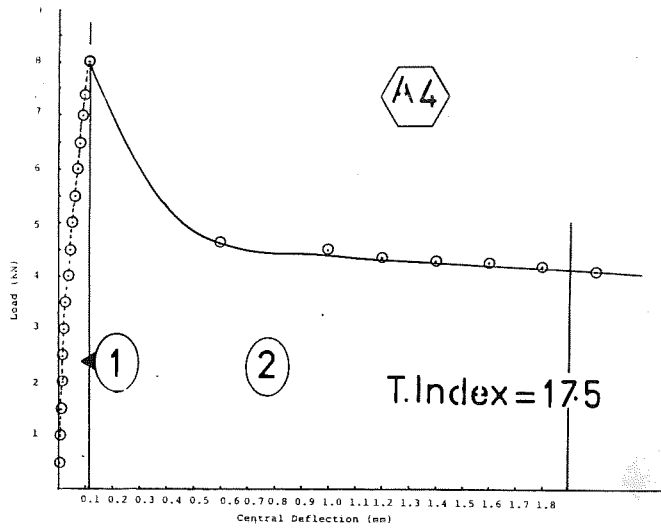


Fig. 5 Load-Deflection (Mix A4)

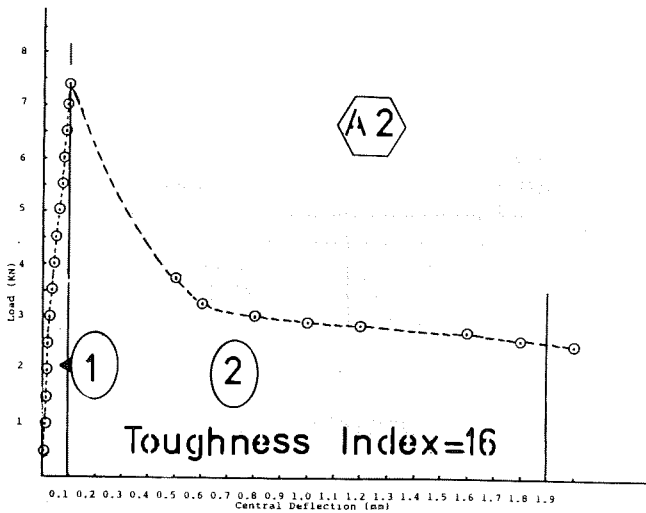


Fig. 3 Load-Deflection of (Mix A2)

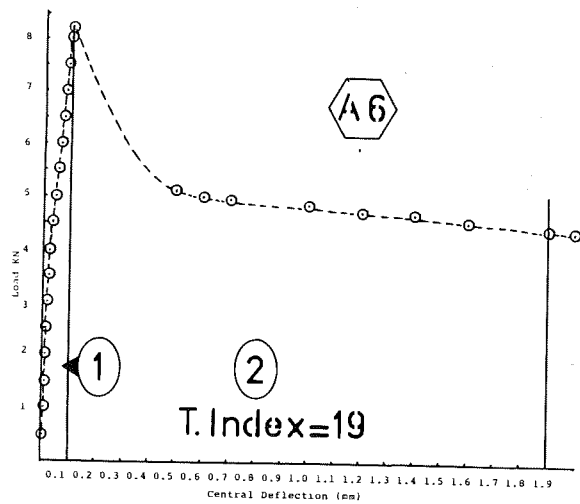


Fig. 6 Load-Deflection (Mix A6)

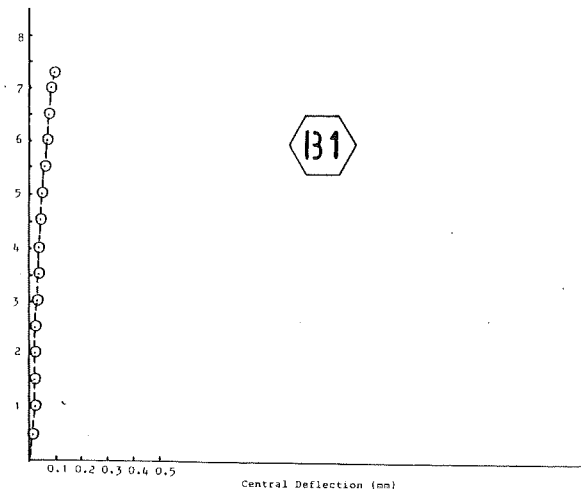


Fig. 7 Load Deflection (Mix B1)

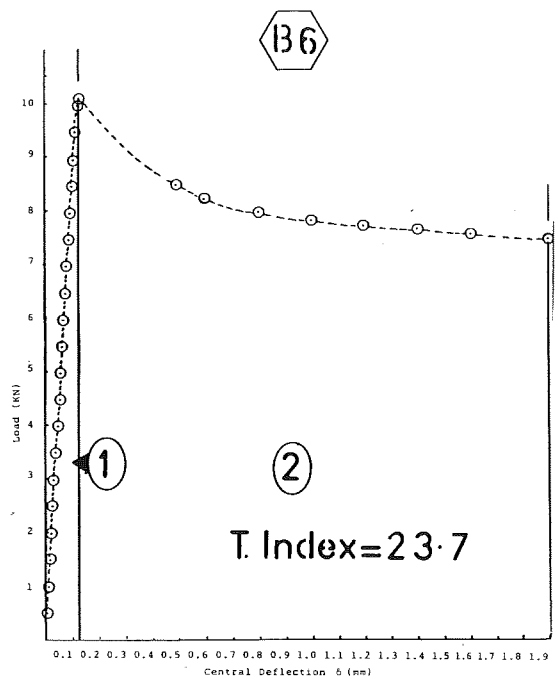


Fig. 10 Load-Deflection (Mix B6)

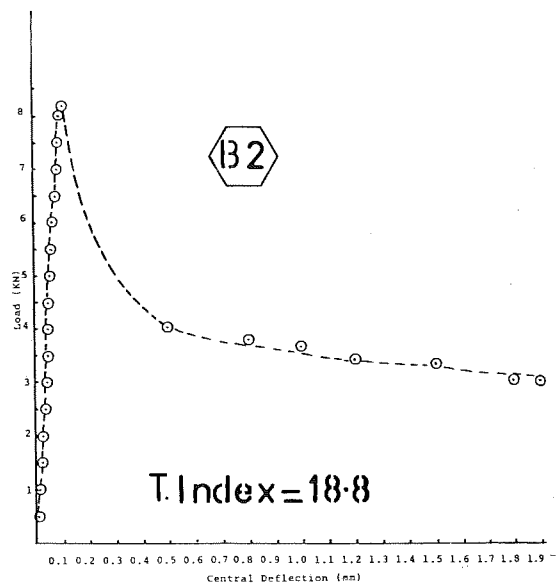


Fig. 8 Load - Deflection (Mix B2)

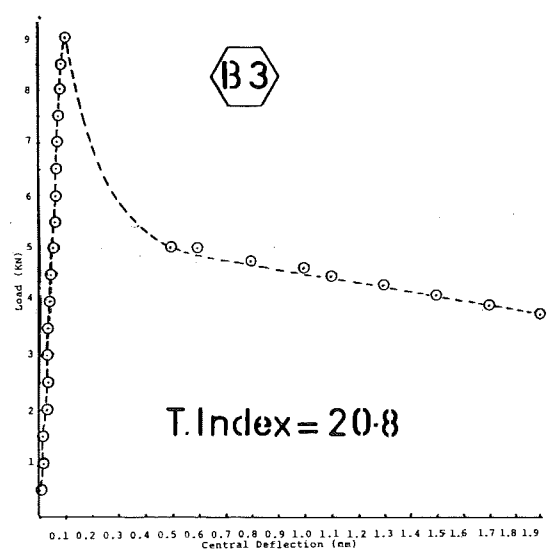


Fig. 9 Load - Deflection (Mix B3)

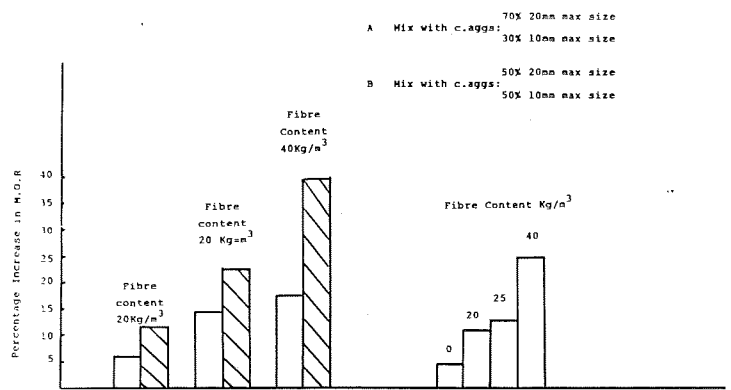


Fig. 11a Percentage Increase in M.O.R. w.r.t plain concrete. Fig. 11b Percentage Increase in M.O.R. w.r.t. A series Central Deflection δ (mm)

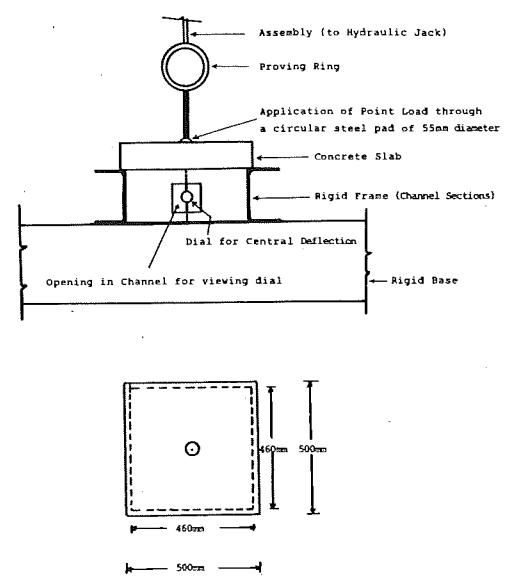


Fig. 12 Test Set-up for Slabs

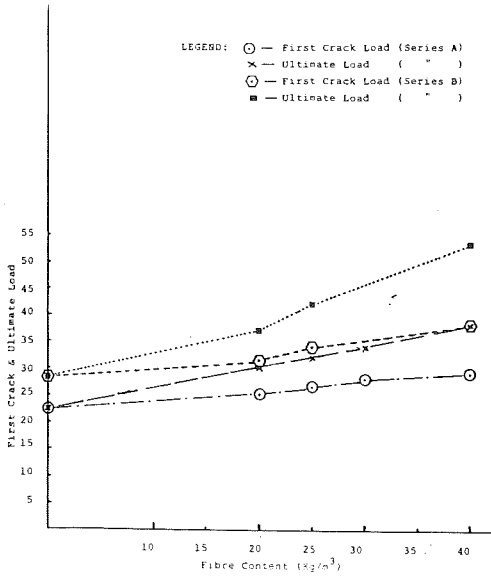


Fig. 13 Influence of Fibre Content on First Crack and Ultimate Loads.

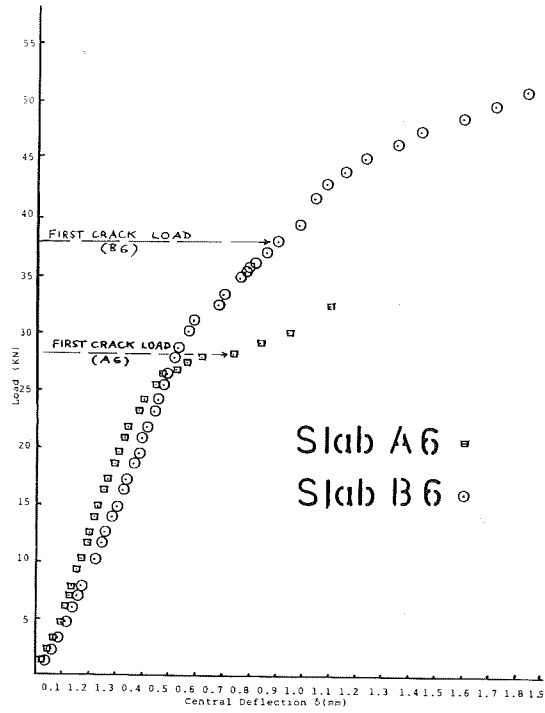


Fig. 14 Load - Deflection (slabs)

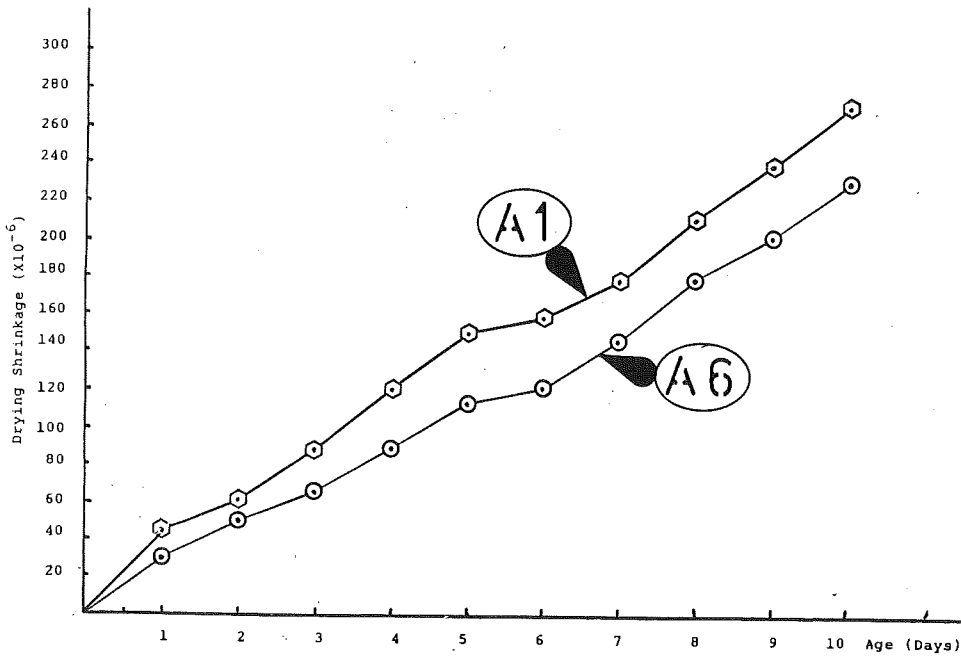


Fig. 15 Influence of Fibres on Drying Shrinkage

UNIMASTER

Η ΣΠΟΥΔΑΣΤΙΚΗ ΕΓΓΥΗ

Τα έχετε όλα προβλέπει για τη μόρφωση του;

UNIMASTER της Universal Life,
το σχέδιο σπουδών
που εξασφαλίζει τα χρήματα
για τη πανεπιστημιακή μόρφωση
του παιδιού σας,
δεν είναι αν συμβεί.

Teia + Pavia

Για να σας δώσουμε περισσότερες πληροφορίες
για το Σχέδιο Σπουδών UNIMASTER και ένα δωρεάν βιβλιόριο «Σπουδαστικός Οδηγός», χωρίς καμιά υποχρέωση,
παρακαλούμε συμπληρώστε και στείλετε το κουπόνι αυτό, στη διεύθυνση, Universal Life, Τ.Κ. 1270 - Λευκωσία.

Όνομα Γονιού _____ Ημερ. Γεννήσεως _____

Όνομα Παιδιού _____ Ημερ. Γεννήσεως _____

Διεύθυνση _____

_____ Τηλέφωνο _____



Acoustoelectronic and Acousto-optic devices for signal processing in real time

Prof. Y. V. Gulyaev
Member of the Academy of
Sciences of USSR

INTRODUCTION

Microwave signal processing in real time, if performed by digital methods, requires, as a rule, the speed of a computer capable of 1 billion operations per second and more. This is very difficult even for the most modern supercomputers and for computers on the board it is so far impossible. In many cases these problems can be solved by analog devices, based on the use of acoustic waves, acoustoelectronic and acousto-optic devices. This brief article reviews relevant work carried out in the USSR over the past twenty five years or so.

1. Surface Acoustic Wave (SAW) Devices

Acoustoelectronic phenomena connected with surface acoustic waves (SAW) have been studied in the USSR for the last 25 years, ever since 1964, when Prof. V.I. Pustovoi and the author showed that SAW can be amplified by supersonic drift of electrons in a similar manner

to bulk acoustic waves. In that work of 1964 we also suggested the use of a layer-structured piezoelectric semiconductor where SAW amplification occurs from one layer to the next due to SAW interaction with the supersonic drift of electrons in the adjacent semiconductor layer. The best amplifier based on this principle and made in IRE Ac. Sci. USSR is shown in fig. 1. At the frequency of 200 MHz the "pure" amplification of a radiosignal is 35 db. Other characteristics make these amplifiers inferior to transistor amplifiers and are not therefore in general use. However, they may be successfully used for amplification of SAW themselves in complex information processing circuits using SAW.

As it often happens, this interesting effect of SWA amplification led to many further acoustoelectronic investigations but the main achievements of acoustoelectronics have been in one direction - that of creating "passive" SAW devices. In the USSR the following outstanding

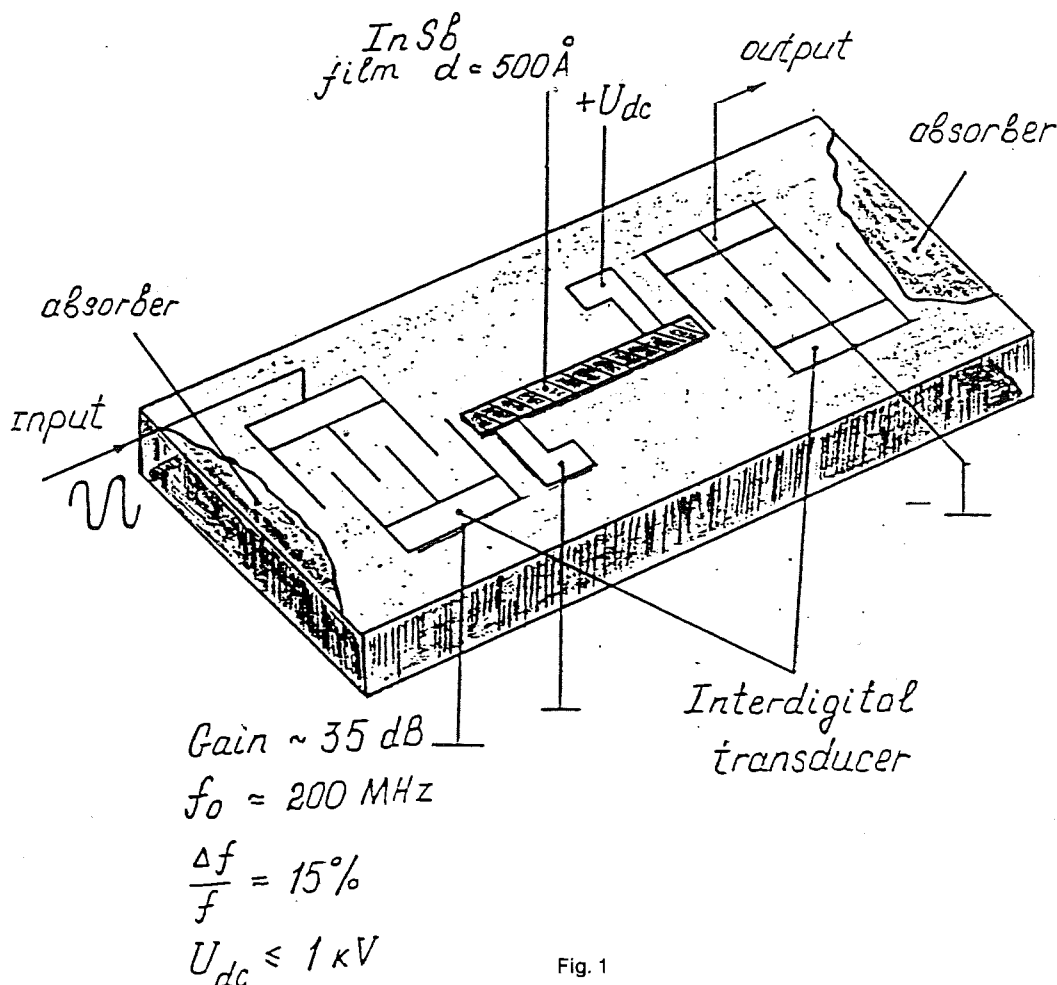


Fig. 1

contributions have also been made: discovery of new types of SWA - shear SAW in piezoelectrics (independently from J. Bleustein, USA), "gap" SAW, the prediction (independently from Auld et al., USA) of shear SAW from a periodically corrugated surface of a solid and investigation of the transverse acoustoelectric effect (where the electromotive force is perpendicular to the surface along which SAW propagates), suggestion of new types of interdigital transducers, etc. Many types of acoustoelectronic (AE) devices (filters, delay lines of different kind, etc.) are now under mass production in the USSR as well as in other countries. More complicated devices such as convolvers, correlators, fast fourier transformers etc. are ready for mass production. The advantages of SAW - processors is their high speed, small size, low power and low cost. The main disadvantage of SAW devices as analog devices is their comparatively low accuracy - which is usually of the order of 1%.

Typically, AE Fourier transformers with dispersive delay lines for processing of the signal can provide speeds of the order of $5 \cdot 10^9$ multiplication operations per second. This substantially exceeds the limiting speed of digital devices ($2 \cdot 10^7$ now and $5 \cdot 10^9$ in foreseeable future).

To improve signal processing for systems employing SAW, combined systems are

developed which use SAW devices in combination with digital techniques. Now SAW-devices are widely used in consumer goods (TV sets, EM radios etc.), industrial production, etc. Oncoming application areas of SAW-devices are new TV networks, including satellite TV, telecommunications, including movable telephone instruments, marking and recognition of objects, SAW sensors of various physical quantities etc. The appearance on the market of high quality SAW-components is forcing manufacturers of radio equipment to change the architecture of many radioelectronic systems.

The efforts of scientists now are directed towards improving the main SAW devices characteristics - reduction of insertion losses, widening of frequency bands, improvement of delay time and dynamic range etc. and to invention of new kinds of SAW devices including those where the interaction of SAW with electrons is used.

One example of an improved SAW device is the SAW-resonator using shear SAW on a periodically corrugated surface (see fig. 2). The Q factor here is 10.000. In the device of fig. 3 another new kind of shear SAW is used - shear SAW which can exist on the boundary of a solid with a viscous liquid. Such SAW are very convenient to use as sensors of liquids and biological objects.

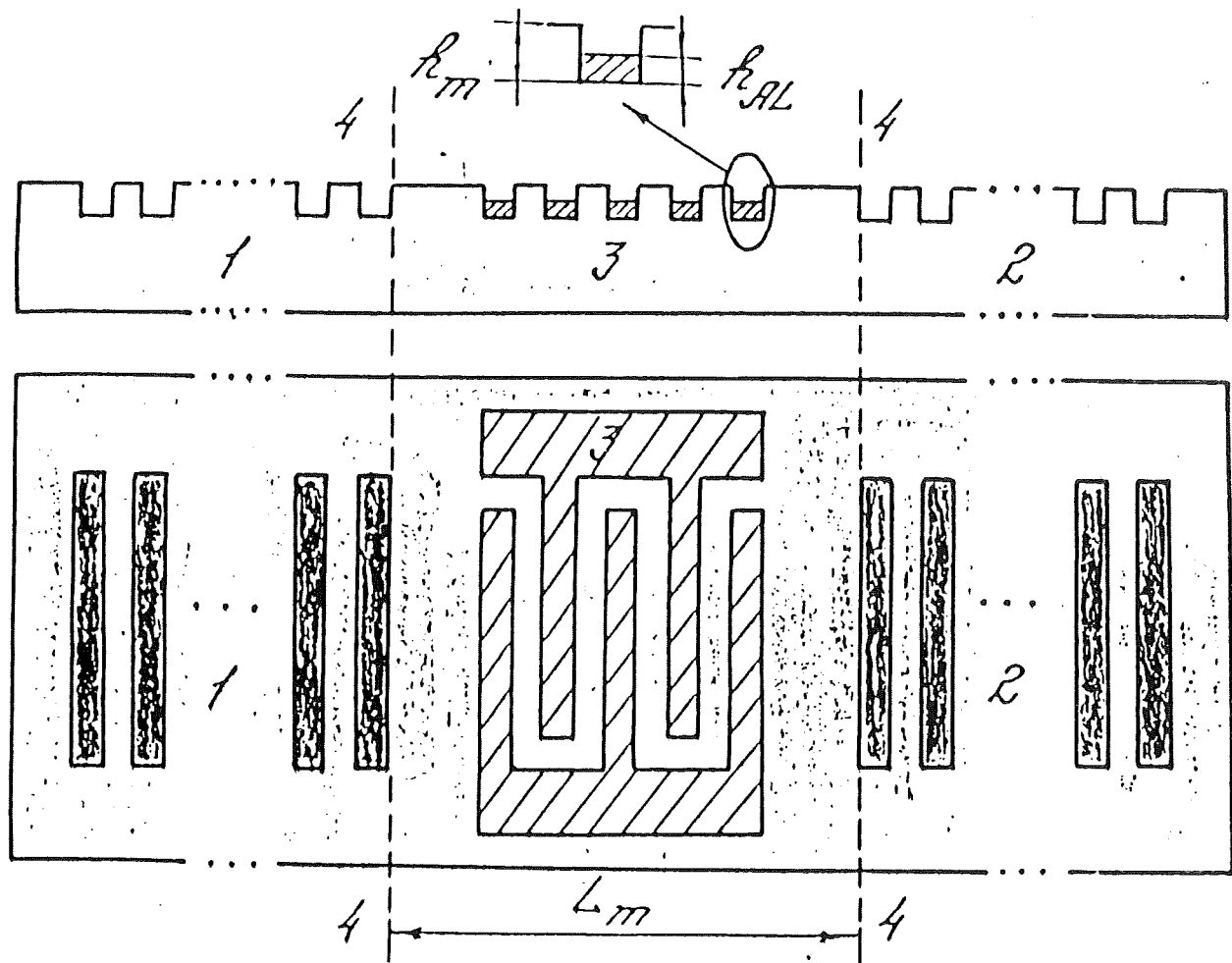
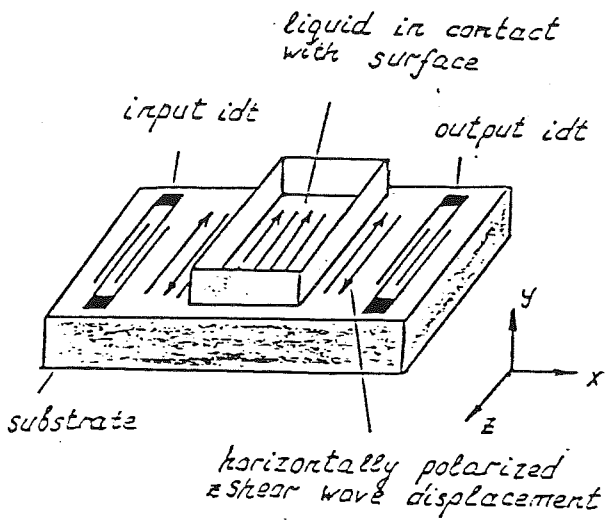


Fig. 2

Shear surface waves on solid/liquid interface



$$U = U_0 \cdot \exp(\alpha y + i q x)$$

$$\alpha = \frac{1+i}{\sqrt{2}} \frac{\omega \cdot \rho_e}{c} \sqrt{\omega \cdot \eta}$$

η - viscosity

Fig. 3

The effect, first predicted and studied by Professor Eric Ash, of bulk acoustic waves transforming into SAW on a periodic grating was used by us to predict and explain the phenomenon of 100% transmission of acoustic waves through the vacuum gap between two piezoelectric crystals, if the edges of the gap are periodically corrugated, (see fig. 4). Under resonance conditions the excited SAW amplitude of the incident wave and by its electric field this SAW excites SAW on the other side of the gap. In the experiment the losses were a few db and a rather narrow band filter was created.

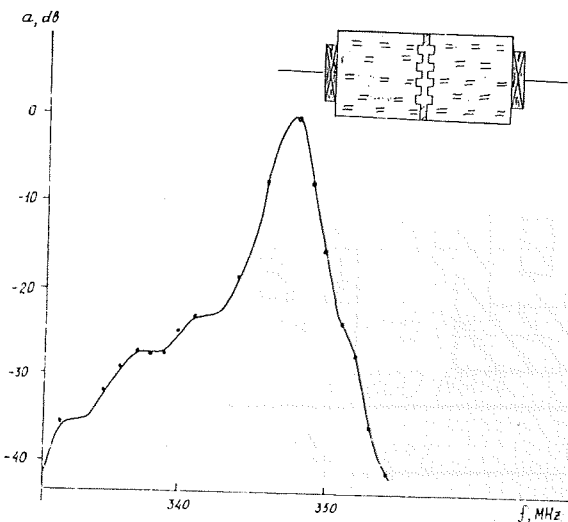


Fig. 4

Fig. 5 illustrates AM or FM demodulators based on longitudinal and transverse acoustoelectric effects. Their characteristics by some parameters are better than in conventional demodulators. On Fig. 6 different kinds of convolvers are shown including one, (c), based on the change in resistivity of a semiconductor film by the acoustic waves. Earlier on this principle we had predicted a new kind of transistor - the acoustoinjection transistor where the drift of electrons caused by acoustic waves is used instead of ordinary diffusion. Finally, on fig. 7 new constructions of interdigital transducers with capacitive tap-weighted electrodes suggested in USSR are shown, which allow one to create acoustoelectronic devices with very high performance.

2. Acousto-optic Devices for Processing Analog and Digital Information

A very fast developing branch of acousto-optics (AO) is optical methods of signal processing with the use of special acousto-optic modulators (AOM) of light both for analog and digital systems. For a typical AOM which is able to store $N=f \cdot T_0 = 10^3$ states during time $T_0 = 10 \mu s$ ($f = 100$ MHz) the calculated speed of one channel optical correlator with such an AOM is of the order

$$S = \frac{N^2}{T_0} = (f)^2 \cdot T_0 = 10^{11} \text{ analog multiplications}$$

or addition operations per second. For a multichannel case this speed can go upto 10^{15} operations per second. The most interesting feature of AO processors is that they perform convolution multiplication as the basic operation, which is usually necessary in radioelectronic problems.

The AO spectrum analysers are well known (see fig. 8). The best devices todate can process signals with $T_0 = 1 \mu s$ and $f = 16$ MHz and work in the frequency range 2-36 MHz with a high frequency resolution of = 2-5 MHz in the dynamic range.

The AO convolution devices are based on the fact that signal "image" in AOM moves with acoustic wave velocity (see fig. 9). These devices to-day solve many radar technique problems, such as compression and reversal in time of microwave pulses, delay, matched correlation filtration and spectral analysis of a signal, determination of the uncertainty function of pulse signal etc. One must note that in the case of convolution with temporal integration the integration time, T, can be much longer (by one hundred times) than in the case of spatial integration. Modern AO correlators with temporal integration reach spectral resolution of = 30 Hz (with spatial integration - 30 kHz). The effective calculated speed here is $S \approx 10^{12}$ operations per second.

AO processors can also perform discrete mathematics, for example carry out algebraic calculations of the type: scalar multiplication, vector on vector, vector on matrix, matrix on matrix etc. An AO processor for multiplication of a two-dimensional vector on a 2 x 2 matrix is

AE-demodulators

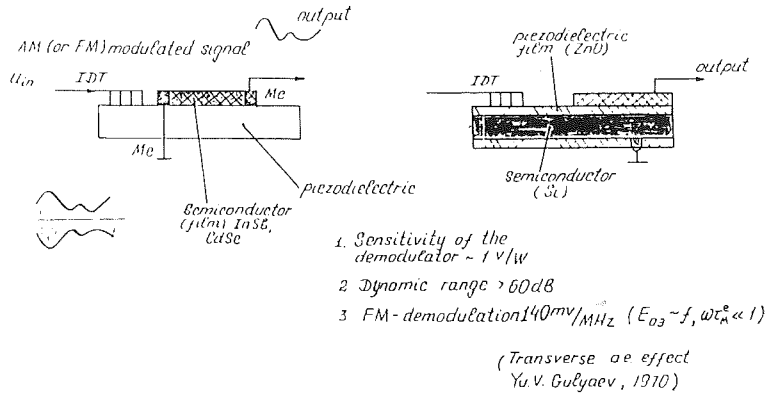


Fig. 5

AE-converters

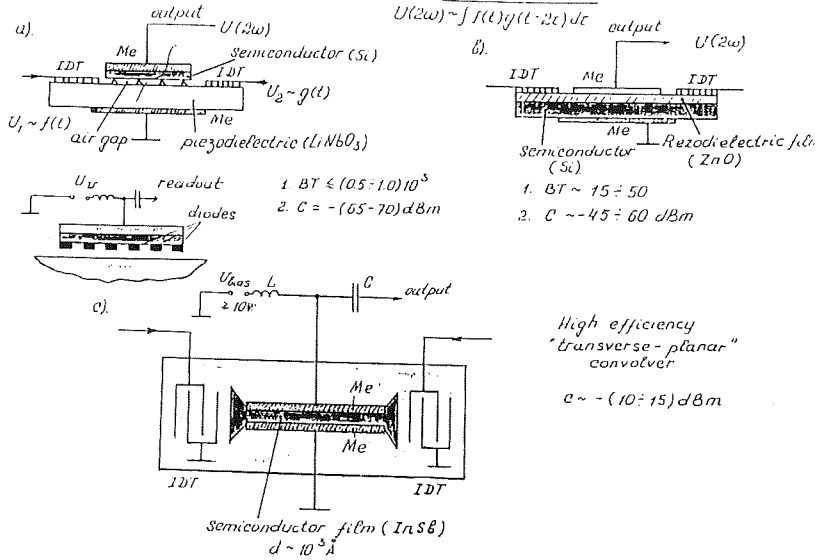


Fig. 6

Capacitive tap-weighted interdigital transducers

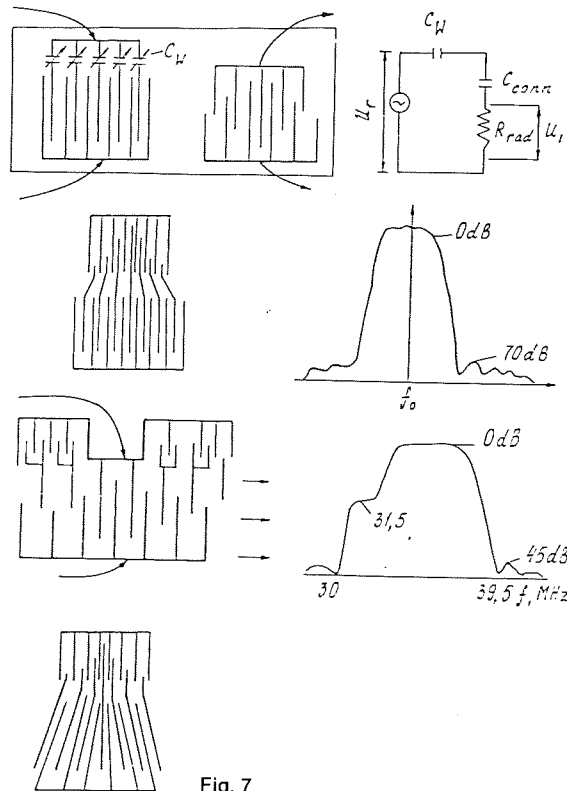


Fig. 7

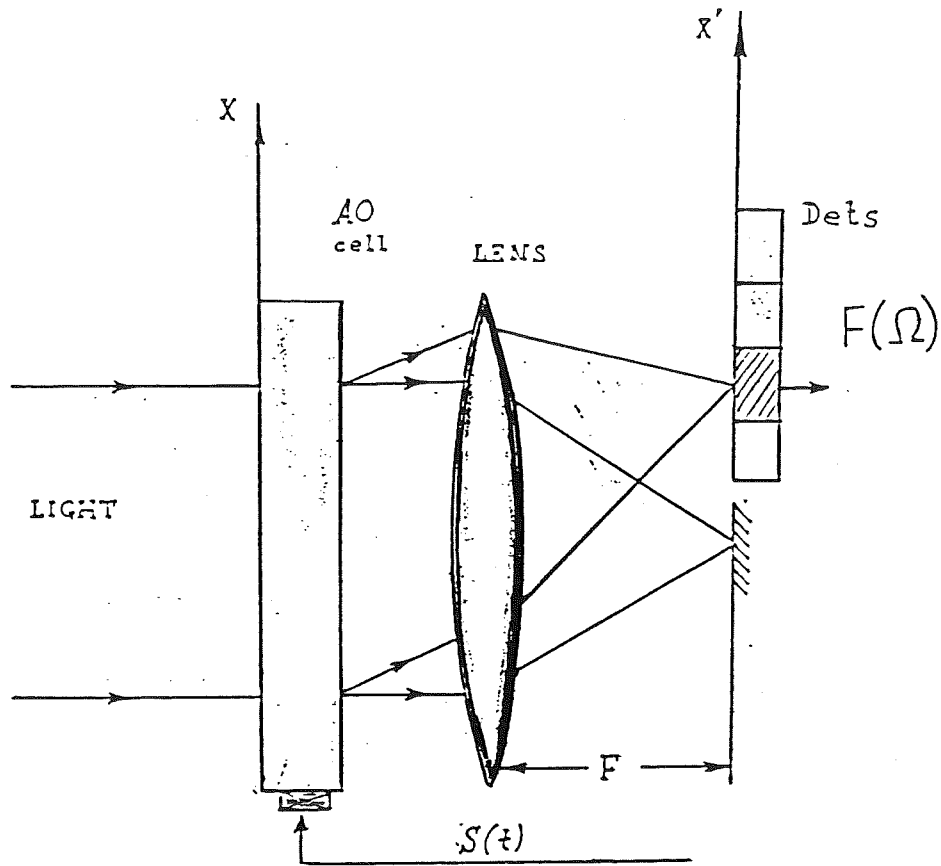


Fig. 8. Schematic diagram of AO spectrum analyzer with space integration

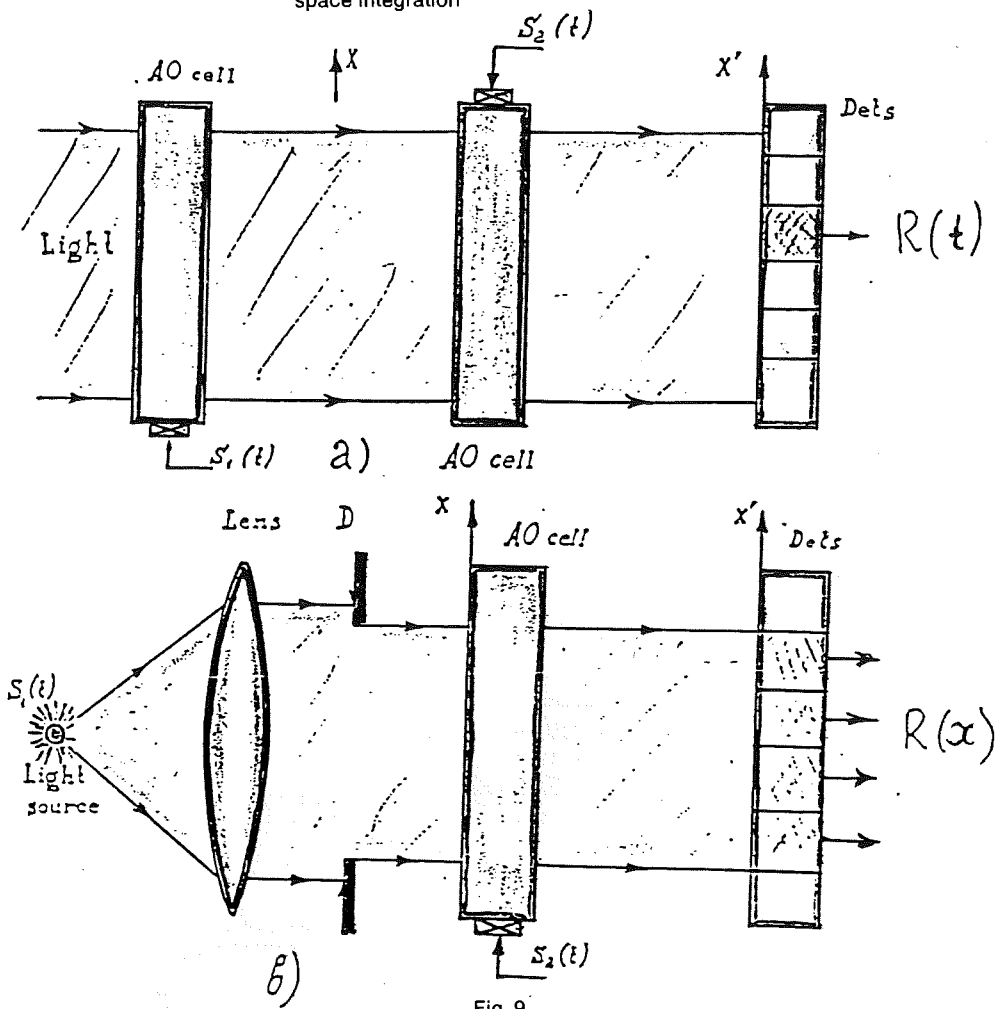


Fig. 9

shown in Fig. 10.

The maximum speed of such a multiplier can be also 10^{12} operations per second.

All AO processors considered above are analog processors, thus their accuracy is usually no more than 8-10 binary digits. To increase the accuracy of AO processors (of course, unfortunately, at the expense of speed!) the analog method of digital multiplication via discrete convolution has been proposed. The principle of it is illustrated in fig. 11. Assume two denary numbers 23 and 25 are to be multiplied to obtain the result 575. If we shall use the binary numerical code one needs to obtain AO convolution for the binary sequences 10111 and 11001 which is possible to do in the scheme of two AOM with two RF acoustic signals modulated consequently by the related

sequences and propagating in opposite directions. After light diffraction by both acoustic signals the photodetector analog output represents the mixed-binary sequence 11123111 (in the form of triangular pulses of different amplitudes) which may be binary digitized with a simple electronic (three-level) A/D conversion, summation by modulus 2 with shift to give the sequence 1000111111. The speed of calculation in such simple system for AOM bandwidth of $f=500$ MHz and N-bit numbers is $S=8 \cdot 10^6$ digital multiplications per second.

Using this principle of discrete convolution in the systolic regime, digital AO multipliers for vector-matrix and matrix-matrix multiplications with an accuracy of 16 bits and even 32 bits are created with a calculation speed of 10^8 operations per second (see fig. 12).

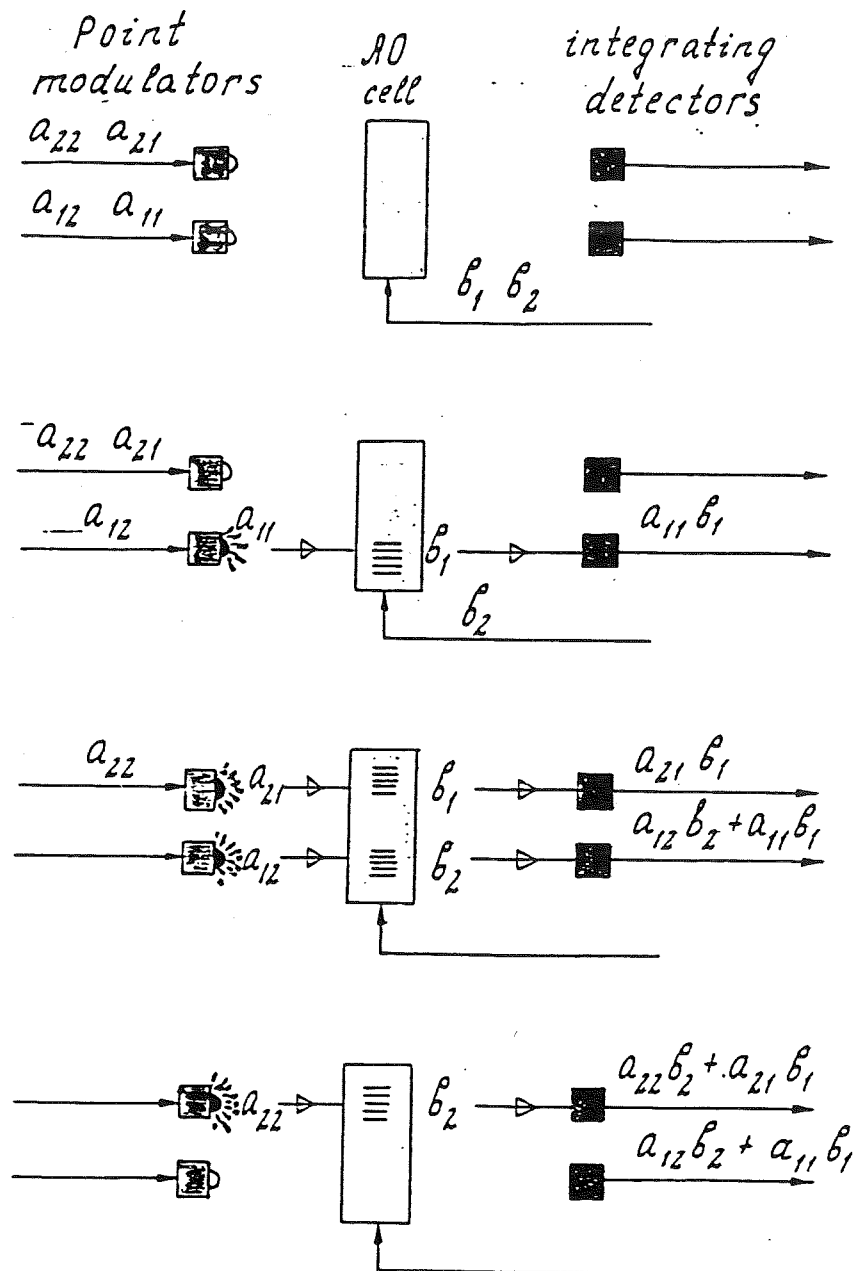


Fig. 10. Example of AO systolic vector-matrix multiplier (2x2)

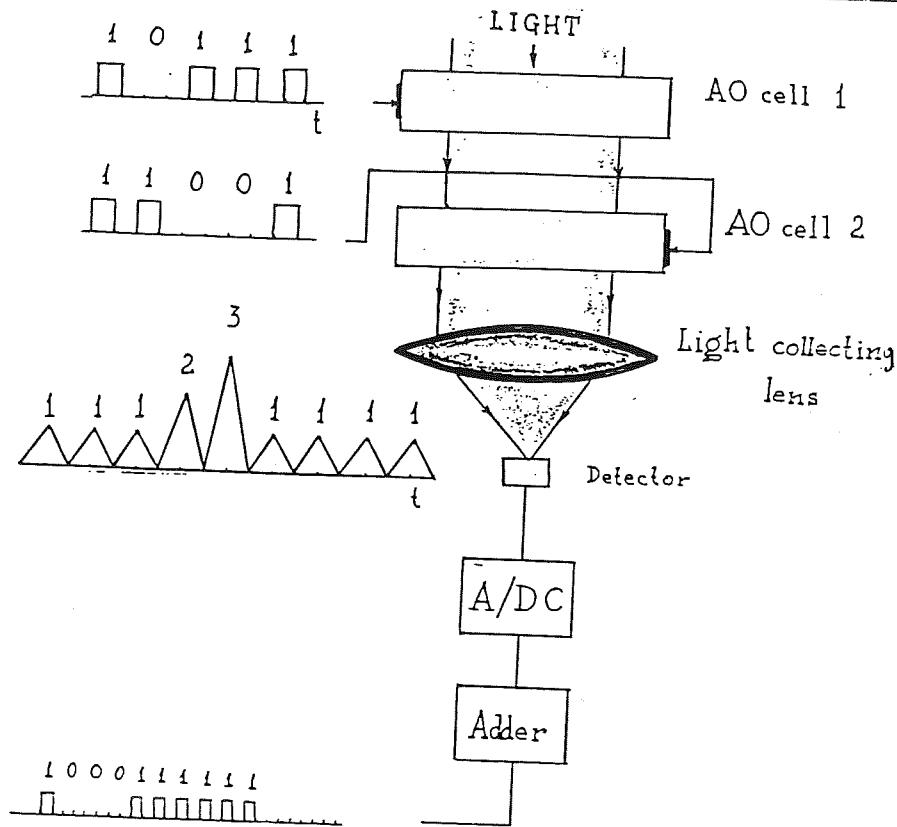


Fig. 11. Digital AO multiplier based on discrete AO convolution with two AO cells

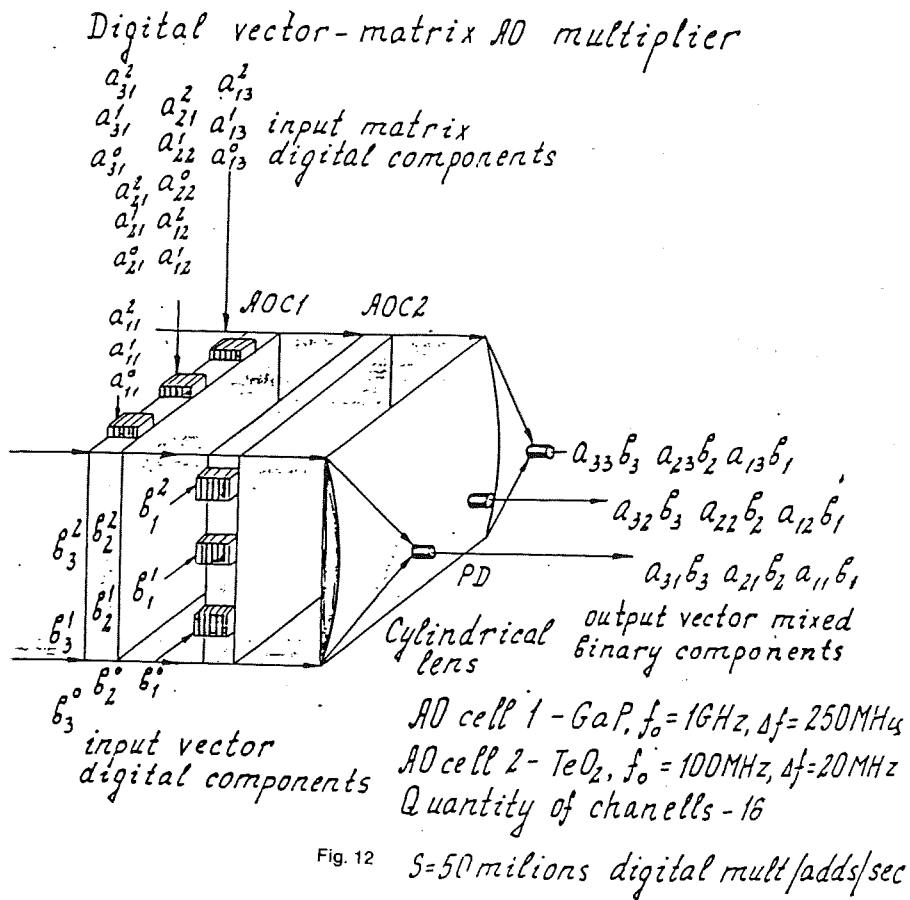
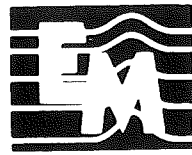


Fig. 12 Published by kind permission of Prof. Gulyaev and based on a lecture he gave to H.T.I. staff and students on the 20 December 1988.



EARTHMETRIX GEOTECHNICAL & MATERIALS ENGINEERS LTD.

OFFERING SERVICES IN:

- Geotechnical Engineering
- Soil Test Borings
- Laboratory Testing:
Soils, Concrete, Asphalt, Aggregates
- Engineering Analyses and Design Recommendations
- Construction Quality Control and Quality Assurance
- Hydrogeological Studies
- Observation/Monitoring Well Installation

TEL. 02-438023, TELEX: 2921 CIPA CY

- P.O.Box 3916 NICOSIA - CYPRUS
- OFFICE: 4 EKATERINES KORNAROU
AGLANTZIA, NICOSIA 123, CYPRUS

Comparative tests on plain, steel fabric reinforced and steel fibre reinforced concrete ground floors

*Derrick Beckett, Head of School of Civil Engineering,
Thames Polytechnic, Dartford, Kent, England*

The merits of the use of plain concrete, steel fabric and steel fibre reinforced concrete for industrial ground floors have been the subject of considerable debate and the Concrete Society Technical Report No. 34⁽¹⁾ refers to the increasing use of steel fibre reinforced ground floors on the Continent and their introduction into the U.K. Increasing static loads arising from rack loading and dynamic loads have necessitated the more frequent use of the thickness design principle⁽²⁾⁽³⁾ that is, an adequate thickness of floor is required to withstand induced tensile stresses. It has generally been assumed that:

- (a) The use of steel fabric reinforcement does not increase the flexural capacity of the slab, but has the primary function of crack control
- (b) The slab depth is related to the flexural strength of the plain concrete.
- (c) If steel fibres are introduced, the flexural capacity of the concrete is increased and that this will allow a reduction in slab depth approximately proportional to the square root of the strength gain.

The purpose of this paper is to report and comment on the first stage of a test programme aimed at rationalisation of the thickness design principle applied to plain, steel fabric reinforced and steel fibre reinforced concrete ground slabs. The programme is sponsored by N.V. Bekaert S.A., Belgium and the tests are being carried out by the School of Civil Engineering, Thames Polytechnic, Dartford. This programme is an extension of a test programme undertaken by Sir Frederick Snow and Partners⁽⁴⁾ in conjunction with Imperial College. The tests at Imperial College were on 1.0m square simply supported slabs with a concentrated load applied at the centre. It was concluded that a reduction in slab depth can be achieved by the introduction of steel fibres. However, it was considered necessary to extend the test programme to compare the performance of slabs on ground. The first stage of the extended test programme has now been completed. It relates to 3.0m x 3.0m slabs, 0.15m deep loaded centrally via a 100mm x 100mm steel plate, see Figs(1) and (2). Three slabs were tested - plain, steel fabric reinforced and steel fibre reinforced with a specification as follows: Concrete grade 40, cement content 325 kg/m³ water/cement ratio 0.55. Steel fabric reinforcement A142 (pitch 200mm, bar diameter 6mm) cover 25mm from top of slab, characteristic strength 460 N/mm².

Dramix steel fibre reinforcement ZC 60/0.8, characteristic strength 1100 N/mm².

The slabs were cast on a polythene membrane below which was a 150mm subbase (Darent Fill, type 2). Plate loading tests on the soil below the subgrade gave modulus of subgrade reaction of 0.030 N/mm³. The slabs were loaded hydraulically by means of a hand pump and deflections were recorded along the two centre lines at 20 kN load increments. A summary of the results is given in table (1).

Table (1)

TEST NO	SLAB	LOAD AND FIRST VISIBLE CRACK kN	LOAD AT FAILURE OR MAXIMUM ATTAINED LOAD kN
P1	PLAIN	180	200
F1	FABRIC REINFORCED	200	320
D1	DRAMIX STEEL FIBRE REINFORCED	290	345

In the three tests, the first visible cracks appeared on the 150mm vertical faces round the slab perimeter, typically as shown in Fig.(3). A small increment of load produced failure of the plain concrete slab (P1), the cracks widening and extending from the perimeter to punching zone round the loading plate, see Fig. (4). This mode of failure did not occur with slabs F1 and D1, the fabric and fibres controlling the development of the cracks through to the top surface of the slab. It is of interest to note that the load at first visible crack for slab D1 was 45 percent greater than that for slab F1 and 60 percent greater than that for slab P1.

The test programme will be continued throughout 1989 but the three tests are already indicative that:

- i) The introduction of Dramix steel fibre reinforcement significantly increases the flexural strength of the concrete. This will allow a reduction in slab depth approximately proportional to the square root of the strength gain.
- (ii) The presence of steel fabric does not make a significant contribution to the flexural capacity of the slab, but controls the development of cracks for loads in excess of the load at first visible crack.
- (iii) The application of still generally accepted theory of elastic slabs on ground (HM

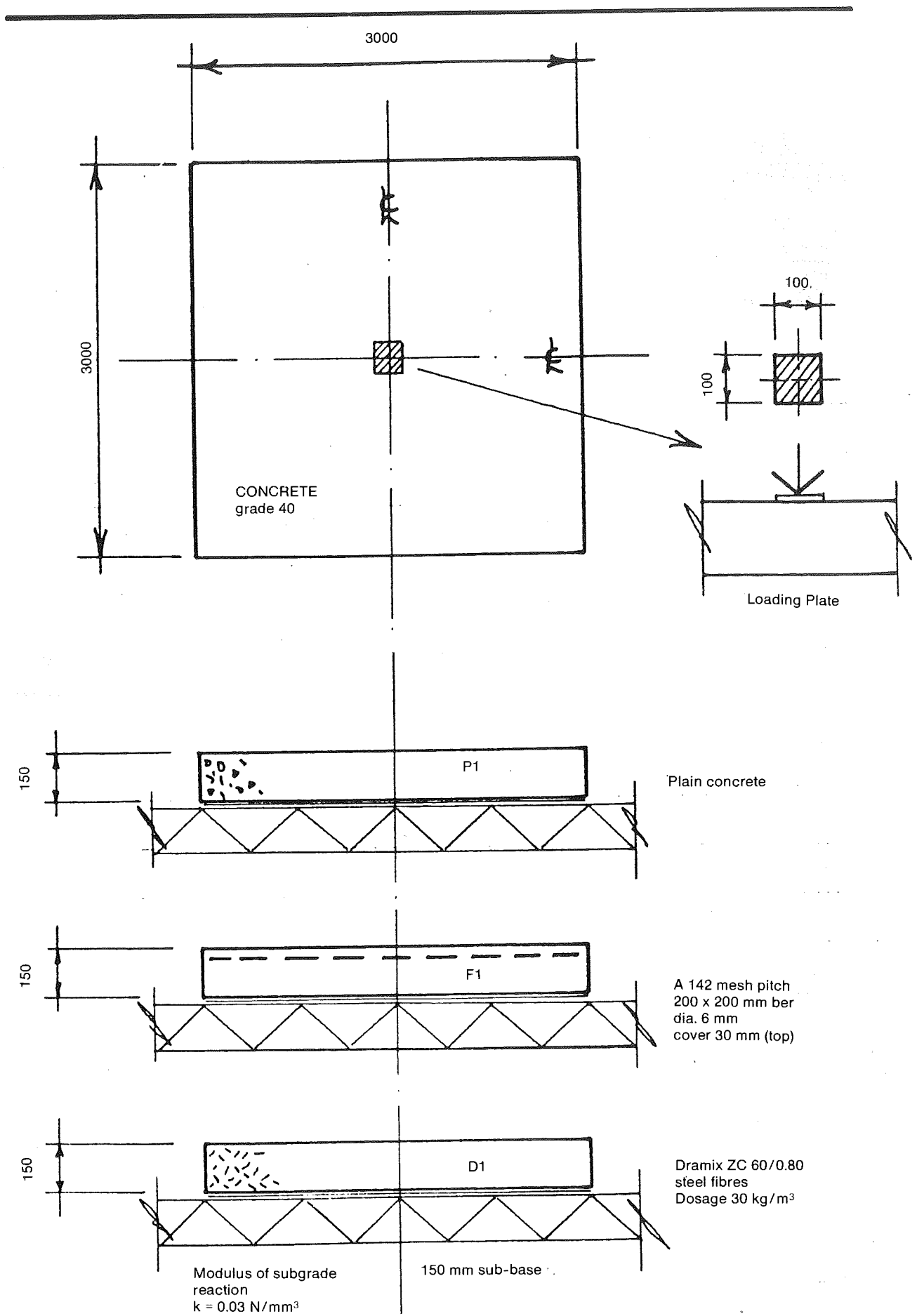


Fig. 1 TEST SLABS

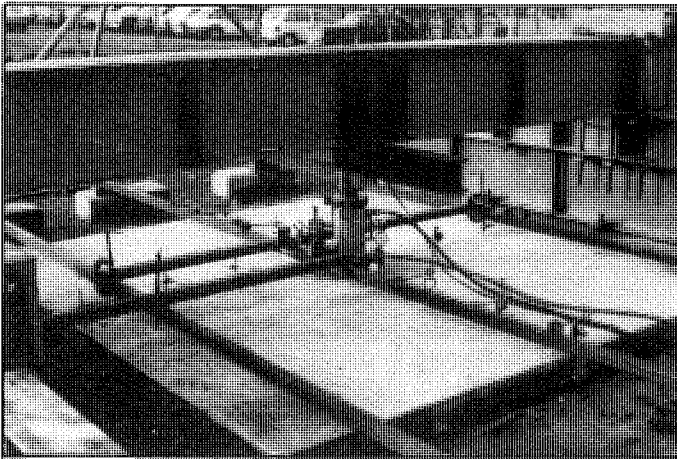


Fig. 2 Test slab showing loading arrangement

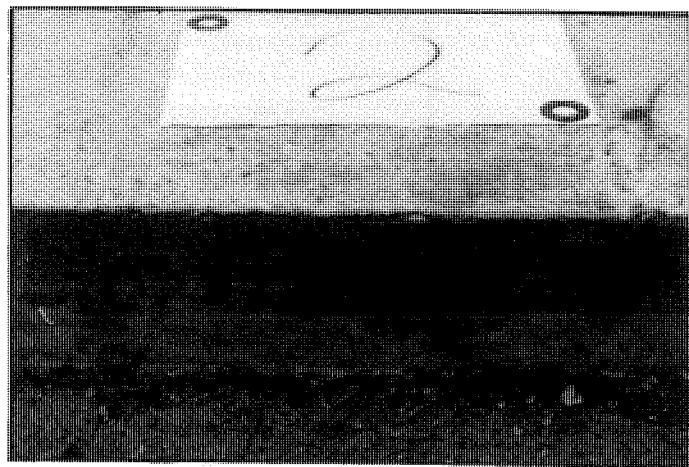


Fig. 3 Typical crack on vertical face of slab

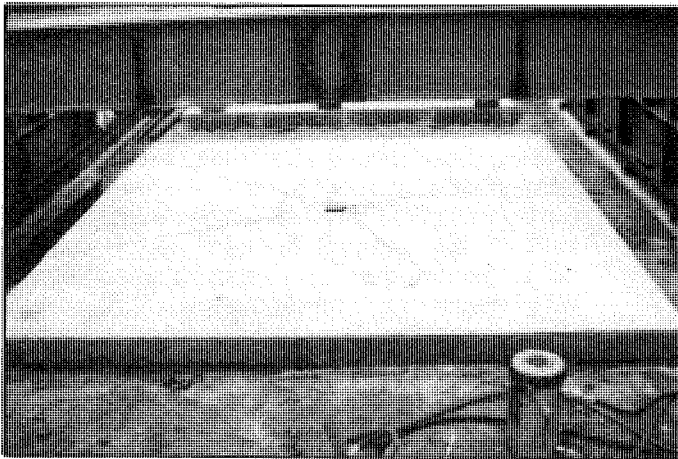


Fig. 4 Failure mode for plain concrete slab P1

Westergaard) will compute unrealistically tensile stresses unless dispersion through the depth of the slab is assumed.

The extended test programme will continue throughout 1989 and will hopefully lead to firm recommendations for the application of the thickness design method to concrete ground slabs.

The co-operation of N.V. Bekaert S.A. Belgium and the technicians of the School of Civil Engineering, Thames Polytechnic in the above test programme is gratefully acknowledged.

A further programme of work on the use of steel fibres in reinforced concrete joints to improve ductile capacity for seismic design is planned to

commence shortly. Collaboration between the HTI and Thames Polytechnic on this important development is anticipated.

References:

1. *Concrete Society Technical Report No 34, Concrete Industrial Ground Floors; The Concrete Society in association with the British Industrial Truck Association and the Storage Equipment Manufacturers Association, 1988.*
2. *Chandler JWE, Cement and Concrete Association Technical Report 550, Design of floors on ground, 1982.*
3. *Chandler JWE and Neal FR, BCA Interim Technical Note 11, The design of ground supported concrete industrial floor slabs, April 1988*
4. *Sir Frederick Snow and Partners, Report on the use of Dramix steel fibre reinforcement for concrete industrial ground floors, March 1988.*

Computer information system for the III games of the small states of Europe

*Dr Christos N. Schizas,
Lecturer HTI*

The Organizing Committee of the III Games of the Small States of Europe, in its efforts to have every possible technical facility available to the delegation officials, press correspondents, trainers and the public in general, has decided to set up a computer information system.

The computer information system had many features which gave a new dimension to the whole event. Some of these features were:

1. Complete up to the second, real time information between athletic centres, information centres and hotels.
2. Lists of participants by function, sport and event.
3. Calendar by day, time, competition site, sport and event.
4. General information about the participating countries.
5. Athletes data including previous or at the time achieved records.
6. Results by day, time, sport and event; current results showing for instance how an event or game was progressing.
7. Generation of rough printed reports for informing VIPs, press and public the progress of the games in other competition sites.
8. Generation of official reports, using desk top publishing facilities, at the end of each day.
9. Statistical results for Basketball and Volleyball at the end of each game and at the completion of all games.

Two state-of-the-art multi-user computers have been employed for receiving, processing, transmitting and storing all the data.

Computer terminals have been connected to the main computers situated at the Higher Technical Institute (HTI). Remote communication has been achieved by using MODEMS and direct telephone lines which were installed and maintained by the Cyprus Telecommunications Authority for this purpose.

The Cyprus Popular Bank provided on loan all the MODEMS which were installed and maintained by their engineers. The Cyprus Popular Bank have also donated to HTI twelve computer terminals and printers for this purpose.

A total of forty-seven leased lines were installed in all competition sites giving them this way the capability of sharing directly the computer resources, irrespective of any geographical distance.

Another thirteen leased lines, computer terminals and printers were installed in nine hotels in Nicosia. At these hotels, the press,

journalists and public were able to receive information about the Games, participation lists, time-tables, results etc. Computer printouts were also provided for the press, journalists, and Country delegations.

The computer was being fed with all the available information concerning the Games and States well in advance, giving thus the opportunity to the journalists to prepare reports and articles for the press of all the participating States.

Another dimension which was added to the system was that of live transmission of the results through the television network. Two computer terminals were installed at the Outside Broadcasting Unit of the Cyprus Broadcasting Corporation for providing a live programme with data about the Games and the athletes; the data was transmitted straight from the computer and mixed with the camera signals with a special equipment which was purchased by the Cyprus Olympic Committee for this purpose.

The analysis, design, development and installation of the computer programs for the Games has been undertaken by the Computer Department of the HTI in March 1988. Two HTI Lecturers and nine senior (third year) students have set as their target to complete and test the whole work with real data before the end of April 1989.

Even though the whole project has been divided into smaller manageable parts for allowing simultaneous and parallel development, the anticipated time for development and testing could not always be predicted, because working conditions were not very good and mainly because most of the committees (basketball, cycling, judo, shooting, swimming, tennis, track and field, volleyball and yachting) have not given the proper attention, interest and time to the development team from the beginning. Eventually at the expense of time, extra effort put by the development team and in some cases the direct involvement and interest of the Chairman of the Organizing Committee of the Games, everything which was supposed to be done was done.

The HTI in general and in particular the classes 1CS, 2CS, 3CS, 3C1, 3C2, 3E1, and 3E2 (partly) and ten members of the staff have contributed to the Computer Information Service of the games by undertaking duties such as supervisors, data entry operators, enquiry operators and report distributors during the Games.

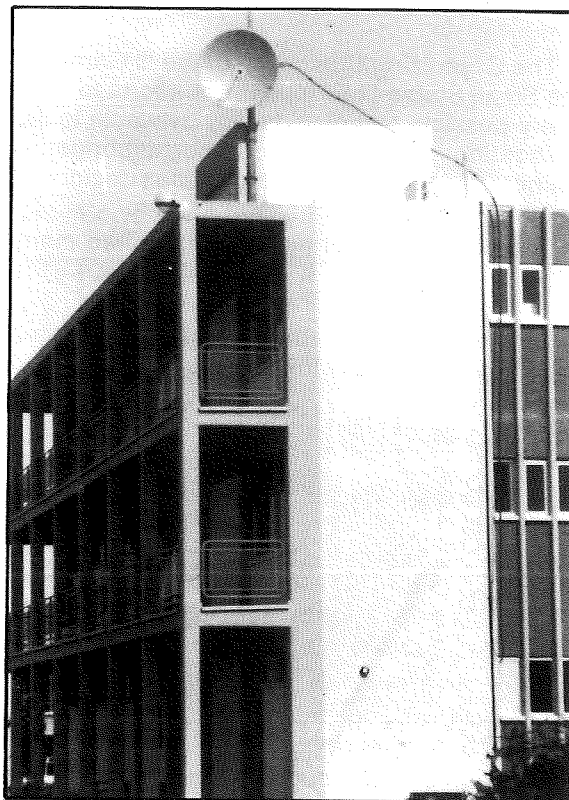
Computer Information Service Team:

Christos Schizas - Project Manager
Viatseslav Rahmatoulin - Software Development
Leader

Development Team (Students) - Athena
Constantinou, Mary Sophocleous, Katerina
Lazarou, Antonis Theodosiou, Tasos Nathanael,
Constantinos Sophocleous, Costas Genethlis,
Costas Potamos, Savvas Lopez



The HTI Vax machines with the CYTA leased lines exchange and MODEMS.



The microwave dish connecting HTI and CYTA.



The computer system Development Team.

BRIDGEHOUSE

BOOKSHOP & STATIONERS

OLON PAPACHRISTODOULOU

BRIDGEHOUSE BLDG., BYRON & GRIVAS DIGENIS AVE. TEL 43297, P O Box 4527
NICOSIA - CYPRUS

International Collection of:

Newspapers & Magazines
School, Language & Literature Books
Technical, Science & Art
Cooking, Housekeeping & Decoration
M & E, Time-Life & Teach Yourself Books
Penguin, Pelican, Pan, Fontana, Gorgi e.t.c.
Chess, Tennis, Bridge & Other Hobbies
Stamps & Coin Collecting Books
Ladybird & Other Children Books
Dictionaries & Reference Books
Books & Model Answers for G.C.E.
Past Examination Papers for G.C.E. L.C.C. e.t.c.
Touring Maps & Guides
School Stationery, Handbags e.t.c.
Office Stationery & Account Books
Office Equipment & Filing Systems
Typing & Duplicating Materials
Envelopes of all Kinds & Sizes
Fountain & Ball Pens
Autographs & Address Books
Drawing & Art Instruments
Albums for Photos, Stamps & Coins
Educ. Toys & Handcraft works
Cards for All Occasions
Christmas Decorations & Candles
Gift Wrapping Papers & Decorations

IT IS OUR PLEASURE TO SERVE YOU

**Books & items not in stock
can be ordered for you**

Concrete pumping and associated problems

Andis D. Ioannides

BSc (Hons), MSE, MIAP, MASCE

When the subject of concrete pumps, their use and economical application is dealt with, the question has to be answered beforehand what requirements will have to be complied with to enable a trouble - free operation of the pump.

A trouble - free concrete pumping is only possible if the concrete can be pushed through a pipeline. This type of concrete is called pumpable concrete. Such concrete must fulfill the following requirements:

The composition of the pumpable concrete must produce adequate lubricating components to maintain a constant lubricating film on the interior walls of the pipeline. Moreover, the concrete must contain ample reserve of lubricating means to envelop each grain completely. Only in this way the wedging of aggregates in the pipeline can be avoided, in other words, blockages cannot occur.

It may be concluded that every good concrete can be pumped, i.e., pumpable concrete is neither of inferior quality nor a special concrete. The requirement that 1 cu m of pumpable concrete must contain approximately 350-400 kg of fines reveals that only a concrete can be pumped which contains approximately 270 kg of cement per cubic meter.

Consequently lean concrete cannot be pumped without further preparation or adding of fines like trass, electrostatic filter ash or the like as lubricating means. To attain a trouble-free operation of the concrete pump great importance furthermore has to be attached to uniform batching, uniform consistency and adequate mixing time (homogeneous mix).

When producing pumpable concrete only standard cements should be used if possible because these are subject of a continuous control and have a uniform fineness of grinding. In view of their better ability to retain water long (slimy) cements such as Portland or trass cements are suited for the production of pumpable concrete. It is known that short (brittle) cements (blast furnace cements) tend to repel the water. If the water is not retained - bound-by the cement the result is the so-called bleeding of the concrete. The lubricating film is destroyed and blockages may occur in the pipeline.

Any concrete to be conveyed through a pipeline must have good lubricating properties. The cement grout serves as lubricating agent. It is necessary that an adequate quantity of same must be available for the pumping operation. The grout consists of cement, fine sand below 0.2mm or other fines and water.

Consequently besides the water the very fine aggregates are of great importance.

It should be mentioned in this connection that not only the lubricating film on the interior walls of

the pipeline is of importance, but also the film between the individual grains. In this way there is no direct contact between them; the concrete is plastic and can be deformed. Consequently the concrete is of good workability. The practice has revealed that the proportion of fines below 0,2mm in a pumpable concrete should amount to approximately 350-400 kg/cu m in order to guarantee a trouble-free operation. In case of crushed or flaky aggregates the proportion of fines should be increased by 10%.

When using washed-out sand, in certain circumstances fines have to be added because the fine sand (below 0.2mm) has been washed out. As admixture quartzite dust, trass, electrostatic filter ash, ground barite or the like are recommended.

For a pumpable concrete only such aggregates are appropriate which are also suitable for dense concrete such as sand, gravel, broken rock, chippings or similar.

The aggregates differ in their geometric shape and individual hardness. The hardness of the aggregates has no effect on the pumpability. However, it inevitably increases the wear. On the other hand, the geometric shape of the aggregates influences the pumpability. Flaky gravel or crushed material need more grout because of their larger surfaces. To achieve a complete envelopment of aggregates the proportion of fine aggregates must be increased by approximately 10%.

As already mentioned, the fine sand is washed out when producing the material size 0/3. Therefore, when the sand is delivered, it has to be checked how much of grain size 0 is contained. According to the grading curve range "especially good" (aggregates 0-30) a concrete may contain up to 9% of fine sand (below 0.2 mm) without this having any negative influence on the concrete quality. If the aggregates have not enough fines, fines must be added correspondingly or the proportion of cement must be increased.

Poor or incorrect storage of aggregates often was the reason for difficulties in concrete pumping. The aggregates should be as uniform as possible and in uniform batches. In order to save the costs of a batching plant, some contractors try to use mixed gravel. To save space, the mixed gravel is then stockpiled to a considerable height.

However, this may result in a segregation. The coarse aggregates accumulate at the bottom of the slope and are later fed into the mixer with inadequate quantities of sand. This results in uneven batches in particular when the scraper operator chooses the easy way of following always the same track.

On the other hand, one sometimes tries to place four sizes of aggregates into 3 partitions only. In this case two different gradings are put into one bin. It is evident that this may cause difficulties during pumping if for example the two grain groups are not mixed by the gravel plant but fed into the transporting vehicle in layers. In case of unfavourable conditions it often happened that instead of the grain sizes 0-7mm only those of 3-7mm got to the mixture. If only 3 partitions are available for four different sizes of aggregates, the grades 7-15mm and 15-30mm must be placed into one bin. It must be ascertained however, that these two grain sizes are delivered in mixed condition by the gravel plant.

As already pointed out, the quality of a concrete as well as its workability and suitability for compaction depend on the grading of aggregates. For an economical production of high-quality concrete it is therefore imperative to pay great attention to the grading of aggregates.

In case of natural, unsorted pit gravel the coarse aggregate or the fine aggregate may prevail. If there is a high proportion of fines, of sand 0-3mm, that means that the total surface of the grains increases correspondingly. In order to envelop each individual grain a relatively higher amount of cement grout will be necessary. In this case one is speaking of "cement eater". This concrete has the advantage that it can be compacted very well but the quantity of cement needed is considerable. In case of concrete having too much coarse aggregates the quantity of cement grout needed to envelop each grain is of course lower. This concrete is difficult to be compacted because the spaces between the individual grains are not filled. The supporting grain is missing.

If a pumpable concrete is produced with crushed material, possibly a natural sand should be used for the grain size 0-3mm because it can retain the water better. It has to be observed that the proportion of fines increases.

The use of absorptive brick may result in a change of consistency of the concrete while on the way through the pipeline. This is due to the tendency of the brick to absorb water a posteriori. To limit the supplementary absorption of water to a minimum, the brick should in any case be stored in wet condition, i.e. constantly sprinkled with water. The same applies to any other aggregates with a tendency to absorb water a posteriori.

It must be born in mind that whenever concrete containing absorptive brick is pumped, water retaining natural sand should be used.

In pumpable concrete the water / cement ratio varies between 0.4 and 0.6. The effectively lowest water / cement ratio cannot be indicated because other characteristics of the concrete are of importance, too, for example the concrete quality, the composition of the grains, the geometric shape of the aggregates as well as the nature of the fines, the lubricating properties of the cement and the concrete additives. But the water / cement ratio should not be lower than 0.4.

Concrete additives are chemical admixtures added to the concrete-before placing time-in small quantities in powder or liquid form.

Wetting agents (BV), air entraining agents (LP), combinations of both (LPV), decelerators and accelerators, compaction agents, anti-freeze, etc. The cements and aggregates react differently upon the various additives, therefore it is recommended to determine by appropriate tests in advance which additives will be best suitable for the concrete pumping on the particular site.

Air entraining agents should be added only in smallest quantities and strictly in accordance with the relevant instructions, otherwise the air pores will act in the pipeline like shock-absorbers.

An important factor for pumping concrete (in addition to careful dosing of the aggregates and uniform concrete consistency) is an adequate mixing of all aggregates. The concrete must be of homogeneous nature! In the mixer, the cement must have an opportunity to be thoroughly bound with the mixing water, otherwise there is danger of concrete bleeding. Great importance must be attached to the proper selection of the mixer. There is no use of having a too small mixer in conjunction with a too efficient pump. The operator will then attempt to adapt the output of the mixer to that of the concrete pump. The too short mixing time resulting therefrom causes time wasting stoppages.

For the pipeline mainly seamless pipes of high-quality precision steel are used. The pipelines consist of straight sections and bends which are connected by means of couplings. The inside diameters of these pipes are indicated as nominal width in mm (for example DN 180=180mm inside diameter).

Normal lengths of straight pipe sections are 0.5, 1.0, 2.0 and 3.0. In addition to 90 deg., 30 deg., 45 deg., and 60 deg. bends are supplied. The radius of these bends depends on the nominal width and can be 1.0 or 2.0m. Further-more there are elbows having a radius of 0.5m, but they are mainly used for slewing joints or at the end of a pipeline only.

The pipeline diameters normally used for placing concrete are: DN 180, 125, 150, 100 and 80. The economical use of the placing equipment depends on the right selection of the pipeline diameter. Large diameter pipes are considerably heavy and their handling is difficult and costly. In this connection particular attention should be paid to the table of weights indicated below. The diameter of pipeline used depends on the following:

- A) Size and type of concrete pump
- B) Required horizontal and vertical placing distances
- C) Quality of concrete to be pumped with regard to the consistency
- D) Maximum size of aggregates

With 80mm dia., pipelines, the speed of the concrete in the pipeline and consequently the

friction increases considerably. That is why the pumping through pipelines of 80mm diameter is limited to a horizontal distance of 150m. One of the most important factors for the choice of the smallest possible pipe diameter is the weight of the pipes. These pipe sections are much lighter! The smaller volume also results in a lower weight of the pipes filled with concrete.

There are also other reasons which speak in favour of smaller diameters:

1) The purchase costs for pipelines of smaller diameter are lower.

2) The use of smaller diameters for distributing concrete by means of flexible hoses at the end of the pipeline is considerably easier. Bearing in mind what has been said about the weight of the filled pipes, it is clear that it is also of importance for an easy handling of the end hose.

3) The negative influence of air pockets will be considerably less in case of smaller pipeline volume.

4) In case of bleeding concrete the segregation will be limited.

5) Mixes which are not pumpable will build-up immediately in the taper piece (150/80mm). Blockages in the pipeline itself are thus excluded.

6) The concrete can be pumped with less cement proportions and higher water/cement ratio.

It is obvious that for pumping concrete through a pipeline it is essential whether it is laid straight and horizontally or whether a pipeline of the same length goes vertically upward. The weight of the vertical conpipe bends. This is generally called "the proportional value of a pipeline".

To ascertain the exact mathematical pipe value, extensive measurements and calculations would be necessary. On building sites only the "approximate value" accrued from practical experience will govern. However, the individual diameters have different proportional values. For "large" pipelines DN 125, DN 150 and DN 180 the following is applicable:

1 m vertical rise equals approximately 6-8m of horizontal pipeline. Each 10 deg. bend corresponds to 1 m of horizontal pipeline. For pipelines DN 80 and DN 100 the following is applicable: 1 m vertical rise equals 2-3 m of horizontal pipeline.

When laying the pipeline the following points should be observed:

1) The concrete pump should be erected at such a point that it will enable the laying of a shortest possible pipeline. If a central batching plant is used, the main feeding point has to be considered.

2) The pipeline should incorporate only those changes of direction which are absolutely necessary. All unnecessary bends should be avoided.

3) When laying the pipeline it should be observed that the first section of the pipeline (behind the pump) should be laid as horizontally

and straight as possible. The minimum distance between the concrete pump and the first change of the pipeline direction should be approximately 10m. If possible, shorter distances should be avoided. In case of high vertical rises the distance between the pump and the vertical pipeline should be as long as possible so that the concrete in the horizontal pipeline creates a counter-weight to the concrete in the vertical pipeline.

4) Ascending or descending pipelines should not be laid transversally but vertically. For gradient of more than 15m it is advisable to install wing or reversing bends, particularly if no longer horizontal pipeline follows the descending pipeline. It is obvious that attempts must be made to hold the concrete in the descending pipeline; the concrete must not escape on its own from the descending pipeline.

5) If possible, the pipeline should not consist of sections exceeding 3m. Longer pipe sections have the disadvantage of difficult handling. Therefore it is recommended to lay only pipe sections of a length of 1 respectively 2m at the placing point. During the pumping operation these pipes have to be dismantled. Short pipe sections then facilitate considerably the work.

6) When assembling the pipeline it must be observed that the sealing rings are inserted in the grooves provided for this purpose. The sealing surface must be clean. A perfect seal must be ensured. No pipe section should be assembled under tension.

7) The pipeline should be laid in such a manner that single pipe sections can be removed during concreting to reach the next placing point. When fitting pipe sections during concreting, the pipeline should be extended always by one section at a time. If the distance is longer, i.e. that the next placing point cannot be reached with one pipe section, the concrete first must be pumped until it emerges perfectly from the pipe section which has been fitted.

8) Ascending or descending pipelines must be supported or tied to the building. The type of anchoring to be used depends on the pipeline length and the conditions prevailing on the site. In the majority of cases simple wiring will be sufficient. A good solution for vertical placing is to lead the pipeline through the individual floors upward. All transitions from horizontal to vertical pipelines must be supported in such a manner that the pipe bend does not carry the whole weight of the pipeline.

9) The practice has shown that it is of advantage for large diameter pipes to lay the discharge end of the pipeline approximately 1.0-1.5 m higher. This will facilitate the distribution of the concrete on a surface by using a chute.

The cleaning of the pipeline deserves particular care and attention. Pipe sections which have not been perfectly cleaned will - due to possible concrete or grout remainders - increase the friction and render the pumping operation difficult.

Above all, long pipelines require a perfect cleanliness. It is of importance that the concrete remainders are not only removed from the inside of the pipeline, but also from the junction points. Pipelines not being tight will cause difficulties and blockages.

The pipeline may also be cleaned by means of water by using a water pump or by connecting the pipeline to a water pressure line. Then one has to proceed as in case of using compressed air. When cleaning the pipeline by means of water, a solid and wet paper plug has to be inserted between the rubber ball and the concrete. The only purpose of this plug is to achieve a good sealing. The water must not expel the cement grout which is needed for the lubrication of the pipe walls. At this, the pipeline must be especially tight. When cleaning with water, the trap basket is not needed. Elbows and distribution base can be fitted to the end of the pipeline.

It should be pointed out briefly that pumping of concrete is also possible in case of extremely hot temperatures respectively in freezing weather. The pipeline is often protected against extreme temperatures either by covering it or by heating it.

With more or less success it is tried to protect the pipeline against the direct influence of heat. The method widely-held is to cover the pipeline system with wet mats or bags. The water evaporates in this manner and thus reduces the temperature of the pipeline. Whereas the concrete sets more quickly in case of high temperatures, the setting process is slower in a cool pipeline. That seems to be the only reason in favour of covering the pipeline because the water of the concrete evaporate out of a tight pipeline. Tight pipelines are generally the necessary condition for a troublefree pumping.

Concrete has often been pumped at temperatures lying 15-20 C below zero. Only seldom the pipeline itself is preheated at extremely low temperatures. It is essential and prescribed to preheat the aggregates and the mixing water, this will prevent the concrete from perishing. Long pipelines can also be preheated prior to pumping in order to avoid a considerable cooling down of the concrete. This is especially valid if prestressed concrete is used which requires an early strength.

At each building site blockages are feared, the causes of which cannot be recognized immediately. Whenever a concrete pump operates properly while running idle, blockages cannot be attributed to the machine but to the material pumped. A concrete pump does not change the properties of the concrete. Blockages are the consequence of concrete difficult to be pumped or not at all pumpable, of leaky respectively dirty pipelines or of human failure.

Blockages are distinguished by certain visible symptoms. A typical blockage always looks like a completely dry concrete plug from which the mixing water has been squeezed out. Very often it appears as if no cement has been

added at all since the coarse aggregates and the fines appear in their original colours.

A sure sign that a blockage has occurred is that the gate valves do not reverse properly. Each blockage in the pump or the pipeline can be recognized by a sudden increase of pressure indicated on the gauge or concrete pump immediately stops any operation. If the valve reacts immediately, this is a sure sign that the blockage has occurred in the pump respectively directly behind the pump. If the pressure rises slowly to maximum in the hydraulic system, this means that the blockage has built-up in the pipeline or at its end.

Difficult to be pumped concrete tends to cause blockages due to its structure. It is obvious that a difficult to be pumped mix can be sucked in only with great difficulties. Asking about the reasons-without considering the consistency-one recognizes that the flexibility of the concrete and its interior friction play a decisive part. A homogeneous and well mixed concrete in any case will have a lower interior friction. If an unhomogeneous mix enters the gate valve housing, the gates will need a considerably higher force to cut through the concrete. The required force may rise infinitely as a result of a hard column formed by compressed concrete which refuses to move in the pipeline due to its structure. This column-compacted to a plug-blocks the whole pipeline and thus the pumping process.

The categories of concrete difficult to be pumped are as follows:

- a) Bleeding concrete
- b) Extreme concrete consistency
- c) Concrete with unsuitable aggregate grading
- d) Concrete with inadequate proportion of fines
- e) Concrete with excessive amount of chemical additives
- f) Concrete setting too quickly
- g) Concrete with chemical, air entraining agents (elastic concrete)

The so-called bleeding concrete has water repellent properties and does not absorb the water. This means that the lubricating properties of the concrete are lost. The cement grout is "watery". Bleeding concrete is easily recognized by the fact that in approximately 2-5 minutes after the pump has been stopped water will set in the hopper. When observing the discharge end of the pipeline it will be noted that in addition to concrete also water will emerge. In this case the concrete plug is not surrounded by an adequate coating of cement grout. Blockages due to bleeding concrete are created by the segregation of concrete in the pipeline because of the repelled water. The coarse aggregates sink on the ground of the pipeline; the water-separated from the cement-fills the upper space of the pipeline. A lubricating film on the pipe wall and in the concrete itself-an absolute necessity for concrete pumping-is not available. Bleeding

of concrete will particularly occur during longer interruptions. If this concrete has to be pumped or blown-out, it can no longer be moved as a column through the pipeline (too high friction). Very often the pipeline then must be cleaned manually.

The bleeding of a concrete can be avoided by reducing the amount of mixing water. The ratio of water to be added should not exceed the quantity that really can be bound by the cement. Generally it should be observed that the water in the mixer must have the possibility to amalgamate intensively with the cement, i.e. the mixing time must be observed very carefully. Primarily in the case of blast furnace cement (short or brittle cements) an adequate mixing time must be adhered to since these cements tend to early repel water. The bleeding of concrete can also be avoided by adding fine sand (0-0.2 mm) or other fines because the grain sized 0 also binds water. In this connection concrete must contain approx. 350-400 kg of fines per cubic meter. Only concrete in extreme consistency ranges (too thin or too stiff) will tend to cause blockages. This applies especially to thin concrete. These blockages will appear in the gate valve housing and are recognized by a sudden jamming of the gate valves. In extreme cases this will happen in regular intervals.

The blockages are caused by too liquid cement grout which becomes free by the pumping pressure and builds-up in the gate valve housing and blocks the movement of the gate valves. Such blockages can be avoided by producing stiffer concrete consistencies. Wrong grading of aggregates is either not pumpable at all or only with great difficulties since the grout is inadequate to provide the necessary film for the aggregates and the pipeline wall. If blockages occur in spite of a good pumping progress the cause will be found in most cases in a failure of the batching plant. On many building sites it has been noted that the content of fines has been reduced unintentionally when supplying different sand. Therefore the sand has to be checked with regard to its proportion of fines. If there is a lack of fines, it must be compensated by cement, lubricating sand, stone dust or trass. If the sand contains too much fines, their proportion must be reduced. If there are too many fines (for example too much cement) in the concrete, the pressure of the piston will no longer be transmitted in a longitudinal direction of the pipeline from grain to grain, but like water in all directions. This means that there are too many fines which try to avoid the pressure and press against the pipeline walls. Thus the friction increases considerably and the concrete pump needs a higher force to overcome it. Due to these high pressures the sand is pressed against the pipeline and builds-up, since the surface of the sand has a higher friction coefficient than the pipeline. In order to avoid these blockages the proportion of sand, fines or cement should be reduced or medium-sized grains should be added in order to increase the surface of the grains.

As already pointed out, blockages may occur

if excessive quantities of chemical additives are used. An excessive quantity of air entraining agents for example is recognized by the fact that in case of long delivery pipelines the concrete flows back into the hopper when the gate valves are reversing. Consequently the concrete can be compressed and expands during the reversing process. In this case the concrete can be heard moving backward and forward in the pipeline and this may cause segregation and blockages. With regard to all chemical additives it must be determined on the site how the used cement reacts upon the used additive in case of different temperatures and dosages. Retarding agents, e.g., may become accelerators merely due to an increase of temperature. By adding a too high dosage of additives or by changing the type of cement the same effect may be reached. Therefore it is necessary to establish a diagramme considering all these facts before a chemical additive is used.

High-grade cements are used if an early concrete strength is needed. The hardening process of such cements is rapid. Blockages may therefore occur because of rapid setting of the concrete if there are long interruptions of pumping. The setting process can be further accelerated by high temperatures.

Blockages caused by such high-grade cement naturally mostly occur during relaying or blowing-out of the pipeline. Whenever concrete containing high-grade cement has to be placed, well-trained operators should be employed. The time for relaying the pipeline must be kept to an absolute minimum and the preparatory time for blowing-out should be as short as possible.

Often blockages may occur because of a too short mixing time-particularly with reverse drum mixers. This applies especially when a stiff consistency of the concrete to be pumped is produced. It is clear that stiff concrete consistencies require a longer mixing time than soft concrete. Difficulties due to too short mixing time will mainly occur if the mixer is too small in relation to the output of the concrete pump.

Blockages may occur at the beginning of the pumping due to insufficient or too thin lubricating mix. The dry pipe walls absorb the grout, therefore long pipelines need more lubricating mix. Blockages occurring while starting the pumping operation are always recognized by a scraping noise at the beginning of the concrete column in the pipeline. If too thin lubricating mixes are used very high pumping pressures will occur due to their great plasticity. It is therefore recommended-particularly in case of vertical pipelines-to use a stiff lubricating mix.

The cause of blockages is seldom found in the pipeline. However, blockages may occur due to pipelines not properly sealed or insufficiently cleaned or when discharge pockets are not used properly.

When a pipeline has not been laid properly there is the danger that pipe joints will leak. Such leaks are caused by dirty or damaged flanges, defective locking stirrups and by assembling the

pipeline under tension. Due to leaky connections water and cement grout may escape from the pipeline thus diminishing the lubricating properties of the concrete. Blockages are the consequence. On the other hand, leaky pipelines impede also the blowing-out process. The compressed air can escape and the air pressure is insufficient to push the concrete column through the pipeline.

Dirty pipelines can cause difficulties right at the beginning of the pumping operation because remainders of old set concrete in the pipeline brake down the flow of the concrete. It has to be mentioned briefly that the lubricating grout is difficult to be pumped due to the high friction values caused by their plasticity.

If a hose is used at the end of the pipeline, blockages can only occur due to improper operation. When using a flexible end section the following should be borne in mind:

- a) The value of friction in the hose is higher than in the pipeline.
- b) Careless manipulation of the hose may easily kink it.

Due to the higher friction value in the hose sometimes blockages may occur at commencement of pumping. To reduce the friction it is recommended to flush the inside with water. When operating with a hose and if a blockage has occurred in the system, it will mostly be found either in the taper piece or at the rear of the hose.

It has been pointed out already what should be borne in mind when using downward sloping pipelines. At the commencement of pumping a blockage may occur if the plug inserted in front of the lubricating mix does not brake it down. The result will be that the mix cannot lubricate the upper wall of the pipeline. This means danger of blockages. Downward sloping pipelines may run empty. The coarse aggregates will then roll at a different speed than the fine aggregates, and the concrete will bleed.

When using downward sloping pipelines generally care should be taken that the flow of the concrete does not break. Here the installation of stowing bends assists. If the "concrete sausage" breaks the concrete will crumble resulting in segregation and blockages.

Blockages mostly occur at certain points of the placing system. To locate them quickly one should know where they tend to occur. All blockages are especially easily occurring in places where the concrete is subjected to deformation. As already mentioned, the taper piece has to be considered as a safety element and therefore it is provided with turn-buckles. This is the first place where an operator must look for a blockage.

If a drop of output is observed during pumping—the hopper of the pump is emptying too slowly and insufficient quantities of concrete reach the end of the pipeline—the cause may be in the pipeline or the concrete to be pumped. It is presumed, of course, that the stroke remains unchanged, other-wise there must be a switching failure. In this case the respective

operating instructions have to be observed. If adjustment has been made, the drop of output must also have been remedied.

The prerequisite of a maximum output is not only a good pumpable concrete but also a normal pipeline. Extremely long pipelines, excessive placing heights and particularly unfavourably laid pipelines will result in a drop of output. If extremely long pipelines are used the concrete must under no circumstances contain air-entraining agents.

For vertical placing it is of advantage if a certain length of horizontal pipeline precedes the vertical pipeline should be long enough to constitute a counter-weight to the concrete in the vertical line. The advantage of this "starting way" outweighs by far the possible disadvantage of such a longer horizontal pipeline.

It would be wrong to attempt to compensate such natural drop of output by using a thin concrete. Practice has shown that the least drop of output is to be noted when using stiff concrete consistencies.

As already mentioned, air cushions have a detrimental effect on trouble-free pumping. This applies in particular to pipeline leading downward where air inclusions will accumulate at the highest point, directly before the slope of the pipeline. However, this will only be detrimental if the highest point of the pipeline is followed by a relatively long pipeline.

Such air inclusions are natural and occur during mixing of the concrete. They should not be taken for micropores intentionally produced by air-entraining agents. The air inclusions are compressed during each piston stroke. If the concrete column between the air cushion and the pipeline highly resists the pressure, the air can only expand towards the concrete pump. During each reciprocating stroke of the gate valves a part of the concrete will flow back into the hopper. This can be seen in the hopper and results in an extremely high wear besides the drop of output.

An air cushion can be removed by drilling a hole in the pipeline so that the air can escape during the concrete placing. It has proven practical to put a nail respectively a piece of wire into the hole (5-8 mm) which is moved by the concrete and keeps the aperture open. The pipeline practically is not damaged by the hole since the bore closes itself lateron. However, it must be ascertained that the hole is closed with a timber plug when blowing-out the pipeline.

As natural air inclusions may affect the output of the concrete pump, so may extreme of additives. Particularly in case of long pipelines a huge number of minute air-pores (micro-pores produced by air-entraining agents) react like a closed air cushion which can be compressed. This process can under certain circumstances become so extreme that the complete piston stroke is absorbed and the output of the concrete pump practically drops to zero. This will frequently result in blockages. A similar effect as with air cushions in the pipeline will also occur with too plastic concrete. Therefore an excessive dosage of wetting agents should be avoided.

Theoretical computation of acoustic emission signal trends for monitoring metal cutting tool wear

V Messaritis, BSc PhD
Lecturer HTI

INTRODUCTION

This paper reports an investigation of monitoring cutting tool wear during turning by Acoustic Emission (AE). Some progress has been made in applying metal cutting theory to predict AE signal levels. Supporting experimental results are presented.

AE is unique in the field of tool monitoring in that it offers the potential to simultaneously monitor progressive wear, chip condition (1), and cracking (2). However, research results have not yet reached commercial standards of robustness. In multi-operation turning centres, calibration of AE instrumentation would be required for each tool. A knowledge based system capable of predicting AE levels theoretically would reduce this disadvantage.

EXPERIMENTAL INVESTIGATION

The experimental work utilised a conventional Colchester Mascot lathe, Sandvik toolholder and carbide insert type TNMM 015 P15. A Dunegan D9201A piezo electric AE transducer was mounted on the end of the toolholder, connected to a 40dB preamplifier. The AE signal was captured on a Nicolet 2090 oscilloscope (2MHz sampling) and signal analysis was carried out off line. The signal could also be passed through a true r.m.s. converter with switchable averaging time. The tool forces were measured by strain gauges on the toolholder.

The ability of AE to detect progressive wear is illustrated in Fig 1. Extracts of 2 millisecond duration of the unprocessed AE signal are shown after: (a) 4 min cutting and negligible wear (b) 52 min and 0.51 mm major flank wear. The speed, feed rate

and width of cut were respectively 150 m/min, 0.2 mm/rev, 2.00 mm. With appropriate initial calibration and choice of threshold level for event counting it is possible to signal excessive wear.

Other authors (3) have found that the spectral characteristics of the AE signal change with progressive wear, the amplitude increasing substantially in the frequency range 80-150kHz. The spectra of the above signals Figs 2(a) show a similar increase in amplitude in the frequency range 100-200kHz. However with current transducer technology it is doubtful whether wear can be reliably predicted from spectral changes, because the AE spectrum is dominated by the transducer's own response characteristics.

The AE signal varies considerably with chip form, as can be seen in Fig 3(a)-(c). This shows 4 sec extracts of the rms AE signal for (a) an untangled continuous chip (b) a chip regularly broken by an obstruction chipbreaker (c) a tangled continuous chip. There is a sharp contrast between the continuous emission in Fig. 3 (a) and the bursts arising from chip fracture in Fig. 3(b). The rms averaging time in (b) has to be selected to conform with the chip breaking rate. Comparing Fig. 3(a) and (c) it is seen that there is also dramatic change in signal level when a continuous chip tangles. Evidently AE offers the potential basis for a chip management system as proposed in (1). The present author's investigation of detecting tool cracking by AE has so far proved unsatisfactory. Small increases in AE are detectable after cracking, but the burst-type emission from chip breaking tends to mask that associated with tool cracking. Further investigation is needed of this important application for AE monitoring.

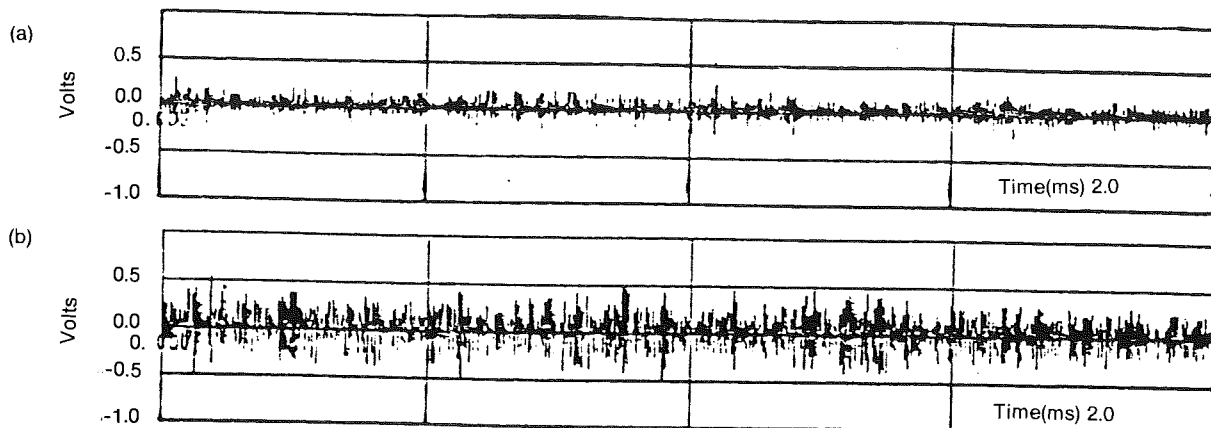


Fig. 1: Unprocessed AE signal after (a) 4 min (b) 52 min cutting

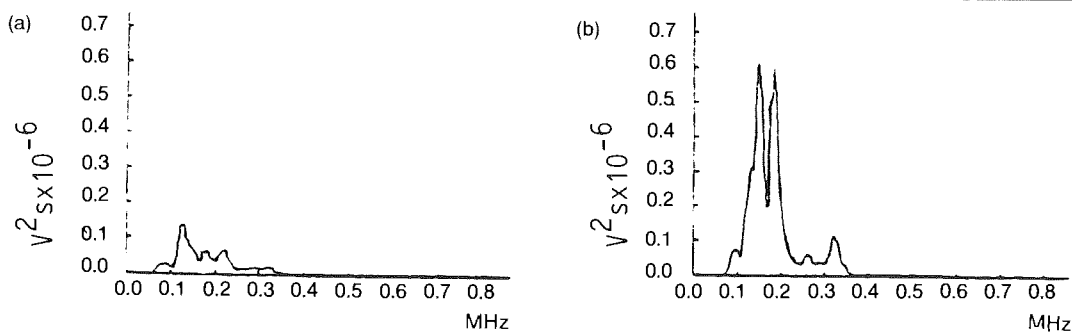


Fig. 2: Spectra of unprocessed AE signal in Fig. 1

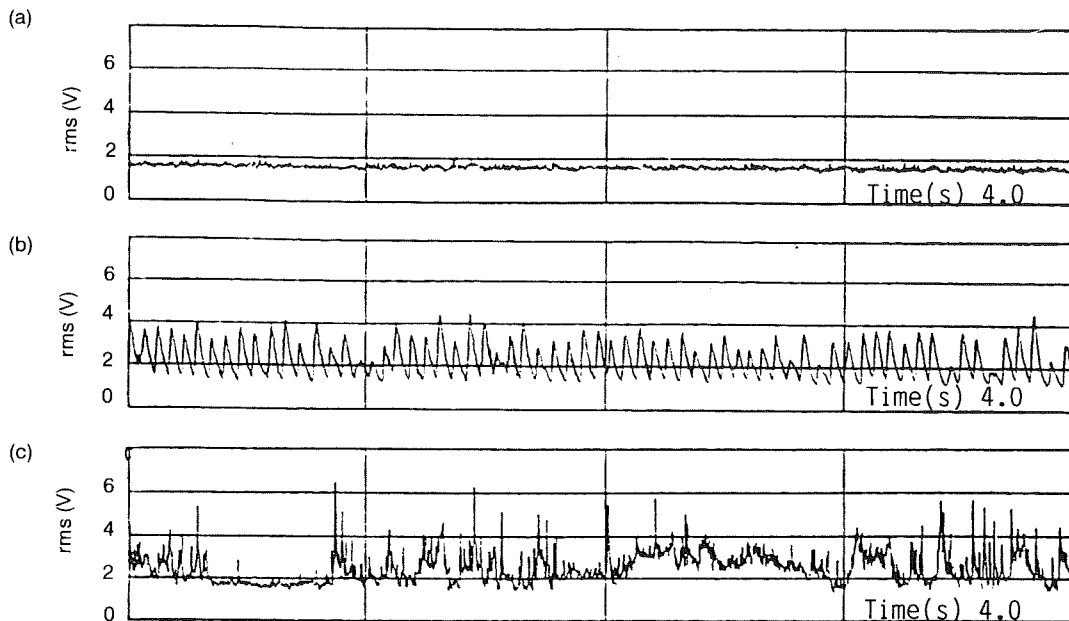


Fig. 3: AE rms signal for (a) continuous (b) broken (c) tangled chip

THEORETICAL PREDICTION OF AE SIGNAL LEVELS

The foregoing illustrates the potential of AE for tool and chip monitoring. A multi-operation turning centre would require calibration for each operation. This might be reducible to a single calibration if it were possible to predict theoretically how the AE signal varies with varying cutting conditions. A previous attempt (4) to establish a quantitative relation between AE and cutting parameters had limited success. This was based on the proposition that the AE signal energy rate is proportional to the cutting work rate

$$\text{rms}^2 \propto \sigma \dot{\epsilon} V \quad (1)$$

The cutting work rate was expressed in terms of the cutting parameters by applying the Ernst and Merchant theory of chip formation. This ignores the dependence of work material shear flow stress on strain-rate and temperature. Strain rate particularly is known to influence AE.

For this reason the present work utilised the cutting theory proposed by Oxley and Hastings (5). This theory, which makes use of the concept of velocity modified temperature to determine work material flow stress at the elevated

temperatures and very high strain rates present in metal cutting, relies heavily on experimental data.

A series of experiments was performed to establish whether the cutting work rate as predicted by the Oxley and Hastings theory exhibited the same trends as the measured AE rms² signal. Some preliminary experiments were also performed to determine the influence on the AE signal of factors such as tool position, workpiece mounting, and the degree of previous surface work hardening. These factors were found to have no measurable effect on the AE signal. A further experiment was carried out to determine the variation between the AE generated from orthogonal cutting and semi-orthogonal cutting. The tool tip nose radius was 0.4mm resulting in minimal cutting on the minor flank. Although Oxley's theory is derived assuming orthogonal cutting, good agreement was observed between experimentally measured and theoretically predicted cutting work rates for both the orthogonal and semi-orthogonal cutting tests. There was also negligible difference in AE and measured cutting work rate between orthogonal and semi-orthogonal cutting, except at very small widths of cut, when cutting on the minor flank becomes significant.

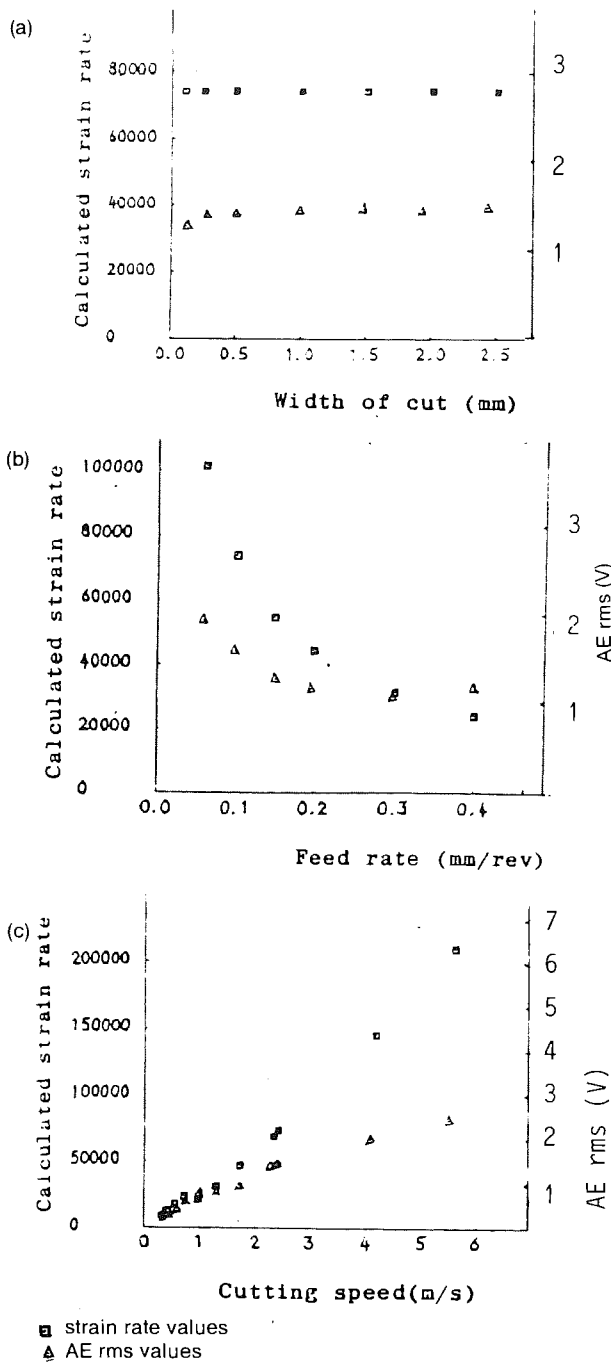


Fig. 4: Variation of AE rms and calculated strain rate with:
 (a) width of cut
 (b) feed rate
 (c) cutting speed

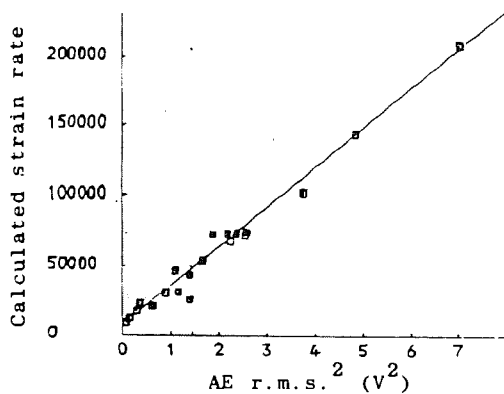


Fig. 5: Correlation between strain rate and AE rms² signal level

The correlation between the AE rms² and cutting work rate was then investigated. Close agreement was observed between theoretically predicted and experimental values for cutting work rate, substantiating Oxley and Hastings theory. However, the AE rms remained constant with width of cut, whereas cutting work rate increases. The only theoretical parameter to exhibit similar trends to the AE rms² was the calculated strain rate. Fig. 4(a), (b), and (c) show respectively the AE rms and calculated strain rate plotted against (a) width of cut, (b) feed rate, and (c) cutting speed. The same information is replotted in Fig. 5 to show the correlation between AE rms² and the calculated strain rate. The apparent insensitivity of the AE rms to volume in Fig. 4(a) is difficult to account for, but has also been observed by other authors. It may be a peculiarity of the particular instrumentation set up. The dominance of strain rate in determining AE activity is easier to accept because the material flow stress in equation (1) is itself dependent on strain rate.

In view of the correlation observed in Fig. 5 it is natural to consider firstly the possibility of a simple linear relation between the AE rms² signal and strain rate. Thus a given toolholder instrumentation set up may be calibrated with a test piece having known material properties. A least squares line is drawn from AE data obtained in cutting tests at three different (calculated) strain rates. This calibration line is then used to predict AE rms levels for other operations for which it is possible to calculate the strain rate from the Oxley and Hastings theory. Within the limited scope of this investigation this was found to be accurate within 10%. Having predicted the initial 'sharp tool' AE level, wear thresholds can be imposed.

Further research is clearly required using alternative workpiece materials, and machining operations. The implementation of intelligent tool monitoring requires a CIM system capable of performing the cutting theory calculations and equipped with a knowledge base for containing material properties data.

References

1. Dornfeld, D.A., and Pan, C., Determination of chip forming states using a linear discriminant function technique with Acoustic Emission. *Proc. 13th. N. Amer. Mfg. Res. Conf.*, 1985.
2. Moriwaki, T., Detection of cutting tool fracture by Acoustic Emission measurement. *Annals of CIRP*, Vol 29, No. 1, pp 35-39, 1980.
3. Lan, M.S., and Dornfeld, D.A., Experimental studies of tool wear via Acoustic Emission analysis. *Proc. 10th. N. Amer. Mfg. Res. Conf.*, pp 305-311, 1982.
4. Kannatey-Asibu, E., and Dornfeld, D.A., Quantitative relationships for Acoustic Emission from orthogonal metal cutting. *Trans. ASME, Inf. Eng. Ind.*, 103, pp 330-340, 1981.
5. Oxley, P.L.B., A mechanics of machining approach to assessing machinability. *Proc. 22nd Mach. Tool Des. Res. Conf., Manchester*, pp 279-287, 1981.

Cold Fusion or Nuclear Confusion?

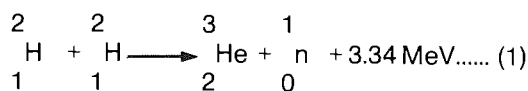
*Dr A.Y. Stathopoulos
B. Sc (Hons), D. Phil (OXON), C. Phys.,
M. Inst. P., F.R.M.S.
Lecturer HTI*

INTRODUCTION

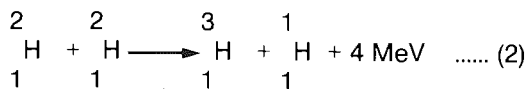
On March 23, 1989 chemists Martin Fleishmann and Stanley Pons shocked the scientific world by announcing at a press conference that they had obtained evidence of nuclear fusion occurring at room temperature, using a simple electrolytic apparatus at the University of Utah, USA. Only a week later physicist Steven Jones of Brigham Young University, also in Utah, USA, announced that he too had been producing 'cold' fusion independently in a similar set up. I will attempt here to set and review the scene as it has evolved over the last two months.

NUCLEAR FUSION - THE SCENE

The excitement generated is clear because for 40 years everyone believed that fusion is a process in need of temperatures in excess of a million degrees which can only come about in enormously expensive machines like the JET (Joined European Torus) project at Culham, UK. This is because, before two light nuclei come sufficiently close together to attract each other via their nuclear forces, they must either pass over or tunnel through a Coulomb barrier. Of the many energy releasing fusion reactions, the most important are between heavy isotopes of hydrogen. For cold fusion, i.e. fusion at room temperature, to occur the possible relevant reactions are:



and



$\begin{array}{c} 2 \\ 1 \end{array}$ H = deuterium or D or deuteron

$\begin{array}{c} 1 \\ 0 \end{array}$ n = neutron

$\begin{array}{c} 1 \\ 1 \end{array}$ H = proton

$\begin{array}{c} 3 \\ 2 \end{array}$ H = Helium-3, $\begin{array}{c} 3 \\ 1 \end{array}$ H = tritium

The energies on the right-hand side of the equations represent the energy release in each

reaction, which for a given mass of fuel is larger than that released by ordinary fission. Now, for the two deuterium nuclei to fuse in any one of the above two reactions, the nuclei must collide with high impact energies. At low impact energy these reactions would be forbidden classically, because Coulomb repulsion between the nuclei prevents them from approaching to within 10^{-15} m required for nuclear forces to become operative. However, the motion of the nuclei is actually governed by quantum mechanics, so there is a finite (but very small) probability for the nuclei to tunnel through the Coulomb barrier, and fusion at low energies is indeed observed. It has, for the past 25 years, been speculated, that the fusion rate can be increased at room temperature by a process known as muon catalysed fusion. Here, the internuclear spacing is reduced by using a negatively charged muon to replace an electron in the D_2^+ molecule. Muons have a mass of 207 electron masses and the D-D-muon molecule is reduced in size by this factor, with a consequent increase in the tunnelling probability of about 85 orders of magnitude over that in the normal molecule.

Hence, if an experimental scheme for releasing energy by fusion at room temperature, as suggested by the Utah teams, is successful, the enormity of the consequences is apparent to everyone: limitless, cheap fuel for ever.

The experimental evidence

The detailed information about the experiments of the Utah teams came after their announcements in two papers, one by Fleishman and Pons (in J. Electroanal. Chem., 261, 301-308) and one by Jones et al (Nature magazine, 1st Week, May). Both groups used electrolysis. Fleishmann and Pons (hitherto referred to as F and P) have employed a conventional electrolytic arrangement with a spiral platinum anode surrounding a palladium cathode, the electrolyte being D_2O (99.5%) enriched, heavy water, i.e. water that contains deuterium, an isotope of hydrogen. The electrolyte was made conducting with LiOD. The cathodes ranged from 1 to 4mm in diameter with current densities ranging from 8 - 512 mA.cm^{-2} . Sheet cathodes and anodes have also been used. The Jones et al experimental set up employed similar electrolytic cells with Titanium and Palladium cathodes and the electrolyte contained Fe, Ni, Pd, Ca and Na in ionic form.

Measurements made in the experiments were of two types: calorimetric and nucleonic. The F and P calorimetric measurements indicate heat generation at a steady rate over periods in

excess of 120 hours. No details are given for the incubation period before heat release in the paper and the calculation of the heat release depends on a range of assumptions about reactions involved, and although later F and P quote a four-fold gain in energy in the form of heat, the total quantity of heat-up to $4\text{MJ}\cdot\text{cm}^{-3}$ - is not compared in the paper with the energy supplied during the incubation period.

The details of the nucleonics experiments are even sketchier. They consist of (i) Detection of 2.5 MeV γ -rays from the interaction of fusion products (neutrons) with water, using a sodium iodide crystal (ii) Detection of neutron flux from the nuclear reaction using a neutron rate monitor and (iii) liquid scintillator measurements of tritium accumulation in the electrolyte. The neutron flux is reported to reach three times background, corresponding to a reaction rate of $4 \times 10^4 \text{ s}^{-1}$ in the 4mm diameter rod and the γ and tritium generation rate measured was consistent with this.

The Jones et al experiment was centred around studying the neutron generation using a very sophisticated spectrometer which established a very definite peak in the 2.5 MeV energy range.

Many other research groups of chemists and physicists around the world have climbed the bandwagon trying to reproduce 'cold fusion'. There have, thus, been two of the strangest months in the history of science. Hardly a day has gone by without a press announcement from somewhere - Texas, Georgia, Italy, India, Czechoslovakia, Soviet Union - that at least some parts of the original experiments have been replicated, providing, however, little in the way of detailed measurements. Nevertheless, many other workers are throwing cold water on cold fusion: None of the major laboratories in the USA (Brookhaven, Yale, M.I.T., Oak Ridge, Los Alamos, Lawrence Livermore et al) or Europe have obtained positive results. Attempts by the Harwell laboratory in Britain and Garsching in Germany have produced nothing, even though Fleischmann himself checked the experiments. Also, scientists in Japan and Switzerland announced that their own experiments convinced them the original work was flawed. Typically contradictory are very recent results from Stanford and Drexel Universities in the USA who specifically carried out the control experiment of using ordinary water instead of heavy water. Fusion is not expected in this case since ordinary hydrogen nuclei are involved.

Meanwhile, F. and P., who submitted their results to Nature magazine, have had their paper rejected for failing to supply, among other things, more information on how their energy output was calculated, to the referees.

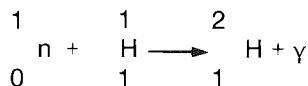
Explanation of results

F. and P. argue that the very high yield of $20 \text{ W}\cdot\text{cm}^{-3}$ obtained in their experiments is higher than any conceivable chemical process can produce.

So it must arise, they say, from a nuclear reaction between deuterium nuclei. Jones et al invoke the same nuclear reaction.

What is beyond doubt to say is that during the electrochemical process the electric current splits the heavy water into oxygen anion and deuterium cations. The latter are absorbed by the palladium (or Titanium for that matter) cathode. Palladium (Pd) metal has an f.c.c. structure and under normal conditions, deuterium can occupy the octahedral interstitial sites. If all these sites are filled, one gets PdD, having the sodium chloride structure and this has a D-D separation of about $2.5 \times 10^{-10} \text{ m}$. At ambient temperatures and pressures the β -phase (condensed lattice gas) is formed at concentrations above 67% but much higher effective pressures are supplied by electrolysis. F and P have claimed an effective pressure of 10^{27} bars which is equivalent to an 'overpotential' of 0.8 eV. This means that the deuterium in the metal will move into sites with potential energy up to 0.8 eV above that of the original octahedral sites. Given that the diffusion activation energy is about 0.4 eV, this means that at this overpotential all the octahedral sites would be filled and that some deuteria could be in either tetrahedral sites or, as F. and P. suggest, in some rather freely diffusing mode. Forced so closely together, the intuitive argument goes, the deuterium nuclei fuse together. A question that arises here is why some at least of the deuterons do not form atoms and then molecules since there are plenty of electrons inside the palladium lattice to do so? This deuterium would be picked up as a gaseous product of the electrolysis. Linus Pauling, himself a chemist Nobel laureate, has openly made it clear that he can explain the heat released by arguing that when absorbing high concentrations of deuterium, the palladium crystal lattice becomes unstable and deteriorates releasing heat.

Most nuclear physicists, as well, are still extremely sceptical about cold fusion taking place. They find the results of F. and P., which differ substantially from those of Jones, much more difficult to explain in terms of nuclear physics. For a close look, the fusion of two deuterons can go either the way of equations (1) or (2). The product easiest to detect is tritium because it is radioactive. In the first process, the neutrons emitted have a characteristic energy which is what Jones measured, unlike F. and P. who did not carry out such measurements, but have instead tried to look for tritium and γ -rays. They have apparently detected γ -rays with an energy of 2.2 MeV which can result from the capture of neutrons by protons in water to form deuterium nuclei:



There is, however, no indication that these came from the cell itself and the rate of neutron production they imply is about a billion times too

low to account for the heat produced. Also, the levels of radioactivity of tritium they quote appear to be far lower than would be expected.

To explain a lot of energy and few neutrons as reported from Utah, P. Hegelstein, an M.I.T theoretical physicist, postulates that two deuterium nuclei fuse to form a single nucleus of helium-4 (^4_2He) sidestepping the difficulties that an isolated deuterium nucleus has in embracing its neighbour. In this way no neutrons and no γ -rays will be produced and the surplus energy will be passed on straight to the lattice. This would, however, require the detection of helium-4 in the experiments. K. Johnson of M.I.T disagrees with Hegelstein saying that only a small amount of nuclear fusion is occurring and the energy is due strictly to chemical reactions.

The other possibility which has been considered is that the fusion reaction occurs but it is catalysed by muons. The muons arise from cosmic rays reaching the Earth's surface from outer space. Variation in cosmic ray intensity could explain why cold fusion has not been reproducible in all laboratories.

Conclusions

The situation as it stands at the moment is very confused both on the experimental and on the theoretical front and one is waiting for the establishment of a consistent experimental picture. The experiments are fraught with difficulties; firstly, measuring the neutron flux is an extremely tricky process and good calorimetry to account precisely for all the heat sources is even more difficult. Secondly, F and P have not given enough details and haven't shown

anybody their set up in Utah, although they are eager to visit and help other labs repeat their experiments. The team have also given conflicting statements about how long, for example, it takes for fusion to start.

More experiments, therefore, must be carried out to establish the results, if they can be established. All the work reported so far has been sloppy to say the least and inconclusive. How do they rule out that heat does not come from a chemical reaction between oxygen and hydrogen released in the experiment? This is why 1500 physicists at a meeting of the American Physical Society during the first week in May in Baltimore, proclaimed their verdict on the experiments: no way have they demonstrated fusion. The physicists challenged both the heat measurements (unstirred solution in the set up, thermometer placed in a 'hot spot', etc) and the radiation measurements (might be coming from radon, background radioactivity, already present in the laboratory's air). Caltech's S. Koonin went a step further to say: "We are suffering from the incompetence and perhaps delusions of Professors Pons and Fleischmann".

However, the debate over cold fusion is not likely to finish here and many of the young, and sometimes conflicting theories, put forward are also likely to be wrong. But a new field has opened up for researchers to delve in; that of nuclear catalysis or the study of ways in which the physicochemical environment can influence or bring about nuclear reactions. Indeed, the stakes are extremely high, although no one knows or can imagine how well cold fusion, if it occurs, might perform on a scale larger than a laboratory bench top.

Nikon

SURVEYING INSTRUMENTS

A Combination of quality and precision.

THEODOLITES, from 1min. to 1sec.

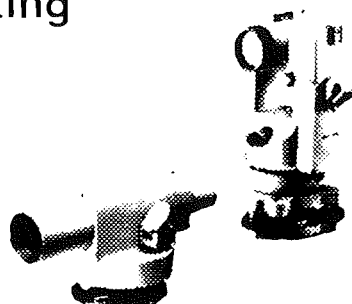
LEVELS, automatic or tilting

EDM instruments

Distributors/ Stockists

NEO. IACOVOU

Tel.: 41664 - NICOSIA



Microprocessor Controlled Three-phase Transistor Inverter

S. Hadjoannou, Msc Power Electronics
Lecturer HTI

1. INTRODUCTION

This article reflects mainly project work carried out at the HTI in relation to third year students' projects.

A three-phase Inverter converts dc into three-phase a.c. Such an inverter consists necessarily of six switching elements, a dc supply and a control circuit.

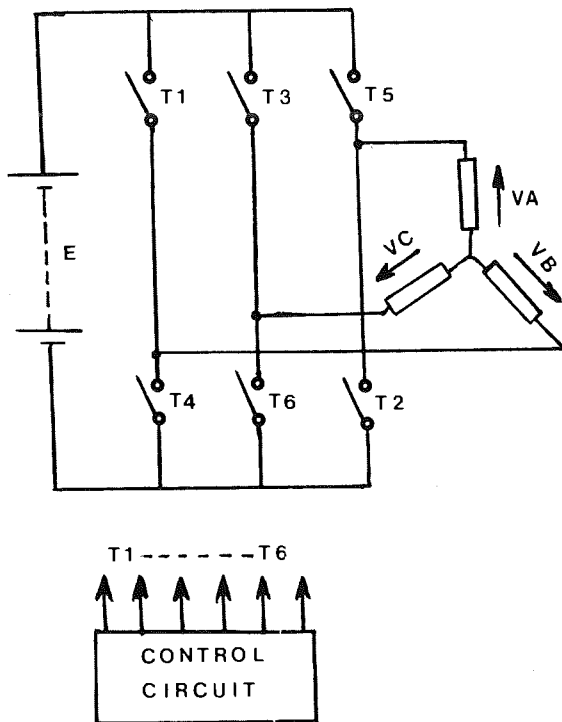


Fig. 1: Outline of a 3-phase inverter

Each switching element shown in fig. 1 can be a Thyristor, a Gate Turn-off Thyristor, a Bipolar Transistor or a MOSFET. The switching elements start conduction in the sequence T1, T2, T3, T4, T5 and T6 with a phase difference of 60° . The duration of conduction for each element can be either 120° or 180° . The 180° duration for conduction gives better output waveforms. Such waveforms are shown in fig. 2. Variable frequency inverters are mainly used for induction motor speed control

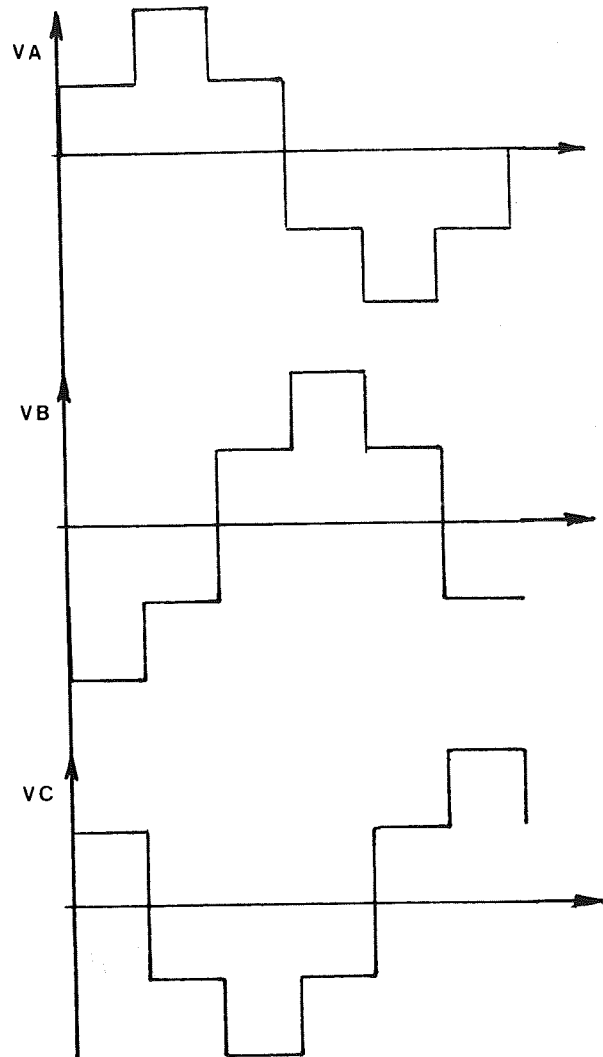


Fig. 2. Output waveforms of a 3-phase Inverter for 180° conduction.

2. A MICROPROCESSOR CONTROLLED 3-PHASE TRANSISTOR INVERTER

With reference to fig. 3, the microprocessor must produce six pulses through output port B in the sequence shown in fig. 4

The time duration of each pulse must be half the period of the output waveforms. The frequency of the output waveforms is selected by the BCD switches through port C. The six optoisolators used provide the necessary isolation between power and control circuits.

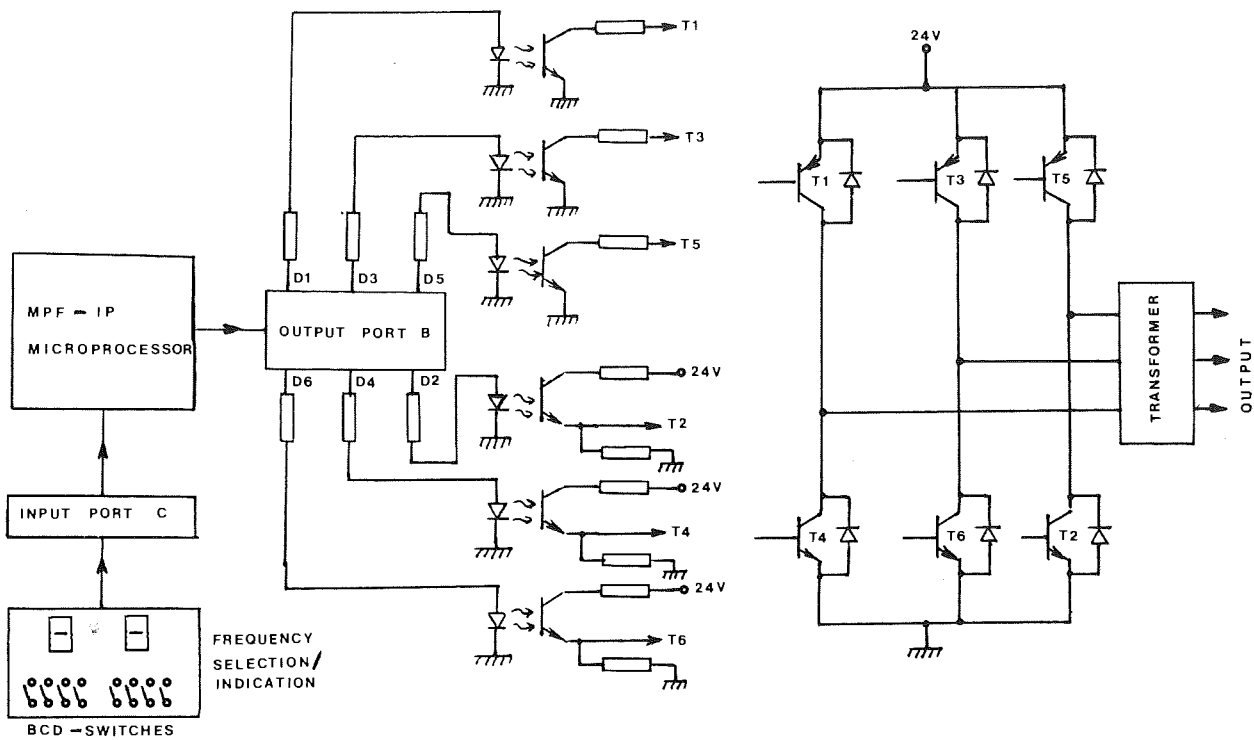


Fig. 3 Circuit Diagram

The diodes across the power transistors provide a path for the return of reactive power from the load to the d.c source.

with a delay between the 6 number equal to: $\frac{1}{6f}$
 The 6 numbers are: 62, 43, 07, 1C, 38, 70

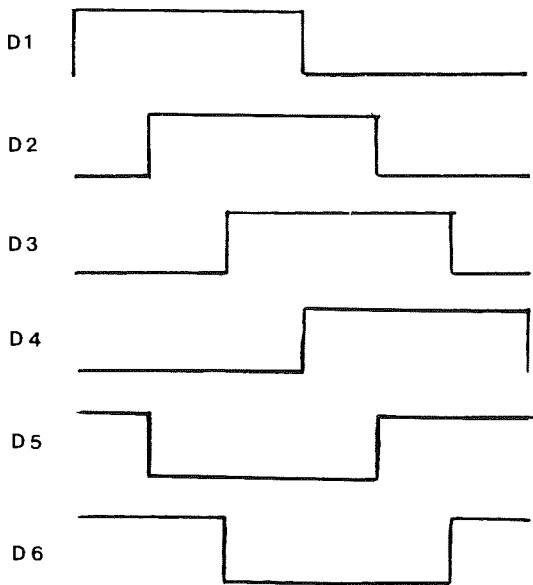
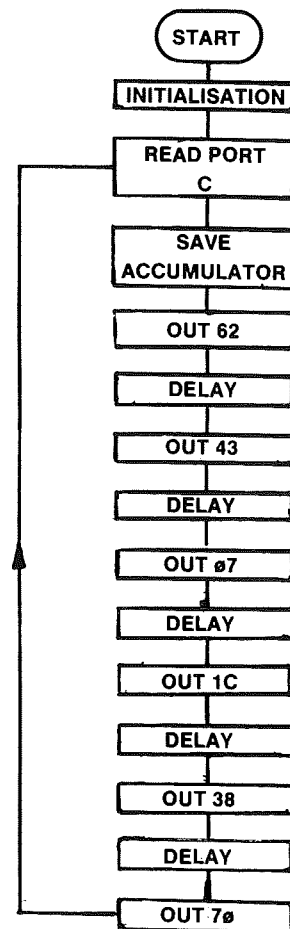


Fig. 4. Control pulses from port B

Program Flowchart



3. THE CONTROL PROGRAM

The purpose of the control program is to instruct the microprocessor to read the frequency required, f, from input Port C and produce the following 6 numbers at output Port B

4. CONCLUSIONS

Three-phase inverters are mainly used for a.c motor control. They can also be used for uninterruptible power supplies and for induction heating. For a.c motor speed control the fundamental harmonic of the output waveform is the one which will produce the useful torque in the motor. All the other harmonics will cause vibrations, losses and some of them will cause reverse torques.

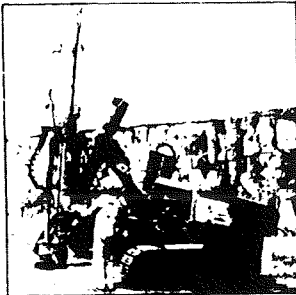
For the purpose of using the maximum power capabilities of the a.c motor, the ratio V/f (voltage

over frequency) at the input of the motor should be about constant. To achieve this the dc supply to the inverter should be variable having a voltage proportional to the output frequency of the inverter. This article reflects the work carried out up to now at the HTI. The work on the inverter will be continued in the future to produce an output having a $V/f = \text{constant}$.

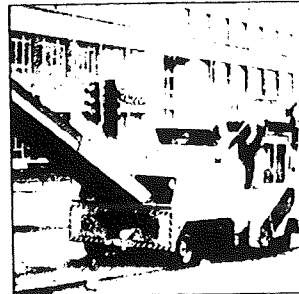
References:

Power Electronics by Cyril W. Lander.

INGERSOLL-RAND®



BLASTHOLE DRILLS



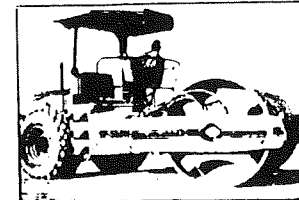
COLD PLANERS
FOR MILLING ASPHALT
AND CONCRETE SURFACES



PORTABLE
AIR COMPRESSORS



WATERWELL AND
EXPLORATION DRILLS



SOIL AND ASPHALT
COMPACTORS

PNEUMATIC TOOLS FOR THE CONSTRUCTION INDUSTRY

HAND DRILLING FOR BLASTING

Jackhammer Drills
Jackdrills with Feedlegs

CONCRETE DEMOLITION / GROOVING / DRILLING

Muffled Paving Brakers — 23, 29, 38 kgs
Diggers — 8.5 through 11.2 kgs
Pick Hammers — 3.5 through 11.2 kgs
Impactcutters / Scalars
Rotary Hammer Drills — cap. to \varnothing 60 mm

CONCRETE / SOIL DENSIFICATION

Concrete Vibrators
Rammers and Tampers
PUMPS

WATER / SLURRY PUMPING

Centrifugal Sump Pumps — cap. to 80 m³ hr
Double Diaphragm Pumps — cap. to 55 m³ hr

FIELD SERVICE AND WORKSHOPS

Stationary Air Compressors — from 3.4 Hp up
Angle and Horizontal Grinders
Sanders and Polishers
Pistol Grip and Horizontal Drills
Screwdrivers
Impacttools
Ratchet Wrenches
Winches and Overhead Hoists
Air Motors
Engine Air Starters
BLASTING SYSTEMS

THE CYPRUS IMPORT CORPORATION LTD

4 Kantaras Ave., Kaimakli, Nicosia. Tel. 435191, Tlx: 2280 IMCOR Telefax 430018
4 Attikis street, Limassol, Tel. 72267

INGERSOLL-RAND

Acoustic Intensity and its applications

Polyvios Eleftheriou
BS, MS, PhD, Lecturer HTI

The decade of 1980's is characterised by a series of developments most of which are due to the growing field of high speed data processing. Computers which were used for mathematical manipulations are also used today for data acquisition. Dedicated systems of a great number of simultaneously sampled data channels can easily be built today.

The use (and advance) of data collection arrived with the "real time processing". This term refers to the data which is processed faster than it can be collected. This capability allows data manipulation at a speed higher than the sampling rate of the computer. In other words the acquired data contain no gap (and no data is lost due to processing).

Acoustic Intensity

Acoustic Intensity is an unknown quantity to many persons who are familiar with Acoustics (!). Even books written before 1984 refer to acoustic intensity as a calculated-non measured quantity. Today though with the real time processing a four-channel data collection scheme can be used to measure three dimensional acoustic intensity.

The Method is based on a finite approximation

technique developed by Fahy [1] in 1977. The technique was first applied by Chung and Blaser [2]. Since the intensity can be calculated from the product of local pressure and particle velocity, Fahy showed that the following formula can be applied to approximate the vector of intensity.

$$\vec{T} = p \cdot \vec{u} = \frac{P_1 + P_2}{2\Delta} \frac{1}{T} \int_0^T \frac{P_1 - P_2}{2} dt.$$

Practically the pressure is found as the average pressure measured by two closely located microphones. The velocity is also calculated from the difference of the signals obtained by the two microphones. One needs to recall here that both the pressure and the velocity are functions of time and so the phase difference between the two microphones (channels) is very important. This fact requires the use of "phase matched" pair of channels and simultaneously collected data. In other words no multiplexing of data channels is allowed if phase is to be measured. Figure 1 outlines the technique of measuring Acoustic Intensity.

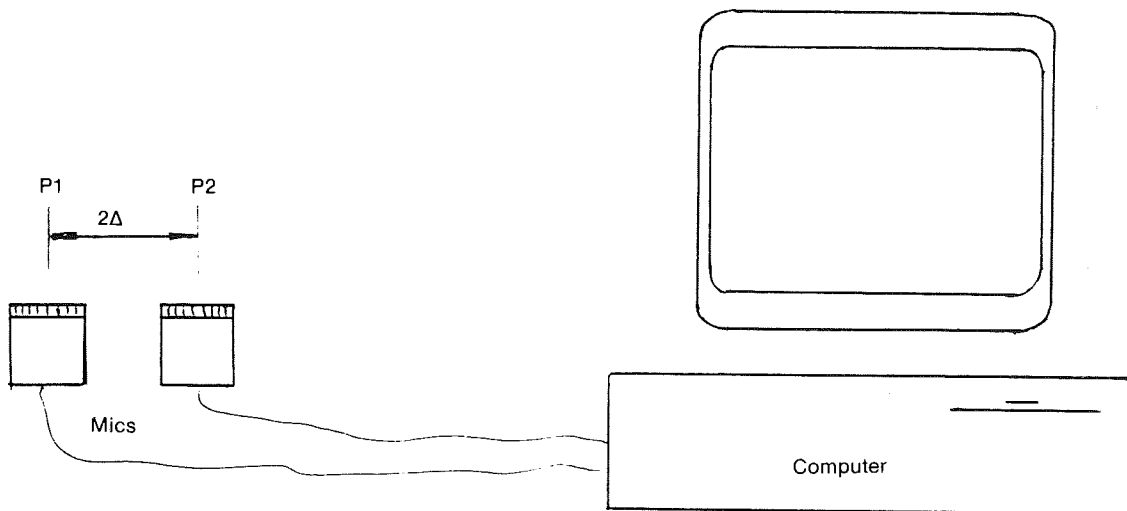


Fig. 1 Measurement of Acoustic Intensity requires the use of two channels and a computer

Areas of Application

The value of the method can be understood if one realises that the large and expensive reverberant rooms **are not** required for traditional acoustic measurements. Fourier transform can easily be applied to the data collected through

the matched channels and frequency analysis is only limited by the speed of data collection (i.e. the speed of the computer used).

In few words to check a device for noise generation one has to map the volume around the device with an "intensity probe" and the total power can be calculated by multiplying the area

and the intensity. The result provides also the operator with the frequency spectrum at different locations. Data mapping is very important because a "small noisy" component of a complicated device can be identified and corrected.

Applications to turbomachines

Turbomachines are used in most areas of our civilization. Cars, air conditioning, etc., use such devices for different reasons. Often those devices are "noisy" and treatment is required. Treatment up to now was based on the "art of designing" (!) rather than true understanding of the mechanism of noise generation. Applying the method of measuring the Acoustic Intensity, the troublesome spots of the device can be found, the frequency analysis can be performed, and the total acoustic energy produced can be calculated.

The method was applied in an in-duct situation for a vane-axial fan. Mapping of the flow area required special treatment. Figure 2 shows the results of this effort.

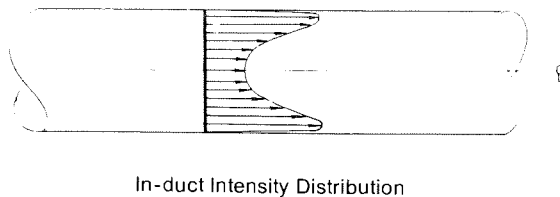


Fig. 2 In-duct mapping of the Acoustic energy flow

A very important observation from the result of Fig. 2 is that the above result represents only the "acoustical energy flow" for a particular operating point of a fan (set pressure rise and flow rate). The energy flow looks like a travelling ring and the pattern reaches its "fully developed" shape downstream. The profile of the acoustic energy flow is very similar to that of fluid velocity as it reaches a fully developed velocity profile downstream.

The biggest problem in applying this method for an in-duct situation is that the flow is fluctuating and analysis becomes very difficult. Separation of noise and flow fluctuation is a rather difficult job. Also, the minor changes due to the variation of the operating point of the device results in drastic changes in the readings. Neglecting those difficulties the simplest test, that of operating point, is presented here.

It is well known that the design point of a device is the "best" for it to operate at. Very commonly though engines are operating over a range of conditions. It is odd to find that for the case of axial fans the best operating point, from the point of noise generation, is not the design point but the peak pressure point. Figure 3 outlines the behavior of a typical axial fan.

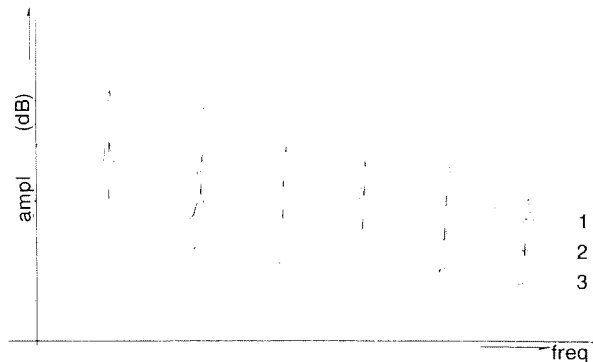


Fig. 3. Narrow band frequency analysis for a vane-axial fan

What is really happening to the flow and what makes the device more noisy? Before answering this question (which is not easy!) it may be wise to take a look at the performance characteristics of a vane-axial fan. Figure 4 outlines this performance.

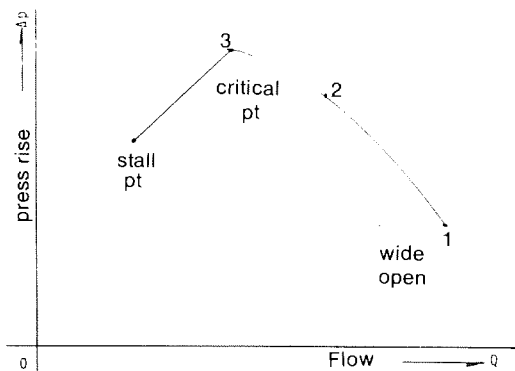


Fig. 4. Typical behaviour of a vane-axial fan

Combining the information from figures 3 and 4 it is clear that the more the flow the more the noise. An immediate suggestion about the noise can be suggested: turbulence might be the problem! Here is a case at which the acoustic intensity helped to overcome the guessing!

After applying the "two microphone technique" the pattern shown in Figure 5 was obtained.

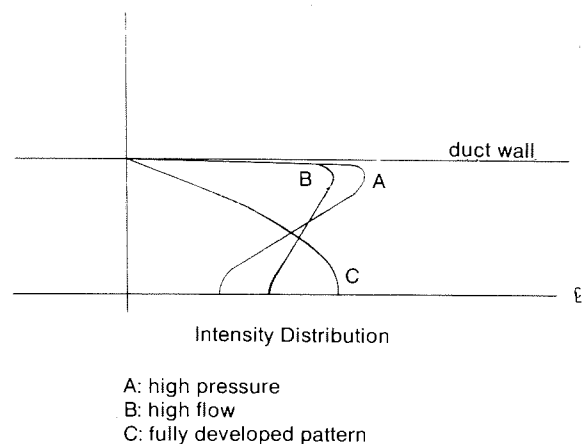


Fig. 5. Mapping using an intensity probe at two different operating points.

Clearly the mapping of the flow area outlines two different distributions. The mapping reveals that there are two distinct noise generation mechanisms. The high flow results in more acoustic energy being generated at the hub of the impeller and the low flow (high pressure) results in higher reading at the tip of the blades.

The above mapping resulted in the examination of the noise generation and gave an answer which is hard to imagine. A detailed explanation of the noise generation is not easy to give due to the speed and loading of the blades. A simple explanation though is that the high

pressure rise across the impeller results in high leakage across the suction and pressure sides of the blades which in turn produces noise. The high flow results in high turning angles and turbulence at the hub of the impeller.

References:

1. F.J. Fahy, 1977. *Measurement of Acoustic Intensity Using the Cross-Spectral Density of two Microphone signals.* JASA, 62, 1957-1059.
2. J.Y. Chung & D.A. Blaser, 1980. *Transfer Function Method of Measuring In-Duct Acoustic properties.* JASA, 68, 907-913.

**Personal Computers
Matrix Printers
Laser Printers
Networks
Disk Drives
Terminals
Telefax
Satellite Antennas**

Total solutions

With so many different standards and daily advancements in the personal computer industry it is very difficult to stay informed

And yet you must in order to select the best products for your company and your own personal computer.

At Galatariotis Brothers Ltd you can find one of the widest range of computer & communication products, of the latest and most advanced technology from leading computer companies, like NEC Corporation, ITT, QUME, ASI etc.

Furthermore, Galatariotis has the backing and resources that assure its customers of proper and continuing support

You are on the safe side ...

Galatariotis



Computers & Communications

NICOSIA 1 Souliou Str. Strovolos Tel 313171
LIMASSOL 87 Gladstones Street Tel 76156
LARNACA 23A Greg Afrentiou Str Tel 55757

Thermography in medicine

A.K. Kaplanis MSc, MBES, AMIEE, FIHospE
Lecturer, HTI

Abstract

This review article attempts to give the general principles and applications of a technique known as Thermography, which is used to provide diagnostic information, non-invasively, for many disorders or diseases.

Introduction

Thermography is a technique by means of which the infra-red radiation emitted by a body is detected, amplified, analysed and processed as to produce a thermogram or thermal image of the surface of the body under examination, on a screen, with distinctive colours.

In effect the technique measures the amount of heat emitted through the skin and the thermograms so produced appear "bright" where there is a "hot spot" area under the skin or "dark" when the area is cool.

Thermograms are used to map out blood vessels and thus circulation of the blood, to detect tumours and arthritic disturbances, to investigate bone fractures which may be undetectable using x-rays, to locate the exact position of tissue destruction for removal by surgery where necessary and many other illnesses.

Theory

All objects emit infra-red radiation.

The intensity of this radiation depends on the temperature of the object, above zero degrees kelvin.

When a body radiates or absorbs all the incident radiation of a given wavelength, that body is said to be a "Black Body" and its emissivity, ϵ , is then said to be one.

The human body emits infra-red radiation, (electromagnetic power), continuously in a restricted wavelength range in the electromagnetic frequency spectrum and its emissivity is about 0.95 which means that it can be considered as almost one, that is a "black body".

The intensity of the infra-red radiation of a black body depends on its temperature and the figure below shows the proportion of the short wave radiation emitted at various temperatures.

Figure 1 shows that as the temperature of the black body increases, the wavelength at which maximum radiation occurs decreases.

This fact is formulated by Wien's Law as follows:

$$\lambda_{\max} \propto \frac{1}{T}$$

$$\text{In fact it can be shown that } \lambda_{\max} = \frac{2898}{T} \approx \frac{2900}{T}$$

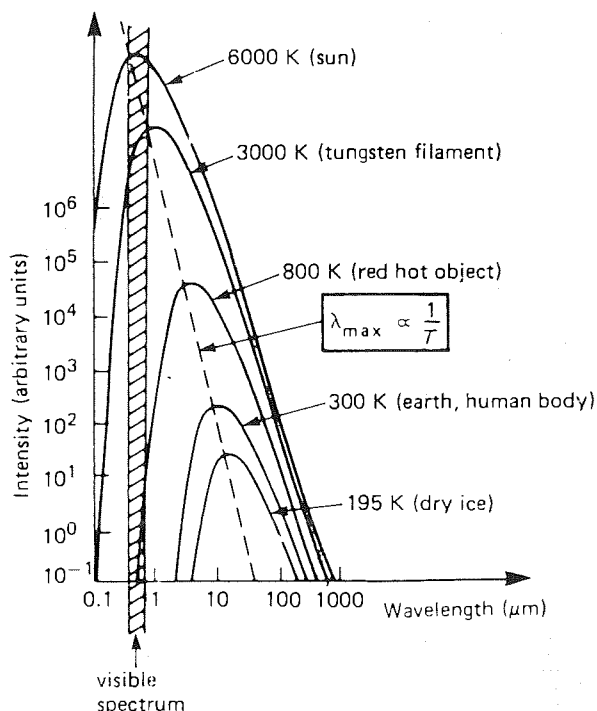


Fig. 1 Black body radiation at various temperatures

Now the core temperature of the central organs of the human body (heart, kidneys, lungs etc), is maintained fairly constant under normal circumstances at 37°C.

However the temperature at the surface of the skin varies from location to location (depending mainly on the circulation below the skin surface), and has an average value of 33°C.

With a skin surface temperature of about 33°C, $T = 273 + 33 = 306^{\circ}\text{K}$, say roughly 300°K, and from the figure it will be noted that the wavelength in microns, (or micrometers), at which the body radiates maximally is about 9.5 microns.

According to the Stefan-Boltzman Law, the total power emitted at all wavelengths by a body is given by the equation:

$$P = \sigma \cdot \epsilon \cdot T^4 \text{ watts/m}^2$$

where

P = Total power emitted at all wavelengths,

σ = Stefan's constant = $5.7 \cdot 10^{-8} \text{ W M}^{-2} \text{ T}^{-4}$

T = Temperature of the body in °K

If the temperature of the surface of the skin is at a temperature of T_s degrees Kelvin and the person under examination is in an environment where the ambient temperature is $T_A^{\circ}\text{K}$, then

Stefan-Boltzman equation becomes:

$$P = \sigma \cdot \epsilon \cdot (T_s^4 - T_A^4) \text{ watts per metre square, (w m}^{-2}\text{).}$$

And if the surface area of the skin, (which depends on the height and weight of the person), is A sq. metres, the energy emitted by the body is:

$$E = \sigma \cdot \epsilon \cdot A \cdot (T_s^4 - T_A^4); \text{ watts per second.}$$

Actually the effective radiating area of the body is about 80% of the body's surface area, hence the energy emitted by the body becomes:

$$E = 0.8 \cdot \sigma \cdot \epsilon \cdot A \cdot (T_s^4 - T_A^4)$$

If we assume a skin surface temperature of 33°C, that is 273+33=306°K and the subject under examination is in an environment of ambient temperature 22°C, i.e 295 °K, then the power radiated from the human body will be:

$$P = 0.8 \cdot 5.7 \cdot 10^{-8} \cdot 0.95 \cdot 1.8 \cdot (306^4 - 295^4)$$

$$P = 93 \text{ Watts approximately.}$$

Since the temperature of the skin varies from location to location, T_s is not constant and thus the energy radiated from the scanned human body will vary.

The above forms the basis of thermography.

In Thermographic examinations the patient lies on a table and a Thermographic camera scans the part of the body to be investigated.

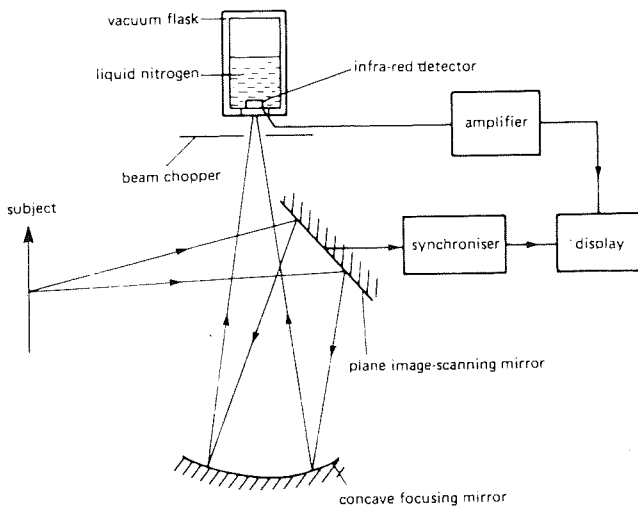


Fig. 2 Thermographic camera

The infra-red rays emitted from that part of the body are reflected by a plane image-scanning mirror onto a concave focusing mirror, which focuses the radiation on a small infra-red detector as shown in figure 2.

The infra-red detector is in effect a photoconductor made of indium antimonide material and a small voltage is produced across its terminals when the incoming radiation from the surface of the skin impinges on it.

This voltage which in effect represents the temperature distribution of the part of the body being examined is applied to a system of amplifiers where it is amplified and processed and thence applied to the cathode ray tube which

displays the signal on the screen, producing a spot of light the intensity of which varies according to the temperature of the point under examination.

The image-scanning mirror is made to oscillate about a vertical axis in order to scan a strip of the portion of the body and after each scan the mirror is made to rotate through a small angle about the horizontal axis thereby scanning a new strip of the subject.

The radiant flux from the body is scanned both vertically and horizontally similar to a television picture and the vertical and horizontal movements of the image-scanning mirror are fed to a synchroniser and thence to a display.

In this way the spot on the screen and the point on the body whose temperature is being monitored are synchronised and a picture is displayed showing the surface temperature distribution of the subject or patient.

The incident infra-red rays are of very low intensity and thus the noise voltage which depends on the temperature, $e_{\text{noise}} = \sqrt{4KTBR}$ can be troublesome.

For this reason the I.R. detector is enclosed in a housing containing liquid-nitrogen which cools down the infra-red detector and keeps the noise voltage down to a minimum.

To improve the accuracy and the clarity of the thermograms it is recommended that the examination room be thermostatically controlled as to be cool and dry and in addition the skin to be examined should have a ten minute precooling period at about 20°C.

As was stated already thermograms are used, amongst many applications, to detect and map out blood circulation.

The pictures in the next page are Thermograms which show how smoking can affect blood circulation in hands and fingers of a smoker are shown in the next page.

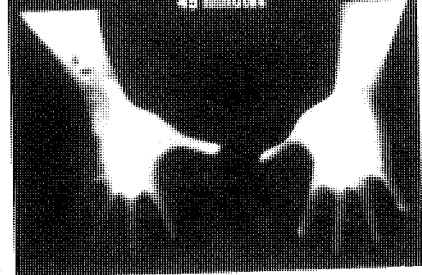
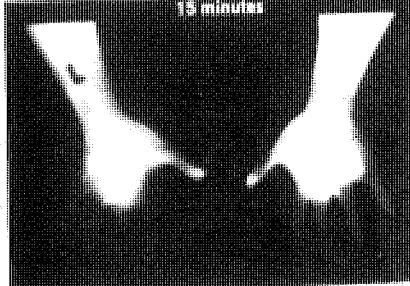
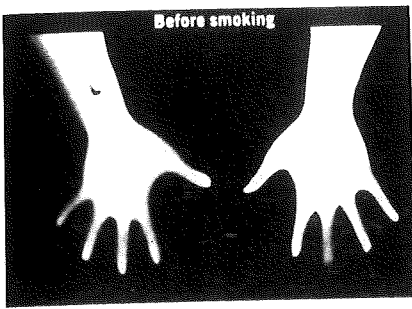
Conclusion

Thermography is a relatively new technique as a diagnostic tool of many illnesses and its future is promising in view of the fact that it is considered to be absolutely safe and, more important, non-invasive.

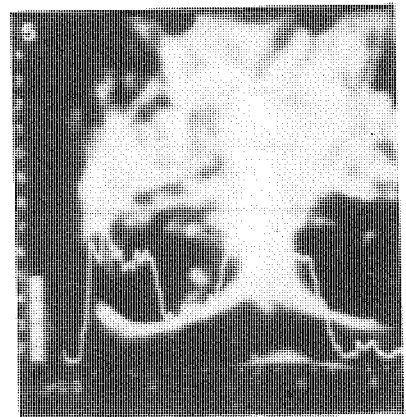
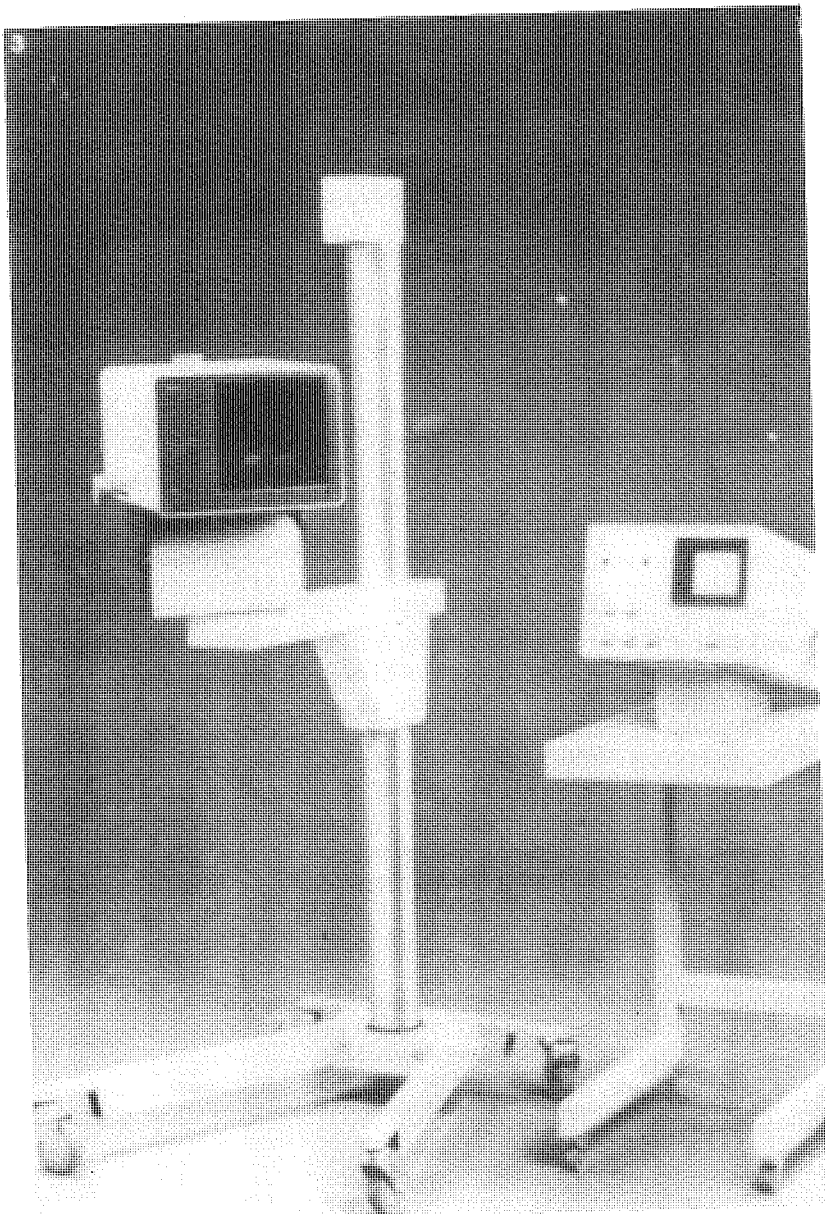
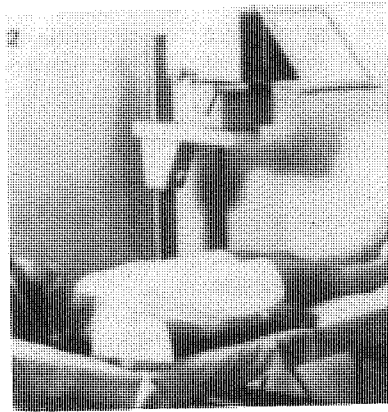
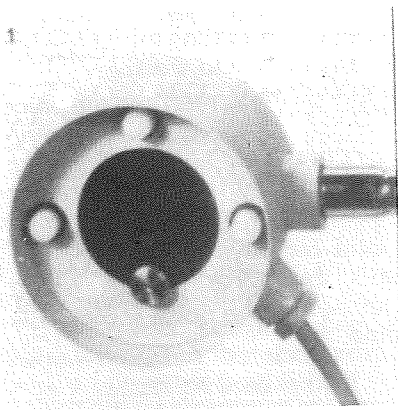
Thermography is expected to be improved further still for prognostic and diagnostic information for many more if not all illnesses with little or no "false" results.

References

- ... MSc Course Notes by Dr. D. Jones.
- ... Medical Physics by J. Pope.
- ... Encyclopedia Americana.
- ... Medical Instrumentation by J. G. Webster.
- ... Various literature from manufacturers of Thermographic units



One of the many types of commercially available Thermographic units is shown below.



1. Temperature Reference Source
2. Medical Thermograph with Mirror
3. Medical Thermograph
4. Vascular Pattern of Female Breast
5. Thermal Profile showing Temperature Distribution along the Scanning Line

Solar Radiation

Sotiris Kaloyirou
HTI Diploma
Laboratory Assistant, HTI

1. INTRODUCTION

For the visitors who come for the first time to Cyprus, the first thing they notice is that practically every single house is equipped with a solar collector. Because of the location of Cyprus 35 Degrees North latitude the solar radiation falling on a surface in the Summer months is quite large, in the range of 1000 W/m^2 . Thus from about 1973 the utilisation of solar energy was steadily increasing primarily due to the oil embargo. Thus it is very important to know the factors affecting the operation of the solar systems. The primary of them, the input of the systems, is the Solar Radiation.

In this article an attempt will be made to analyse the various factors influencing the solar radiation for the locality of Cyprus. These will include the Solar Angles determination, the direct normal intensity and the diffuse solar radiation. At the end the various factors will be analysed by means of a computer program written for this purpose.

2. SOLAR RADIATION

The intensity of solar radiation on a surface normal to the sun's rays beyond the earth's atmosphere at the mean earth-sun distance of $92,897,400 \pm 100$ miles is defined as the solar constant, I_{sc} . The currently accepted value of I_{sc} is 1372 w/m^2 . This reflects recent spacecraft measurements. Because the earth's orbit is slightly elliptical and the extraterrestrial radiation intensity I_0 varies inversely as the square of the earth-sun distance. I_0 ranges from a maximum of 1417 w/m^2 on January the 3rd, when the earth is closest to the sun, to a minimum of 1328 w/m^2 on July the 6th, when the earth-sun distance reaches its maximum. I_0 is not related to the earth's tilt i.e. season.

The earth's orbital velocity varies throughout the year, so the Apparent Solar Time (AST) varies slightly from the mean time kept by a clock running at a uniform rate. The variation is called the Equation of Time (ET). In solar radiation calculations, Apparent Solar Time must be used to express the time of a day. Apparent Solar Time is based on the apparent angular motion of the sun across the sky. The time when the sun crosses the meridian of the observer is the local solar noon. It usually does not coincide with the clock time of the locality. The standard clock time is reckoned from a selected meridian near the centre of a time zone. Since the sun takes four minutes to transverse one degree of longitude, a longitude correction term of $4 (\text{longitude}_{st} - \text{longitude}_{local})$ should be added to the standard clock time of the locality. For the locality of Cyprus the Longitude is the Greenwich which

have a longitude of zero degrees. If we consider the city of Nicosia for which the longitude local is 33.33 degrees the correction is:

$$-4 (0 - 33.33) = +133.32 \text{ min.}$$

But 120 min are estimated so the difference is $+13.32$ min.

The general equation for calculating the Apparent Solar Time (AST) is:

$$\text{AST} = \text{LST} + \text{ET} - 4 (\text{longitude}_{st} - \text{longitude}_{local}) \quad \text{---(1)}$$

where: LST= Local standard Time

ET= Equation of time (minutes)

The values of the Equation of Time as a function of time of year can be obtained from the following empirical equation:

$$\text{ET} = 9.87 * \sin 2B - 7.53 * \cos B - 1.5 \sin B \quad \text{---(2)}$$

$$\text{where } B = \frac{360}{364} (N - 81)$$

Where N = day of the year (1 to 365)

In passing through the earth's atmosphere, the sun's radiation is reflected, scattered and absorbed by dust, gas, molecules, ozone and water vapour. The extend of this depletion at any given time is determined by atmospheric composition and length of the atmospheric path traversed by the sun's rays. This length is expressed in terms of the air mass, m , the ratio of the mass of the atmosphere in the actual earth-sun path to the mass which would exist if the sun were directly overhead at sea level ($m = 1.0$). For all practical purposes, the air mass at any time equals the cosec of the solar altitude, multiplied by the ratio of the existing barometric pressure to 760 mm Hg ($10.343 \text{ m H}_2\text{O}$). Beyond the atmosphere, $m = 0$.

Most ultraviolet solar radiation is absorbed by the ozone in the upper atmosphere, while part of the radiation in the short-wave portion of the spectrum is scattered by air molecules, imparting the familiar blue color to the sky. Water vapour in the lower atmosphere causes the characteristic absorption bands observed in the solar spectrum at sea level.

Some shortwave radiation scattered by air molecules and dust reaches the earth in the form of diffuse radiation I_d . Since this diffuse radiation comes from all parts of the sky, its intensity is difficult to predict and varies as moisture and dust content of the atmosphere change throughout any given day. On a completely

overcast day, the diffuse component accounts for all solar radiation reaching the earth.

Some energy absorbed by carbon dioxide and water vapour in the sky reaches the earth in the form of long-wave atmospheric radiation.

The total shortwave radiation I_t , reaching a terrestrial surface is the sum of the direct solar radiation, I_b , the diffuse sky radiation, I_d , and the solar radiation reflected from the surrounding surfaces, I_r . But

$$I_D = I_{DN} * \cos \theta \quad \text{---(4)}$$

where I_{DN} is the direct normal irradiation, and θ is the angle of incidence between the incoming solar rays and the normal to the surface.

$$\text{So: } I_t = I_{DN} * \cos \theta + I_d + I_r \text{ [w/m}^2\text{]} \quad \text{---(5)}$$

3. SOLAR ANGLES DETERMINATION

The earth's orbit around the sun is elliptical. While the earth makes its daily rotation and yearly revolution, the sun also rotates on its own axis approximately once every earth month. The earth's axis of rotation (polar axis) is always inclined at an angle of 23.5 degrees from the ecliptic axis which is normal to the ecliptic plane. The ecliptic plane is the plane of orbit of earth

around the sun. The inclination of earth from the straight-up position in reference to the plane of orbit makes the northern hemisphere tilting toward the sun in summer and away from the sun in winter, therefore producing the seasonal variation on earth. At the winter solstice (December 21), the north pole is inclined 23.5° away from the sun. At the summer solstice (June 21) the reverse is true. At the spring and fall equinoxes (March 21 & September 21 respectively), the north and south poles are equidistant from the sun, thus all points on the earth's surface have 12 hours of daylight and 12 hours of darkness.

Because the solar radiation is a function of the geometry of the receiving surface relative to the sun it is imperative to notice several geometric angles showing the sun earth's surface relations. The various angles of interest are shown in figures 1 and 2. The mathematical equations, of them are given below. A further description of each angle can be found in the bibliography.

1. The solar declination angle: δ

$$\delta = 23.45^\circ \sin \left[\frac{360}{365} (284 + N) \right] \quad \text{---(6)}$$

where N is the day of the year (1-365)

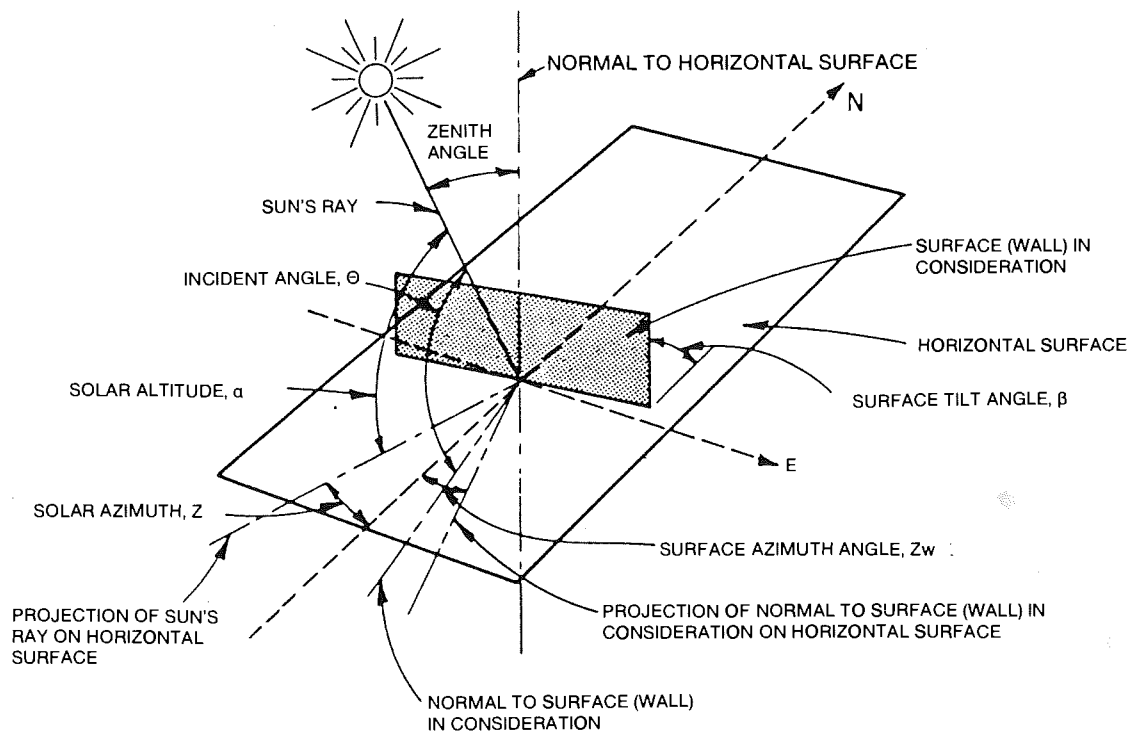


Figure 1 Solar Angles for Tilted and Horizontal Surfaces

2. The hour angle: h

$$h = \pm 0.25 * (\text{Number of minutes from local solar noon}) \quad \text{---(7)}$$

where the + sign applies to afternoon hours and -sign to morning hours.

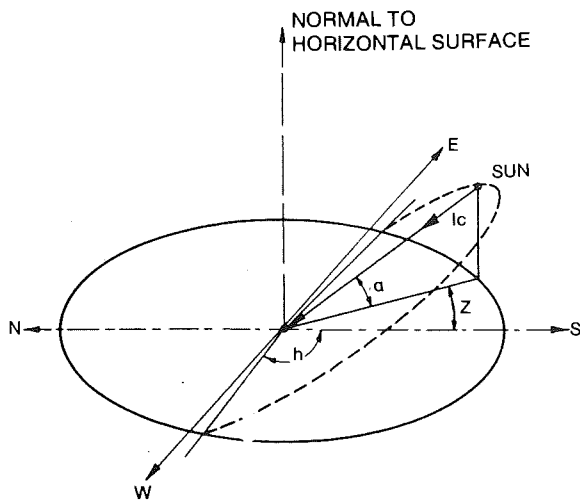


Figure 2 Schematic Showing Apparent Path of Sun and Hour Angle

Note:

Hour angle h , is an expression of the Apparent Solar Time (AST) in degrees. At solar noon $h = 0$ and $AST = 0$. Therefore from equation (1), Local Standard Time (the time shown by our clocks at solar noon) is:

$$LST = -ET + 4 (\text{longitude}_{St} - \text{longitude}_{local}) \quad \text{---(8)}$$

OR $LST = 13.32 \text{ min} - ET$

3. The Solar Altitude angle: a

$$\sin a = \sin L * \sin \delta + \cos L * \cos \delta * \cos h \quad \text{---(9)}$$

where L = Latitude

4. The Solar Azimuth angle: z

$$\sin z = \cos \delta * \sin h / \cos a \quad \text{---(10)}$$

5. The Incident angle: i

$$\cos i = \sin L * \sin \delta * \cos \beta - \cos L * \sin \delta * \sin \beta * \cos \psi + \cos L * \cos \delta * \cos \beta + \sin L * \cos \delta * \cos \beta * \sin \psi + \cos \delta * \sin h * \sin \beta * \sin \psi$$

where ψ = surface azimuth angle

It is often necessary to determine the sunrise and sunset hours and the length of a particular day. The hour angle at sunset, h_s , can be found by solving Eq. 9 for h when $a=0$. Thus

6. Sun Set hour, h_s

$$\cos h_s = -\tan L * \tan \delta \quad \text{---(2)}$$

where h_s is taken as positive at sunset. Since the hour angle at local solar noon is zero, with each 15° of longitude equivalent to one hour, the sunrise and sunset time in hours from local solar noon is then:

$$h_s = \frac{1}{15} \cos^{-1} (-\tan L * \tan \delta) \quad \text{---(13)}$$

and the length of the day is given by:

$$\text{Day length} = \frac{2}{15} \cos^{-1} (-\tan L * \tan \delta) \quad \text{---(14)}$$

4. DIRECT NORMAL SOLAR INTENSITY

At the earth's surface on a clear day, direct normal Solar Intensity, IDN is represented by:

$$IDN = \frac{A}{\exp(B/\sin \alpha)} \text{ (w/m}^2\text{)} \quad \text{---(15)}$$

where: A = apparent solar irradiation at air mass = 0
 B = atmospheric extinction coefficient.

Values of A and B vary during the year because of seasonal changes in the dust and water vapour content of the atmosphere, and because of the changing earth-sun distance. Values for A and B are shown in table 1. These data do not give the maximum value of IDN that can occur in each month, but rather are representative of conditions on average cloudless days. For very clear atmospheres, the value of IDN can be 15% higher than indicated by Equation (15), using values of A and B in table 1.

TABLE: 1
DATA FOR THE 21st DAY OF EACH MONTH

MONTH	A	B	C
	w/m ²	(Dimensionless Ratios)	
JAN	1208.8	0.142	0.058
FEB	1193.3	0.144	0.060
MAR	1165.3	0.156	0.071
APR	1115.7	0.180	0.097
MAY	1084.8	0.196	0.121
JUN	1069.4	0.205	0.134
JUL	1066.2	0.207	0.136
AUG	1056.4	0.201	0.122
SEP	1132.1	0.177	0.092
OCT	1171.6	0.160	0.073
NOV	1199.6	0.149	0.063
DEC	1211.9	0.142	0.057

5. DIFFUSE SOLAR RADIATION

The diffuse radiation falling on any surface consist of radiation from the sky and part of the reflected solar radiation from adjacent surfaces, particularly the ground lying south of the surface in question. The radiation from the sky does not come uniformly from all parts of the sky, and the ratio of diffuse radiation incident on a vertical surface to that falling on a horizontal surface has been related approximately to the sun's incident angle for the vertical surfaces. This ratio of vertical-to-horizontal radiation from the sky varies from low 0.45 for the sun behind the surface at high incident angles, up to 1.2 with the sun coming in at very low angles.

A simplified general relation for the diffuse solar radiation I_{ds} that falls on any surface from a clear sky is given approximately by:

$$I_{ds} = C * I_{DN} * F_{ss} \text{ (w/m}^2\text{)} \quad \text{--- (18)}$$

where: C is the diffuse radiation factor given in table 1

C * I_{DN} is the sky radiation falling on a horizontal surface, and

F_{ss} is the angle factor between the surface and the sky.

i.e., the fraction of shortwave radiation emitted by the sky that reaches the tilted surface (dimensionless)

F_{ss} is 0.5 for vertical surfaces and 1.0 for horizontal surfaces.

For other surfaces,

$$F_{ss} = (1.0 + \cos \beta) / 2 \quad \text{--- (17)}$$

where β is the surface tilt angle measured upward from the horizontal plane (fig. 1)

diffuse reflection at an adjacent surface is the intensity falling on the reflecting surface times its reflectance multiplied by the angle factor between the receiving surface and the reflecting surface.

Ground - reflected radiation includes the diffuse sky and direct solar radiation incident on a horizontal surface. The intensity of the total solar radiation falling on the ground is given by:

$$I_{tH} = I_{DN} (c + \sin \alpha) \quad \text{--- (18)}$$

In equation (18) the term I_{DN} * sin α is the direct radiation falling on the ground. This ground - reflected diffuse radiation incident to any surface can be estimated by:

$$I_{dg} = I_{tH} * \rho_g * F_{sg} \quad \text{--- (19)}$$

where: ρ_g is the reflectance of the foreground (dimensionless)

F_{sg} is the angle factor between the surface and the ground (dimensionless)

The sum of the angle factors equals 1.0, and the angle factor for surface to ground is:

$$F_{sg} = (1 - \cos \beta) / 2 \quad \text{--- (20)}$$

If the surface is exposed to only the ground and the sky, then the sky angle factor is:

$$F_{ss} = 1 - F_{sg} \quad \text{--- (21)}$$

The reflectance values for different types of materials can be found from handbooks. Values for a number of common types of ground surfaces are given in table 2. These values apply for various angles of incidence and surfaces.

**TABLE 2:
SOLAR REFLECTANCES OF VARIOUS SURFACES**

FOREGROUND SURFACE	INCIDENCE ANGLE (Deg.)					
	20	30	40	50	60	70
New concrete	0.31	0.31	0.32	0.32	0.33	0.34
Old concrete	0.22	0.22	0.22	0.23	0.23	0.25
Bright green grass	0.21	0.22	0.23	0.25	0.28	0.31
Crushed rock	0.20	0.20	0.20	0.20	0.20	0.20
Asphalt	0.09	0.09	0.10	0.10	0.11	0.12

6. COMPUTER PROGRAM

As the reader realises there is a lot of calculation work that has to be performed in order to get the values of the various parameters. For that purpose a computer program has been written in order to make life easier. The results of such program are shown in table 3. For that results the input was: Latitude 35 Deg. North, surface tilt angle = 0 Deg., i.e. horizontal, at noon each 21st day of the month. The output of sun set and sun rise time is in "hours. hundreds of hour". The units of solar radiation is w/m².

7. BIBLIOGRAPHY

- A. PRINCIPLES OF SOLAR ENGINEERING By Frank Kreith & Ian F. Kreider.
- B. ASHRAE FUNDAMENTALS HANDBOOK.
- C. ASHRAE APPLICATIONS HANDBOOK.

TABLE 3

ESTIMATION IS FOR THE 21 st DAY OF EACH MONTH

MONTH	DECLINATION ANGLE	ALTITUDE ANGLE	AZIMUTH ANGLE	SUN RISE TIME	SUN SET TIME	TOTAL RADIATION
JAN	-20.12	34.57	-7.00	7.40	17.42	836.51
FEB	-11.22	43.33	-9.29	6.99	17.93	792.58
MAR	-0.66	54.00	-9.02	6.38	18.32	715.03
APR	11.09	65.93	-7.30	5.68	18.73	629.53
MAY	19.83	74.67	-8.74	5.19	19.14	590.43
JUN	23.45	78.01	-16.57	5.07	19.43	578.43
JUL	20.45	74.84	-17.62	5.31	19.33	584.57
AUG	11.78	66.50	-9.87	5.71	18.83	598.81
SEP	0.12	55.10	-2.37	6.08	18.10	687.97
OCT	-11.22	43.78	0.88	6.49	17.42	768.62
NOV	-20.12	34.88	-0.02	6.99	17.01	823.35
DEC	-23.45	31.48	-3.31	7.38	17.03	842.11

Contingency Plans for Time-Constrained Systems

Christophoros A. Solomou BSc MSc MIEEE
Lecturer, HTI

1. Introduction

Applications such as Computer Integrated Manufacturing (CIM), distributed network management, chemical and nuclear process control, automatic mobile units, and knowledge source control in expert systems require the time-constrained processing of large amounts of data. In traditional real-time applications (e.g., banking, reservations) the timing constraint or deadline for a transaction is normally specified to be 2-3 seconds since for humans this is an optimal response time. No disaster will result if at one time the actual response time is 5 seconds. In contrast, in a truly time-constrained environment the correctness of a result produced by a task (a program unit in execution) depends also on the timeliness of the result.

Contingency plans are alternate actions that can be invoked whenever the system determines that it cannot complete a task in time. Contingency plans become particularly attractive for handling long overload conditions. Contingency plans should be provided for selected tasks in a way that is transparent to other tasks also being served by the local/short-term scheduler.

In time-constrained real-time systems, tasks are expected to complete before their prescribed deadlines. Failure to meet a deadline in hard real-time systems, results in financial or environmental disaster; for soft real-time systems, results produced after the task deadline will simply have a reduced value. In the scheduling of tasks, the scheduler receives as input the task execution time (if known), its criticality or priority and deadline. In a static environment where the number of tasks and their requirements are static, i.e., they are known in advance, a schedule can be produced so that all tasks are guaranteed to complete before their prescribed deadlines. However, the situation is more complex in a dynamic environment. For example, in a radar tracking system, the number of objects being monitored vary with time. Also, failure of one processor may cause other processors to be assigned execution of the tasks on the failed processor; this may have an effect on the completion time of tasks.

2. Related Work

Related work [1] obtains and returns results from partially complete computations due to tasks which have failed to complete by their prescribed deadline. These are called *imprecise results* because the task which was producing them did not complete. Partial results are obtained using two different methods. In the first method, the *milestone* approach, results are recorded at different points in the execution of a

task. If the task deadline is not met, the last recorded values are returned as the result. In the second method, called the *sieve* method, selected code sections may be skipped in order to reduce execution time (execution of this code merely improves existing results; not executing them results in the production of less precise results). It is up to the scheduler to decide whether or not the selected (or marked) code sections should be skipped.

The disadvantage with these methods is that they are only suited to iterative algorithms (e.g., Newton's method, Fast Fourier Transform, etc.). Also the schemes proposed, especially the sieve method, require a powerful task scheduler and may involve extra overhead. Consequently, we take the position that both imprecise results and contingency plans should be supported in a real-time environment. We believe that they are complements and not replacements of each other.

3. Task Progress Notion

Task progress is a measure of how well the task is proceeding to completion. The progress made by a task may be based on the amount of resources allocated to it. In particular, task progress can be best estimated in terms of the amount of work completed so far (both CPU - and I/O-bound task work). The estimation must take into account the slack time for the task (defined as the time remaining before the task deadline is reached minus the estimated remaining task runtime).

The success of CPU scheduling depends upon the following observed property of tasks: a task execution is a cycle of CPU execution and I/O wait. Tasks alternate back and forth between these two states. Task execution begins with a CPU burst. It is followed by an I/O burst, which is followed by another CPU burst, then another I/O burst, and so on.

4. Task Progress Check-Points

An important question is the following: when should a new estimate of task progress be taken? We propose estimation of a new value of the task progress made so far, on occurrence of any of the following events:

- (1) task transition from state WAITING to READY, and
- (2) time-out condition if event (1) does not trigger in time

Occurrence of the first event signifies completion of one complete CPU-I/O cycle on behalf of the task. In a real-time environment, a CPU-I/O cycle is expected to have the following state transitions: READY -->CURRENT-->WAITING-->READY. It is being assumed that

tasks are preempted only when they are about to perform an I/O operation or wait for locked resources to become available. Consequently, the transition from CURRENT to READY is assumed not to exist. A closer examination of the CPU-I/O cycle, reveals the following:

- in the READY state the task is waiting to use the CPU,
- in the CURRENT state the task is using the CPU,
- in the WAITING state, a task waits for its I/O request to be serviced by the lower-half of a device driver, and once serviced, waits for the actual device to complete the operation.

Thus at different points in a cycle, a task is either active (using a resource such as the CPU or disk) or passive (waiting to use a resource).

The only information which needs to be collected about a task is the length of the period for which the task is active. The lower-half of a device driver, can record the time taken by a task to complete its I/O (waiting time to use the device is excluded; We are only interested in the time for which the device was in use by the task). Also, the task dispatcher can record the length of the period during which the task is in state CURRENT.

5. Progress Estimation for Tasks with Known Exec Times

We define task progress factor (TPF) to be the ratio of the actual task execution time and expected task execution time at the point in time where the value for TPF is being computed. As already pointed out above, during a CPU-I/O cycle a task is normally both active and passive. If the system is overloaded, tasks spend most of the cycle time in the passive state. If the system is underloaded, tasks spend most of the cycle time in the active state. Thus, a possibly good time for computing a new value for TPF is at the end of C CPU-I/O cycles (where C, may be a static or dynamic parameter of the scheduler).

For the calculation of TPF, it is assumed that the task deadline D, and estimated task execution time EET are given/known (EET is defined to be the task runtime in a system where it is the only task i.e., where there is no contention for resources). Calculation of TPF for a specific task at time T_i (relative to its execution) is based on the following simple formula:

$$TPF = AAT / ((T_i * EET) / D)$$

where AAT (actual active time) represents the amount of time for which the task was active.

To illustrate, consider the following example task, for which the TPF is computed at the end of some CPU-I/O cycle 600 milliseconds after task execution was initiated. It is being assumed that D is 1200 ms, EET is 500 ms, and that at $T=600$ the $AAT=150$ ms

$$\text{at } T=600 \quad TPF = 150 / ((600 * 500) / 1200) \\ = 0.6$$

rationale:

at $T=D=1200$ task is expected to be active for $EET=500$

at $T=T_i=600$ task is expected to be active for EAT thus,

$$EAT = \text{Expected Active Time} = (EET * T_i) / D \\ = (500 * 600) / 1200 \\ = 250$$

AAT = Actual Active Time = 150

$$TPF = \text{Task Progress Factor} = AAT / EAT \\ = 150 / 250 = 0.6$$

A TPF value of 1.0 implies that the task is moving to completion at just the right rate; a value less than 1 implies that the task is progressing at a rate which if continued will make it impossible for the task to meet its deadline; a value greater than 1 implies that task is progressing at a rate which if allowed to continue will allow completion before the deadline.

As already mentioned, new values of TPF are to be computed at the end of every C CPU-I/O task cycles. We define TPF-i to be the task progress factor computed at the end of the i-th cycle set. For a task which has completed N sets, the following set of TPF values becomes available: {TPF-1, TPF-2, ..., TPF-n}. Thus, TPF-n is in fact the last measure available of task progress. If this is greater than an upper critical value (UCV), say 0.85, then the task is progressing at a rate that is satisfactory. On the other hand, if it is less than a lower critical value (LCV), say 0.60, then the task will probably not make its deadline.

However, in the case where TPF-n, is greater than LCV and less than UCV, then any scheduler action on the task must also take into consideration very recent progress data. This may be necessary, because unpredictability and occasional overloading during the last task cycle may cause the task to spend a large proportion of the last task cycle may cause the task to spend a large proportion of the cycle time in the passive state, thus also yielding a value for TPFn which is lower than TPFn-1. We propose that under such conditions, any scheduler action must take into account the K recentmost TPF values of the task (where K may be a parameter of the task scheduler).

5.1 Trend in Task Progress

In particular, we propose use of the K recentmost TPF values to compute an estimate of task trend towards progress. Trend is computed using the following formula:

$$w_1 * (TPF_n - TPF_{n-1}) + \\ w_2 * (TPF_{n-1} - TPF_{n-2}) + \\ \dots \dots \dots + \\ w_k * (TPF_{n-k} - TPF_{n-k-1})$$

where w_i = weighting factors

A positive value indicates an increase in the rate with which the task is proceeding to completion, whereas a negative value is an indication that the opposite is occurring. Weighting factors are being proposed so that most recent TPF values are given greater weight.

For real time systems, the value of K should be small, as task schedulers are expected to use the

"earliest-feasible-deadline", "smallest-slack-time" algorithms, or variations of these. A task at the start of its execution is unlikely to have the earliest feasible deadline or the smallest slack time among all tasks. Consequently, during the very early stages of its lifetime, a task will be mostly passive and as a result its first TPF values will be rather low.

5.2 An Example

To illustrate, consider a task which has just finished its sixth CPU-I/O cycle (assume $C=1$) and the scheduler has to decide whether to continue or abort the task.

It is known that,

$K=3$
 $w_1=3$ $w_2=2$ $w_3=1$
 $LCV=0.50$ $UCV=0.80$

It is known about the task that:

TPF1	TPF2	TPF3	TPF4	TPF5	TPF6
0.40	0.60	0.68	0.77	0.82	0.77

Thus, $LCV \leq TPF_6 \leq UCV$, implying that there is a need to compute the trend in task progress.

Trend = $w_1(TPF_6 - TPF_5) + w_2(TPF_5 - TPF_4) + w_3(TPF_4 - TPF_3)$

Trend = $3(-0.05) + 2(+0.05) + 1(+0.09)$

Trend = +0.04

5.3 Contingency Plans Using Auxilliary Tasks

Time-constrained systems should provide for the definition of some sort of contingency plans for some tasks which can be invoked when the task scheduler realizes that a time constraint cannot be met. We describe a method for implementing contingency plans which relies on the replacement, if necessary, of the executing primary task by an auxilliary task with a much lower estimated execution time. The primary task is normally an I/O-and/or CPU-intensive job, e.g., high resolution spatial search, image analysis. It is being assumed here, that the auxilliary task is less intensive and thus contention for disk and/or the CPU will be reduced significantly. Examples of auxilliary tasks are use of low resolution spatial search, partial image analysis, use of old aggregate data, and guess-making.

The basic idea is to replace the primary with the auxilliary task at some point in the lifetime of the primary task such that enough time is available for the auxilliary task to complete before the specific deadline. The decision will be made long before the task deadline by a component of the system kernel, the task scheduler. This is different from exception handling normally found in systems programming languages such as Ada. In an Ada program, the application will be informed on the failure of the primary task to meet its deadline long after the deadline.

Let

EET_p = estimated execution time of primary task

EET_a = estimated execution time of auxilliary task

D = task deadline

T_p = time at which primary task starts executing

T_a = time at which auxilliary task may have to start executing i.e., replace the primary task

In the interval $T_p - T_a$, it is guaranteed that only the primary task will be executing. At the point in time $t = T_a$, a decision will have to be made on whether the primary task will be allowed to continue or be replaced by the auxilliary task. The decision will be rather premature if the interval $T_p - T_a$ is much less than the interval $T_a - D$, i.e., we decide the action too early in the life of the primary task. On the other hand, if the interval $T_p - T_a$ is much greater than the interval $T_a - D$, it may be too late to start executing the auxilliary task, i.e., the latter may not have enough time to complete before the deadline D . Clearly, there are tradeoffs involved and an optimal value for T_a cannot be determined.

We propose, a simple method for computing a value for T_a such that the ratio of total time available to a task and estimated execution time is the same for both tasks. For the primary task this value is known to be equal to $(D - T_p)/EET_p$. Thus,

$T_a = D - (D - T_p)/EET_p * EET_a$

An example: If $D=1200$, $EET_p=500$, $EET_a=200$, $T_p = 0$

$T_a = 1200 - ((1200 - 0)/500 * 200) = 720$

Thus, $(D - T_p)/EET_p = (1200 - 0)/500 = 2.4$

and $(D - T_a)/EET_a = (1200 - 720)/200 = 2.4$

Any, or variations, of the following two algorithms may be used to decide the action to be taken at time T_a .

Algorithm 1:

```

If  $TPF_n < LCV$  Then
    Abort primary task
    Start execution of auxilliary task
Else
    If  $TPF_n > UCV$  Then
        do nothing
    Else
        Compute progress trend  $P_{Tr}$  using last N TPF values
        If  $P_{Tr} < 0.0$  Then
            Abort primary task
            Start execution of auxilliary task
        EndIf

```

Algorithm 2

Compute trend P_{Tr} using last N TPF values:

If $(TPF_n + P_{Tr}) < UCV$ Then

Abort primary task

Start Execution of auxilliary task

EndIf

6. Progress Estimation for Tasks with Unknown Exec Times

When approximate task execution times are not known, it is both theoretically and practically impossible to foretell whether or not the task will meet its deadline, since at any point in the lifetime of a task, the runtime remaining is unknown.

However, task progress can at least be monitored by viewing the execution process as a discrete process, where discrete points are the completion of CPU-I/O cycles. In turn, cycles may be grouped into segments of length S. Calculations on task progress can be made upon completion of the last cycle for the segment. For example, if S equals 3, then the length of each time segment will be given by the sum of the durations of 3 consecutive task CPU-I/O cycles.

As already pointed out, during a CPU-I/O cycle a task spends some of the time in the active state (using a resource) and the remaining time in the passive state (waiting to use a resource). We define cycle activity factor (CAF), to be the fraction of the cycle time during which the task was active. The CAF values of the cycles belonging to some segment may be used to produce an overall estimate of the fraction of segment time during which the task was active, defined as segment activity factor (SAF). The value of SAF may be used by the scheduler to decide possible actions. Segmentation is used, so that the action to be decided will be based on data for a long period of time; in this way biasing due to overloading or underloading conditions during one cycle only is removed. At the end of a segment, a value SAF may be computed by the scheduler using the following weighted formula:

$$\text{SAF} = \frac{w_1 \cdot \text{CAF}_1 + w_2 \cdot \text{CAF}_2 + \dots + w_S \cdot \text{CAF}_S}{w_1 + w_2 + \dots + w_S}$$

6.1 Contingency Plans using SAF

As already pointed out, the scheduler should not take any direct action such as abortion on tasks which are progressing at a very slow rate and whose execution times are unknown. However, indirect action may be taken by the scheduler. An obvious action would be to increase task priority or criticality. However, this would have an effect on the completion times of other tasks also served by this scheduler. This is unacceptable, as it would violate the principle of providing contingency plans for selected tasks in a way that ought to be transparent to tasks already admitted by the local scheduler.

An alternative action, is to temporarily disable the admission of new tasks by the local scheduler whenever the most recent SAF value of selected tasks happen to be less than some lower critical value. New tasks will have to be redirected by a global scheduler to some other processor. Admission of tasks may be reenabled when the most recent SAF value of all tasks being monitored, reaches an acceptable upper level. The main justification for the type of action proposed here, is that since admission of new tasks is disabled, the load on the system will be eventually reduced; consequently, tasks already admitted will tend to spend more of the CPU-I/O cycle time in the active state.

The following simple algorithm will be executed at the end of a segment and immediately after calculation of SAF.

```

If (SAF < LowerCriticalValue) Then
  If TaskId Not in Id-TABLE Then
    Disable admission of new tasks
    Insert Task-Id in ID-TABLE
  EndIf

Else
  If (SAF >= AcceptableUpperValue) and
    (Task-Id in ID-TABLE) Then
    Remove Task-Id from ID-TABLE
  If (ID-TABLE Is Empty) Then
    Enable admission of new tasks
  EndIf
EndIf
EndIf

```

6.2 Contingency Planning using Task Signals

For tasks with unknown execution times it is impossible for the scheduler to foretell whether they will be able to make their prescribed deadline. However, an executing task may inform the scheduler on the amount of work completed so far. For example, in a "template-matching" program, after half the templates are searched the task may send a signal to the local scheduler (possibly via a system call) informing it that fifty percent of the work is completed. Knowing the task deadline D, and the amount of time that elapsed since creation of the task, the scheduler may produce an estimate of task progress so far. If this turns out to be less than some lower critical value, the local scheduler may reject requests for admission of new tasks on this processor until progress rate for the task in question is restored to some upper acceptable value. Moreover, the signalling task may be informed on its progress so far and may take special action if necessary. Examples of such action include the use of old aggregate data, or the use of low resolution search on the remaining search space.

To illustrate, consider a process which reads records from a very volatile real-time file on which insertions and deletions are performed very frequently. Consequently, the execution time for a run is not fixed and depends on the number of records in the file at the time of the run; as far as the scheduler is concerned the execution time is not known. For this example, it may be assumed, that the task deadline is at $t=D=2000$ time units, and that at $t=1500$ a "signal" is sent to the scheduler by means of the "SignalScheduler" system call, informing it that 50% of the work is complete.

At normal progression rate, the task is expected at $t=1500$ to have completed $(t \cdot 100) / D = (1500 \cdot 100) / 2000 = 75\%$ of its total execution time. However, the task has completed only 50% of the total execution time, implying that an estimate for task progress at $t=1500$ is $50 / 75 = 0.67$.

```
Process ReadVolatileFile
```

```
l:=0;
while (Not End Of File) do
  Get Next Record
  ...
  l := l + 1
  If (l = FileSize/2) Then
    /** 50% of work completed ***/
    SignalScheduler (50%, Status)
  If (Status = PossibleDeadlineMiss) Then
    /** invoke optional special action **/
  EndIf
EndIf
EndWhile
EndProc
```

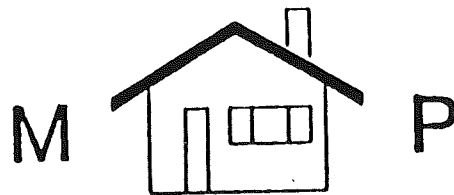
7. Closing Words

Contingency plans are alternate actions that can be invoked whenever the system determines that a task will not complete in time.

Unpredictability in execution time and data requirements is responsible for the failure of a number of tasks to meet their deadlines, despite the sophistication level of the task scheduling algorithm. The ideas presented in this paper for monitoring the progress task require further refinement. Perhaps, simulation experiments are needed to assess them. We believe, that contingency plans should be applied especially in advanced distributed real-time systems consisting of multiple processors and I/O storage devices with support for data replication. In this way, whenever the local scheduler of some processor inhibits admission of new tasks, the latter may be redirected by the global scheduler to a contingency processor.

References:

1. Lin K. J., Natarajan S., Liu J. W., "Imprecise results: Utilizing Partial Computations in Real-Time Systems", IEEE Real-Time Systems Symposium, p. 210, Dec 1987.
2. Stankovic J. A., Ramamritham K., "The Design of the Spring Kernel", IEEE Real-Time Systems Symposium, p. 146, Dec 1987.



Vassiliou Estates Property Services

P.O.BOX 3671, NICOSIA - CYPRUS

Κτηματικές Συναλλαγές, Αγορές, Πωλήσεις
Ενοικιάσεις, Διαχειρήσεις Περιουσιών

"You can trust us"
For further information please contact
Mrs Maroulla Vassiliou

29 Kasos Str., 1st floor, apt 105, Acropolis, Nicosia,
Tel: 02-466592, Fax: 02-466290

Calendar of Activities

Academic Year 1988-89

SEPTEMBER

- Final enrolments for the academic year 1988-89 were: 61 for Civil Engineering, 64 for Electrical Engineering, 65 for Mechanical Engineering, 26 for Marine Engineering and 33 for Computer Studies.

9 students enrolled for the Electromedical Course of the Regional Training Centre.

- Lectures commenced on Monday, 12 September.

- The HTI Director, Dr. Themis Drakos, visited the University of Pennsylvania between 9-17 September within a bilateral exchange programme.

During his visit Dr. Drakos led an "Operations Research" seminar and lectured on "Mathematical Modelling of Energy Systems".

- Mr Bryan Preece, Ag. Head of the Construction Centre of the Polytechnic of Wales, came to HTI on an exchange programme and lectured on Strength of Materials and Structures.

In exchange the Head of the HTI Civil Engineering Department, Mr D. Lazarides, lectured at the Polytechnic of Wales.

- Mr Savvas Savvides, Senior Instructor in Electrical Workshops, attended from 16-18 September a 16 hour seminar on "Occupational Safety and Health," organised by the Cyprus Professional Engineers Association and the Factory Inspectorate of the Ministry of Labour and Social Insurance.

OCTOBER

- Mr Douglas Veasey, Senior Lecturer at Luton College, U.K., visited HTI 3-28 October and lectured on Physics.

In exchange Mr Andreas Achillides Senior Lecturer at HTI, lectured at Luton College on Physics for the same period of time.

- Mr Ioannis Economides, HTI Lecturer, was awarded a scholarship by the U.K. Government under the British Technical Co-operation Training Programme.

He left on 7 October to pursue studies in Highway Engineering at the Birmingham University leading to a Masters of Science degree.

- On 12 October HTI celebrated the 20th Anniversary of its establishment.

The ceremony was attended by H.E. the Acting President of the Republic, Dr. Vasos Lyssarides, the Minister of Labour and Social Insurance, Mr Takis Christofides, the Minister of Education, Dr. Andreas Philippou, the Minister of Justice, Mr Christodoulos Chrysanthou, members of the Diplomatic Corps, members of the House of Representatives, guests, staff and students.

*D. Charalambidou-Solomi, D.E.S, BA (Hons) M.A.
Lecturer HTI*

The Minister of Labour and Social Insurance inaugurated the new Computer Building and later addressed the meeting.

Addresses were also delivered by Dr Themis Drakos Director HTI, Mr Antis Constantinou, member of HTI Board of Governors, Dr. Tribor Szentmartony ex-chief Technical Adviser of UNESCO at HTI and the President of the HTI Students' Union.

All speakers expressed admiration for the excellent work accomplished by HTI during the first twenty years of its existence.

Commemorative plaques were presented by the Minister of Labour and Social Insurance, Mr Takis Christofides to Dr. T. Szentmartony and Mr G. D. Christodoulides, first Director of HTI.

- The IEE (Cyprus Centre) in co-operation with HTI and the Industrial Training Authority organised a course on Electrical Services Design, Installations and Maintenance between 15-25 October.

23 practising engineers and technicians participated.

The course was presented by Mr E. Michael, Lecturer and Mr. S. Savvides, HTI Senior Instructor.

- Dr. Christos Schizas, HTI Lecturer, participated in a seminar from 20-23 October on computers.

The seminar was organised by the International University Consortium in Halkidiki, Greece.

- The HTI Regional Training Centre organised a course on "Refrigeration Repair Technician" in collaboration with the WHO Expanded Programme of Immunization with 23 students from 14 different countries.

The course was run in four languages simultaneously English, French, Arabic and Persian.

- Mr D. Lazarides, Head of Civil Engineering Department, visited the Polytechnic of Wales from 24 October - 11 November on an exchange programme and lectured on Structural Analysis and Design in Earthquake Regions.

- On October 19, HTI staff and students offered blood for the needs of the Blood Bank of Nicosia General Hospital.

NOVEMBER

- The IEE (Cyprus Centre) in collaboration with HTI and ITA organised the following short courses:

- (a) Advanced Trouble Shooting: 16 Bit Processors and the PC, 31 October - 4 November.

- (b) Electronics and Microprocessors, 3 October - 4 November.

(c) The IBM PC for Engineers and Managers, 7-11 November.

(d) Electrical Services: Refresher Workshop, 21-25 November.

Courses (a) and (b) were delivered by Neal Huthinson, Head of Microcomputer Unit, London Course (a) had 11 participants and Course (b) had 12 participants. Course (c) was delivered twice by Ms Carol Weaver, an associate of the Microcomputer Unit with 55 participants.

Course (d) was delivered twice by Peter Smith and Ron Taylor, IEE accredited lecturers, with 33 participants.

● Mr Jindrich Kratena, a Principal Researcher of the Czechoslovakian Academy of Sciences Institute of Theoretical and Applied Mechanics, visited HTI from 2-30 November according to the Cultural and Scientific Protocol between Cyprus and Czechoslovakia.

Mr Kratena held discussions with Dr. H. Stavrides, HTI Senior Lecturer, on the possibility of introducing photoelastic techniques in the testing of concrete elements both in the laboratory and real structures.

● The Regional Training Centre organised a course on Solar Refrigerator Technician during 7-18 November in collaboration with WHO Expanded Programme of Immunization (EPI)

The course was attended by 16 students from 11 different countries.

The course was run in two languages simultaneously English and Arabic.

● The HTI Director, Dr. Themos Drakos, visited London between 21-23 November.

Dr Drakos participated in a meeting of the IEE Overseas Board and attended the 150th Anniversary Graduation Ceremony of the Polytechnic of Central London as a special guest.

Dr. Drakos also visited Luton College and discussed their Higher National Diploma (HND) in Applied Biology.

● Mr. D. Lazarides, Head of Civil Engineering Department, and Dr. H. Stavrides, Senior Lecturer, attended a one day Symposium on the Construction Industry at the Philoxenia Hotel organised by ITA on 22 November.

● UNESCO Day, an annual event, was celebrated on 17 November.

Students and staff visited the churches of Archangelos and Panayia Tis Podithou near Galata village.

Mr Andreas Petrides, Secretary of the Church Committee, guided them around the churches and talked on the historical value of the two churches and their frescoes.

Students and staff offered voluntary work for the embellishment of the area around the churches.

Prior to departure the HTI Director, Dr Themos Drakos, and the President of the Students' Union, spoke outlining the significance of UNESCO and its international role in Letters, Education, Science and Culture. They also mentioned the

special ties between UNESCO and HTI.

The gathering voted a resolution to be sent to Director General of UNESCO.

DECEMBER

● Mr C. Neocleous, HTI Lecturer, left for Czechoslovakia to visit Czechoslovakian Technological institutions in order to gain experience in automation, control and instrumentation as well as computer aided-design.

● HTI organized an introductory course in computers of 20 hours duration for the technicians and engineers of P.W.D. The course was presented by Mr Christos Makarounas, HTI Lecturer, 18 November - 23 December.

The course was attended by 17 participants.

● The distinguished scientist Academician Yuri Gulyaev of the USSR Academy of Sciences visited Cyprus for two weeks, 15-30 December.

Professor Gulyaev visited HTI as a guest of IEE (Cyprus Centre) and HTI and delivered a series of lectures on various scientific and technical matters.

JANUARY

● Mr Pantelis Vasiliou, the National Secretary of IAESTE Cyprus, participated in the Annual General Conference of IAESTE which was held in Graz, Austria, 13-18 January.

The Cyprus IEAESTE offered 16 places for training in Cyprus and received 25 places for HTI students to receive training abroad.

The next Annual General Conference will take place at Sao Paulo, Brazil in January 1990.

● The IEE (Cyprus Centre) in collaboration with HTI and ITA organised a course on "An Introduction to Industrial Electronic Control" from 16-20 January.

The course was developed and presented by Professor R.J. Simpson, Lancashire Polytechnic, U.K., and attended by 43 participants from local industry, Government sector, and overseas.

● Classes for the Second Semester of 1988-89 began on 30 of January.

FEBRUARY

● Mr Anastasios Gregoriou, RTC Laboratory Assistant, attended a two week fellowship on Mechanical Medical Equipment from 12-24 February sponsored by CFTC at Falfield National Health Service Training Centre.

MARCH

● In March IEE (Cyprus Centre), ITA, and the London Microcomputer Unit, organised two short courses:

(a) "Data Communication and Local Area Networks"

(b) "UNIX/XENIX"

The first course was attended by 38 participants and the second one by 23 participants.

APRIL

● Sports Day was celebrated on 4 April. The finals of tournaments were held. Staff and students engaged in various sports activities and games.

- Environment Day, another annual event, was celebrated this year on 12 April.

On that day students and staff offered voluntary work for the embellishment of the grounds and facilities of HTI.

- A course of 60 hours in Industrial Quality Control commenced on 12 April.

The course was presented by HTI staff Mr M. Pattichis, Senior Lecturer, D. Roushas, Lecturer, L. Lazari, Lecturer, and V. Messaritis, Lecturer, between 12 April - 31 May. The course was attended by 18 professionals from the local industry and 5 HTI staff.

- The Institution of Electrical Engineers IEE (Cyprus Centre) in collaboration with HTI and ITA organised two courses on "The IBM PC for Engineers and Managers" between 17-21 April.

The courses, which were aimed at engineers and managerial staff working in industry, were developed and presented by the London Microcomputer Unit.

The duration of each course was 20 hours and it included theoretical and practical sessions.

- HTI students and staff donated blood on 17 April for the needs of the Blood Bank of the Nicosia General Hospital.

This was the second time in this academic year that HTI staff and students donated blood.

MAY

- The Annual Graduating students Dinner was held at the Philoxenia Hotel on 11 May at 8.00 p.m.

During the Dinner, the HTI Director, Dr. Themos Drakos, proposed a toast to H.E. the President of the Republic, Mr George Vasiliou.

Mr Phaedros Economides, Chairman of the Cyprus Employers and Industrialist Federation proposed a toast to HTI students. Mr Alecos Tryfonides, President of the HTI Students Union acknowledged.

HTI staff and official guests of HTI from the local industry participated.

The Annual Graduating Students Dinner was

honoured by H.E. the Minister of Labour and Social Insurance.

- The Third Games of the Small States of Europe took place between 17-20 May.

HTI contributed considerably in the organisation of these Games.

Two members of staff and nine third year students of the Computer Science course worked for more than a year to prepare the Computer Information System.

Moreover, HTI computer hardware resources, VAX, terminals and printers were made available to the Organising Committee for use.

During the Games all computer students were used as operators at the various athletic Centres and Sites.

HTI staff was utilised during the Games for supervision of students' activities and the smooth operation of the system.

All third year students of the Engineering courses were recruited to act as computer operators, drivers, judges, engineers, and guides to guests.

- The IEE (Cyprus Centre) in collaboration with the London Microcomputer Unit organised a course on "Data Communication and Local Area Network" between 22-26 May.

36 participants attended the course.

- Mr Andreas Achillides, HTI Senior Lecturer, gave a lecture on "Cold Fusion" on Wednesday, 31 May at the HTI Lecture Theatre.

Dr. T. Drakos participated in a meeting of the IEE Overseas Board in London and thence visited the Helsinki University of Technology as well as the Tampere University of Technology in Finland.

JUNE

- Final year exams are scheduled for 29 May-12 June.

- Exams for the first and second year students will take place between 5-16 June.

- The Graduation Ceremony is set for Wednesday, 28 June 1989.



PERGAMON

BOOKS — STATIONERY — CAKE DECORATION SUPPLIES

16A, King Paul Str., P.O. Box 5062, HERMES Court
(Behind Nicosia Stadium)
Tel. 456343 - Nicosia

- Books
- Book binding
- Stationery
- Duplicator supplies
- Calculators
- Rubber stamps
- Typewriters

**SPECIALISTS IN BUSINESS MANAGEMENT, HOTEL,
CATERING & BANKING BOOKS**

WE HAVE:

the largest selection of books on:

Economics & Statistics
General Management
Personnel, Marketing
and Production Management
Management Accounting
Hotel & Catering
and Banking

All the recommended books for:

The Institute of Marketing
Certified and International Accountants
Institute of Bankers
as well as other professional bodies

WE ARE:

the exclusive suppliers of books for:

The PHILIPS COLLEGE
The INTERCOLLEGE
The CYPRUS INSTITUTE OF MARKETING
The PITMANS COLLEGE

as well as the main suppliers for:

The MEDITERRANEAN INSTITUTE OF MANAGEMENT
The HIGHER TECHNICAL INSTITUTE
The FREDERICK POLYTECHNIC
The CENTRAL HOTEL SCHOOL
The G.C. SCHOOL OF CAREERS
and other private and public educational Institutions

WE ACT AS:

sole agents in Cyprus for the:

Mc-Graw-Hill Encyclopedia of Science and Technology (15 volumes)
Management English (Coursebook, activities book, 2 cassettes)
Haynes car and m/cycle workshop manuals
Virtue Hotel, catering and general books
Wilton cake decorating supplies of U.S.A.
Autodata publications incl. data for diesel engines
Car service data, by Seale

(N.B. last two titles are translated into Greek and are very useful for mechanics in servicing all makes and models of cars.)

Finally please note our following special discounts:

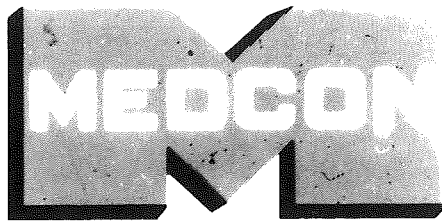
For cash purchased orders totalling £15 — £49 10% discount

For cash purchased orders totalling £50 — £99 15% discount

For cash purchased orders totalling £100 or more 20% discount



PERGAMON

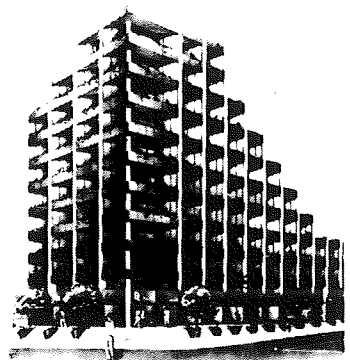


The Best in Civil Engineering and Building

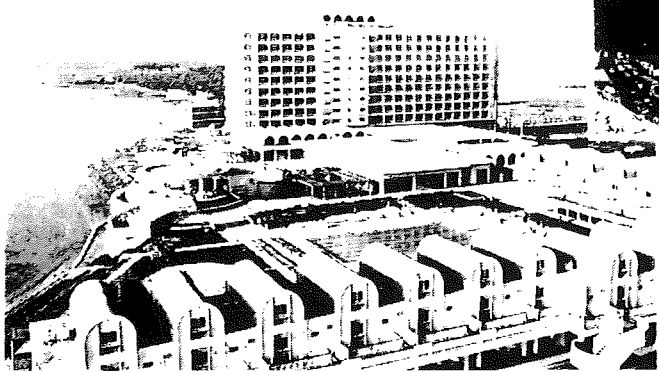
Από το 1950 κτιζουμε και δημιουργουμε τοσο στην
Κυπρο όσο και στο εξωτερικο.
Μια δυναμικη παρουσία. σ όλα τα επιπεδα.
Διαθέτουμε και τα μέσα και την πείρα. Κερδισαμε την
εκτίμηση και την εμπιστοσυνη χαρη στη συνεπεια και
την ποιότητα της δουλειας μας.
Με έργα... όχι μόνο λόγια.



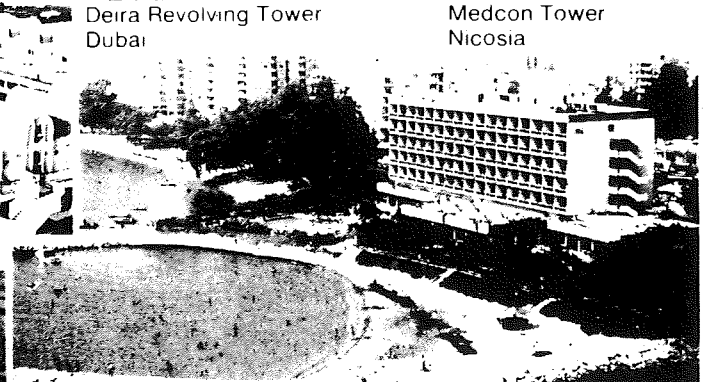
Deira Revolving Tower
Dubai



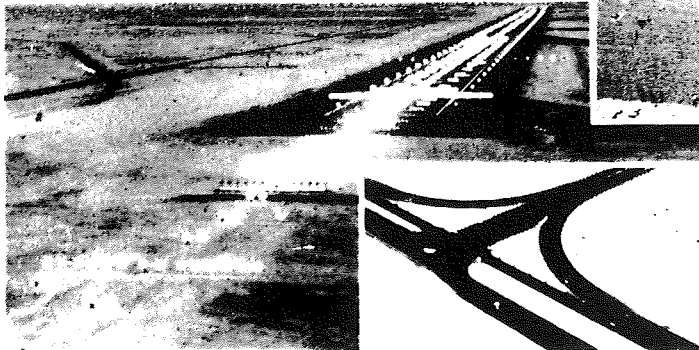
Medcon Tower
Nicosia



Salamis Bay Hotel - Famagusta



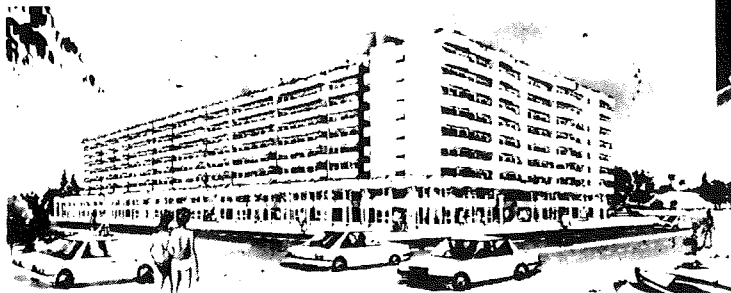
The Churchill Hotel - Limassol



Dubai Runway & Highway



Lefkara Dam



Eden Hotel Apartments - Limassol



MEDCON CONSTRUCTION LTD

24, Voulgaris St. P.O. Box 1054, Nicosia - Cyprus.
Tel 02-475111, 2, 3 Telex 2548 CY Telegrams Builders
Telefax 02-452549

advantage

SKF The largest manufacturer of ball and roller bearings

S K F is an international group with factories in twenty countries, an international sales network, and its own service organisation spread around the world.

S K F bearings are made in 8,000 basic types and sizes and many thousands of variants ranging from 3mm to several metres in outside diameter and from a weight of 0.036 grammes to more than 6,000 Kg. There are S K F bearings which can run at a speed of 400,000 r.p.m. and others which at low speed can carry loads of more than 2,000 tons.

S K F research efforts stretch from theory right through applied mathematics by computer to manufacturing process and product development. To illustrate the degree of accuracy required we may cite the example of any one medium sized bearing where ball diameters must not deviate more than 0.00002in., and where errors in sphericity in one particular ball must not exceed 0.0000 in.

MUCH MORE THAN BEARINGS

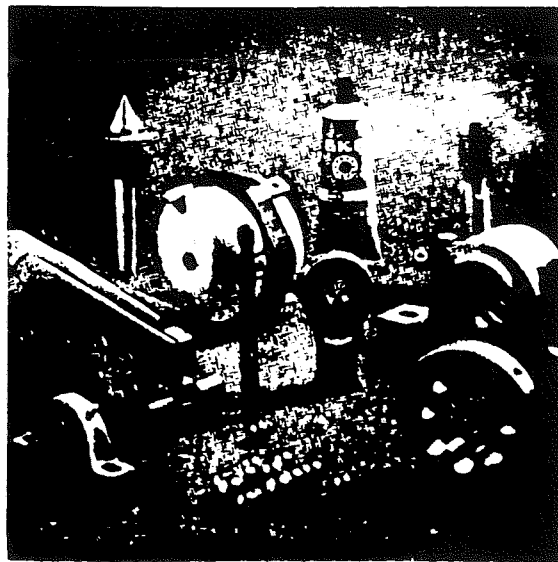
BALL BEARINGS

ROLLER BEARINGS

CASTINGS

MACHINE TOOLS

TOOLS



TEXTILE MACHINERY

COMPONENTS

PLANETARY ROLLER

SCREWS

FLUIDICS

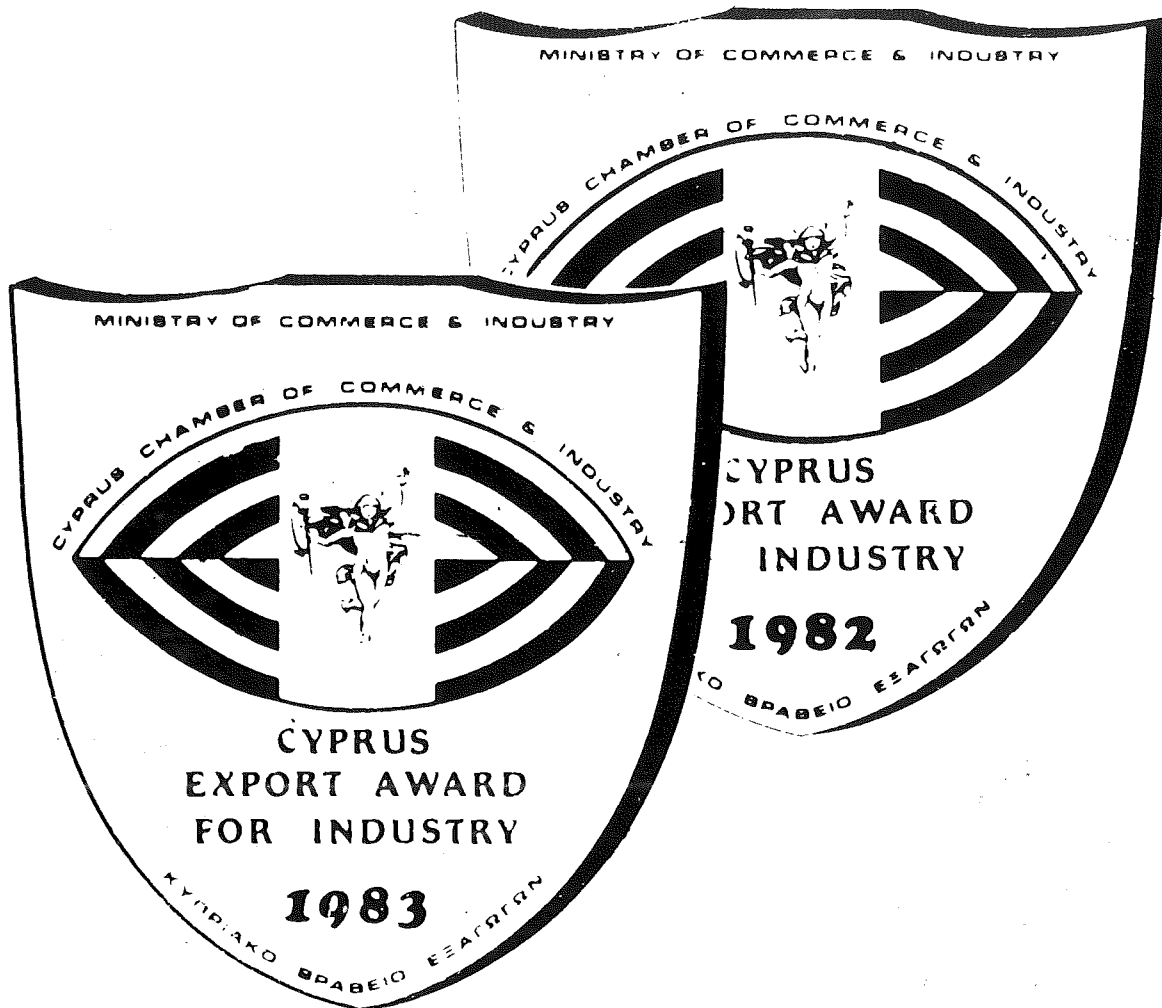
SKF

SKF Best possible service to customers

Research and development in the S K F group is applied in three directions. The first is the development of production technology the second is the development of new products and the third is a continuous process of developing the traditional product ranges to changing market requirements.

S K F faces strong competition in all the most important industrial countries. It is, however, true to say that S K F is foremost in the field of roller bearing engineering, in addition to being the most important exporter of ball and roller bearings.

S K F has attained this pre-eminent position for several reasons. One of them being that S K F was the first bearing firm to undertake systematic theoretical and experimental research in ball and roller bearing engineering.



twice awarded to
NEMITSAS INDUSTRIES LTD
for their outstanding performance
in the export of
TURBINE PUMPS & BUILDING MACHINERY



NEMITSAS INDUSTRIES LTD
MANUFACTURERS OF TURBINE PUMPS & BUILDING MACHINERY
P O BOX 124 LIMA SSOI - CYPRUS TELEX 2666 CABLE NEMITSAS TEL (051)69222 8